Deltares

Maasvlakte 2: Site evaluation

Geological and geotechnical characteristics and hazards

Maasvlakte 2: Site evaluation
Geological and geotechnical characteristics and hazards

Maasvlakte 2: Site evaluation
Geological and geotechnical characteristics and hazards

Client	Ministerie van Economische Zaken en Klimaat
Contact person	
References	None
Keywords	Nuclear Power Plant, desk study, geology, geo-engineering, earthquakes, liquefaction

Document control	
Version	1.0
Date	01-07-2025
Project number	11209639-004
Document ID	11209639-004-GEO-0003
Pages	104
Classification	
Status	Final

Management Summary

This report describes the site evaluation for the possible Maasvlakte 2 (MV2) nuclear power plant. This includes an evaluation of risks associated with the build-up of the subsurface, subsidence, settlement, bearing capacity, seismicity and volcanism. No major risks have been identified. It is a first-assessment desk study based on currently available data and does not provide sufficient information for the design phase. The main attention points are:

- A part of the site is still open water, while the other parts were reclaimed about 15 years ago. The landfill in the latter parts is about 20 m thick and is still consolidating. This results in relatively high subsidence rates of several millimetres per year for the coming years. The parts that are still to be reclaimed will need considerable consolidation time (>15 years) if the reclamation technique will be similar to the previously used technique.
- Large settlements, in the order of 0.5 m, are expected during and after constructing with the given loads of the reactor building. These settlements are partly caused by fluvial and shallow marine clay layers situated between depths of 25 and 200 m. A lack of information about the geotechnical properties of these layers causes large uncertainties around the expected settlements.
- In these parts of The Netherlands new buildings commonly have their foundation within the sandy Kreftenheye Formation. At MV2 this formation starts around -23 m NAP, but at places at -28 m NAP. This means that piles of considerable length are needed if that foundation technique is chosen.
- At the level of -21/-22 m NAP aeolian dune deposits are present, known to be archaeologically important. If the construction design will lead to significant disturbance of these deposits, archaeological research will need to be executed. It is advised to contact the Cultural Heritage Agency in an early stage of planning.
- There are plans for the construction of a third Maasvlakte. These plans are not concrete yet and will most likely not directly impact the technical construction of the MV2 NPP itself. Depending on the design for the third Maasvlakte, however, the construction can have impact on aspects like the design for the cooling-water systems or logistics. It is advised to obtain as much details about the plans for a third Maasvlakte in an early stage of planning.
- No groundwater monitoring wells are present at the project site. It is advisable to already install monitoring wells with filters at different depths to measure the piezometric head. Monitoring should continue for at least one year to capture seasonal effects.
- Based on preliminary assumptions it is concluded that the risk of full liquefaction of the subsurface due to earthquakes is very low. These assumptions need further consideration once the full Probabilistic Seismic Hazard Analysis (PSHA) has been carried out.

From the above, the PSHA and more insight into the plans for a third Maasvlakte would be essential information when ranking the four proposed locations in terms of suitability. The other attention points can be addressed in a later phase.

Technical Summary

The Ministry of Economic Affairs and Climate Policy of the Netherlands requested Deltares to conduct a subsurface site evaluation for the possible Maasvlakte 2 (MV2) nuclear power plant site in the South Holland province of The Netherlands. Within the scope of this study are the external hazards as described in chapter 5 of IAEA-SSR-1:

- Evaluation of fault capability.
- Evaluation of ground motion hazards (including human induced seismicity).
- Evaluation of volcanic hazards.
- Geotechnical characteristics and geological features of subsurface materials.
- Evaluation of geotechnical hazards and geological hazards.

The evaluation is based on currently available data and encompasses first-level assessments of the geological build-up and geotechnical properties of the subsurface, the geohydrological setting and hazards associated with subsidence, seismicity and volcanic activity. It does not provide sufficient information for the design phase.

Fault capability and Ground motion hazards
No major upfront constraints for the development of MV2 were identified. With respect to seismicity, this needs to be reevaluated after a full Probabilistic Seismic Hazard Analysis (PSHA) has been carried out.

Volcanic hazards
No major upfront constraints for the development of MV2 were identified.

Geotechnical characteristics and geological features of subsurface materials
The site can be divided into three subareas. The southern (1) and northern (3) subareas consist of a landfill up to 5 m NAP, while in the central (2) subarea water is present and the landfill starts at -4 to -8 m NAP. The landfill is internally heterogeneous as the result of a three-staged construction phase, but in general shows a downward-fining trend. The base of the landfill lies around -15 to -16 m NAP.

Below the landfill a mostly sandy unit is present, in general consisting of shoreface deposits from the Southern Bight Formation (0.5 m thick) on top of tidal deposits from the Naaldwijk Formation. This latter formation shows frequent alternations between clay/silt and sand. At locations of former tidal channels the Naaldwijk Formation is thickest and lies incised into the Kreftenheye Formation, locally to depths of nearly -30 m NAP.

The Naaldwijk Formation is underlain by a complex sequence of clayey freshwater-tidal fluvial deposits (Echteld Formation), a peat layer (Basal Peat Bed of Nieuwkoop Formation) and a loamy and stiff overbank deposit from the Kreftenheye Formation (Wijchen Member). The Wijchen Member below the peat is absent on the higher parts of the underlying aeolian river dunes (Delwijnen Member) and is in general quite thin. The dunes are mostly present as a blanket of ~1 m thick, but higher dunes reach thicknesses of 3 m and are often truncated at the top by tidal deposits. The dunes are known for their archaeological importance and additional geoarchaeological research will need to be executed when disturbed during the construction of the NPP. The Kreftenheye Formation is 20-25 m thick and consists of stacked sandy deposits from both meandering and braiding rivers.

Evaluation of geotechnical hazards and geological hazards
There are no publicly available piezometric measurement at the project site. With the Dutch Hydrological Model a simulation of groundwater is computed, indicating average groundwater levels between 0.5 and 1.0 m NAP, with fluctuations of 0.1 m between seasons and of 0.5 m between years. Daily fluctuations due to the influence of the tidal cycle can be expected. It is expected that tidal effects influence the groundwater level on a hourly base. The salt concentration in the uppermost part of the subsurface is simulated to be currently ~2.0 g/l. It is expected that in 2045 a six metre thick freshwater lens will be present.

The geotechnical properties vary with depth and geological formation, but are, except for the landfill, laterally quite homogeneous. The landfill consists of sands and silts and is especially loosely packed towards the bottom. This may require densification before construction can take place. Due to the heterogeneity of the landfill and varying thickness of the internal soft (clayey) layers, uneven settlements may be expected.

The bearing capacity of the subsurface is below the given surcharge load of the reactor building. Large settlements, in the order of 0.5 m, are expected during and after constructing with the given loads of the reactor building. These settlements are partly caused by clay layers between 25 and 200 m deep, such as the fluvial and shallow marine clay layers from the Kreftenheye, Waalre and Maassluis Formations . A lack of information about the geotechnical properties of these layers causes large uncertainties around the expected settlements.

Need for additional data and analysis
Based on the current assessment of the subsurface at the MV2 site, no additional geological or geotechnical data is needed for the current, reconnaissance, phase of the project. If a Nuclear Power Plant will be built at MV2, more subsurface data will be required for the design phase of the project. For a proper characterization of the geohydrological setting, however, more data is urgently needed. It is advised to install piezometric monitoring wells with filters at different depths as soon as possible. Monitoring should continue for at least one year to capture seasonal effects. With respect to seismic hazards a full Probabilistic Seismic Hazard Analysis according to the latest scientific standards and SSHAC guidelines is recommended.

Contents

1 Introduction

1.1 Aim of this study

This report provides a subsurface site evaluation for the possible nuclear power plant locality Maasvlakte 2 (MV2) at the most seaward part of the Port of Rotterdam (Figure 1-1). This includes a data inventory, a geological desk study, a description of the geohydrological situation and the geotechnical parameters. Within the scope of this study are the external hazards as described in chapter 5 of IAEA-SSR-1:

- Evaluation of fault capability.
- Evaluation of ground motion hazards (including human induced seismicity).
- Evaluation of volcanic hazards.
- Geotechnical characteristics and geological features of subsurface materials.
- Evaluation of geotechnical hazards and geological hazards.

The geological, geohydrological and geotechnical models and profiles should all be regarded as first assessments to characterize the site, based on the currently available data. In addition, the report provides first assessments of expected rates of subsidence, seismic hazards and volcanic risks. Hence, the report is not part of a Senior Seismic Hazard Analysis Committee procedure. All geological data and interpretations are made available in a GIS project that is included as supplementary material to this report.

1.2 Content and structure of this report

This report is divided into 10 chapters and 3 appendices. The introduction (1) covers the aim of this study, while chapter 2 introduces the available datasets and the datasets specifically used for the geological and geotechnical desk study. In subsequent chapters first the regional geological background is given (3), while the geological interpretation and creation of the geological model are covered in chapter 4. Detailed descriptions of the relevant geological units are part of Appendix A, with cross-sections including all used point data are provided in Appendix B. Chapter 5 uses, amongst others, the geological model to describe the geohydrological situation, including insights from existing groundwater-level monitoring systems. The geotechnical aspects of the site are described in chapter 6, that ends with proposed soil profile parameters for the initial design of the site. Additional geotechnical properties are listed in Appendix C. Chapters 7 to 9 give first assessments of expected rates of subsidence, seismic hazards and volcanic risks. In a separate report, the Royal Netherlands Meteorological Institute (KNMI) describes the seismological and climatological data.
The report finishes with conclusions and recommendations (10).

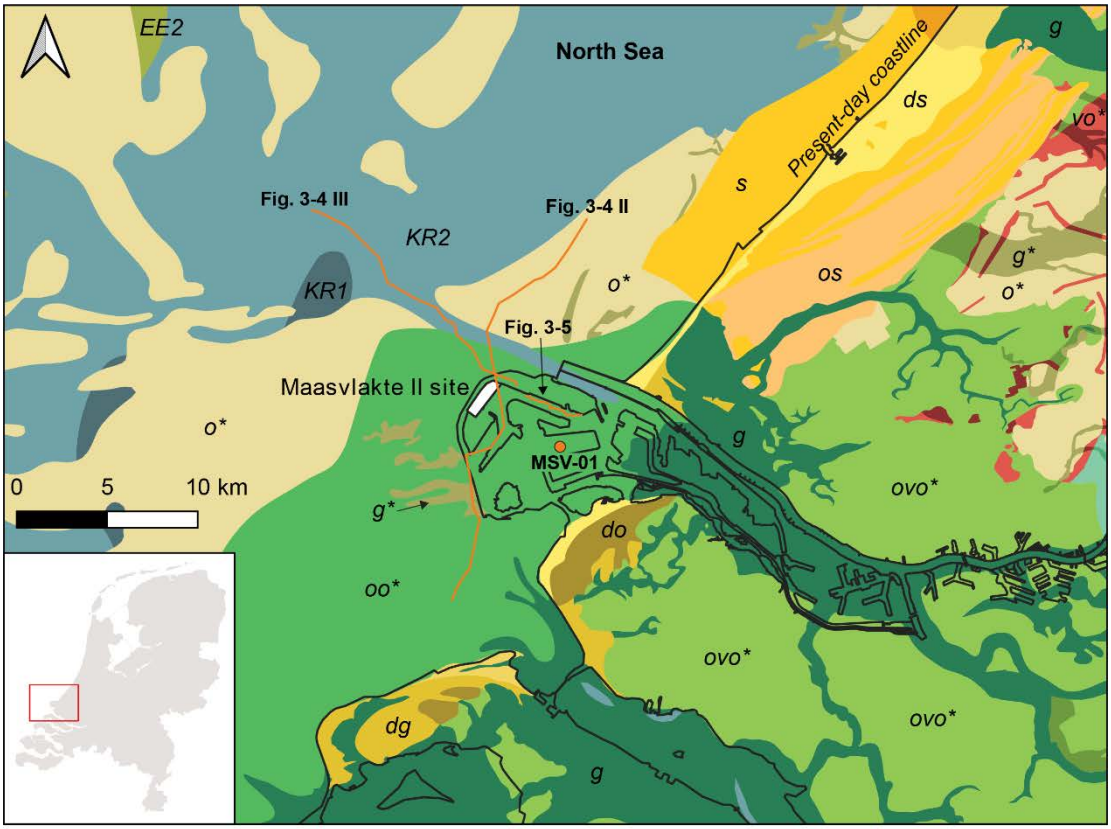

Units geological map

Holocene units

d	Coastal dune sand	ds	dsg	dg	do		
s	Beach and foreshore deposits	s	sg				
g	Tidal channel deposits	g					
o	Tidal deposits	o	os	ovg*	ovo*	oo*	
v	Coastal peat	vg*	vo*				
b	Sandy fluvial channel deposits	b					
k	Overbank deposits	kvo*	kg*				
*	Indicating older deposits	g*	o*				

Note: The order of the letters in the multiletter codes indicates the top-to-bottom stacking order of the deposits. e.g. ds = Coastal dune sand (d) on top of beach and foreshore deposits (s). The star behind a letter indicates that this part of the code (e.g. g in ovg) represents older Holocene deposits.*

Pleistocene units (underneath Holocene marine deposits)

KR1	Solid fine-grained Late Pleistocene flood deposits	KR1
KR2	Coarse-grained Late Pleistocene fluvial deposits	KR2
EE2	Open marine sandy and shell-rich Last Interglacial sediments.	EE2

Figure 1-1 Geological location map for Rotterdam Harbor region surrounding the MV2 site. Cross-section lines of figures 3-4 and 3-5 are indicated in orange. The location of borehole MSV-01 (Figure 3-2) is indicated as an orange dot. Geological map units follow the geological map of the Netherlands (TNO-GDN, 2023). The Maasvlakte II site is located within unit oo, which represents tidal deposits on top of older tidal deposits. Note that the darker green colour represents (tidally influenced) incised channel facies that were active in the past 1000's of years. Light green areas are those where a relatively complete Holocene succession can be found. Yellow colours represent coastal (dune) sands, red colours indicate areas with prominent deposits of early Holocene coastal peat.*

2 Subsurface data sources

The geological subsurface model and lithological descriptions in the current report are based on several databases. The following sections will provide a more detailed description of the various datasets stored in these databases. Locations of all datapoints are available in a GIS file (see Section 2.4) and are indicated in Figure 2-1.

The Netherlands has multiple open-source databases from which a wide range of subsurface data can be retrieved in standardized format. The 'shallow subsurface', in the Netherlands typically any data up to a depth of 500 m below Amsterdam Ordnance Datum zero or Normaal Amsterdams Peil (NAP) can be obtained from DINOloket (https://www.dinoloket.nl/en). This database is maintained by the Geological Survey of the Netherlands and is actively updated with both new data and digitized legacy data. For an explanation on how data can be retrieved from this database, see https://www.dinoloket.nl/en/help-subsurface-data.

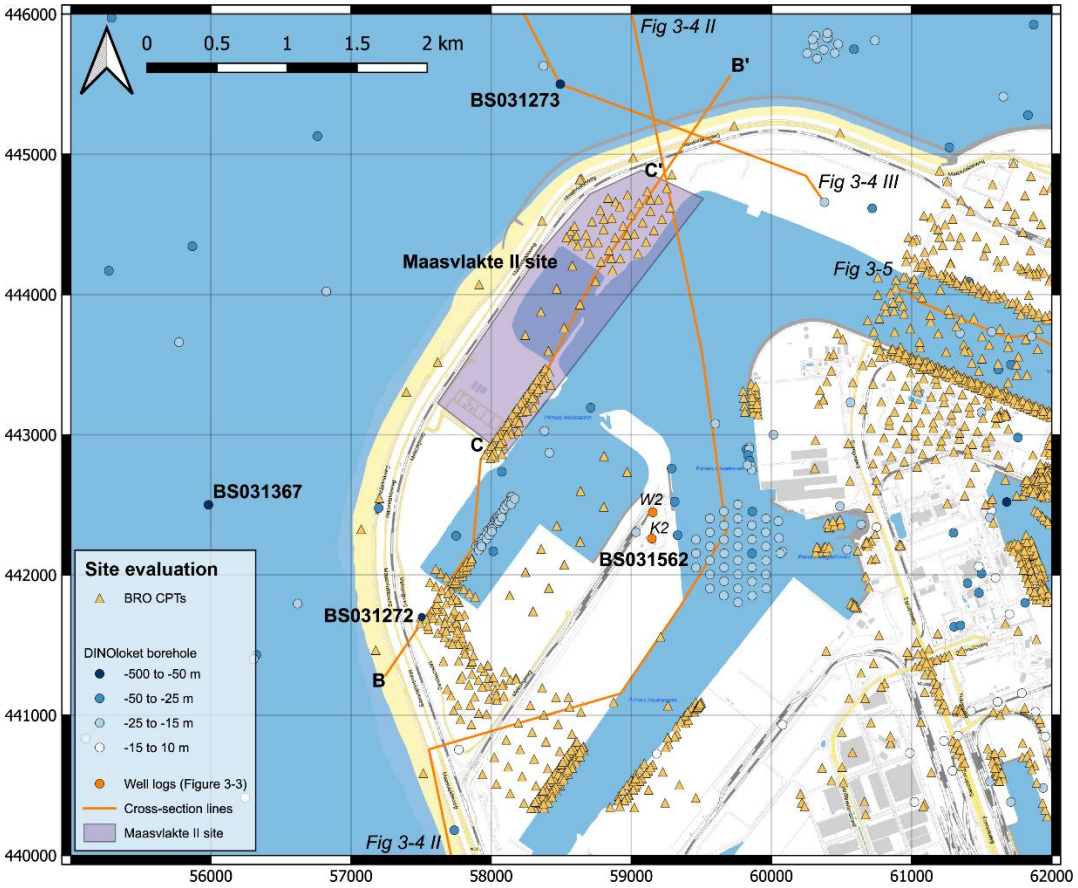

Figure 2-1 Location map of the MV2 site with locations of relevant publicly available subsurface data. Triangles indicate cone penetration test (CPT) locations, circles represent boreholes. Maximum depths of DINOloket boreholes are given in meter below surface level and classified in four classes depending on the end depth. In orange cross-section line B to B' (Figure 4-1) is indicated. Along the same line a zoomed-in version represents profile C to C' (Figure 4-2). The locations of parts of the cross-sections of figures 3-4 and 3-5 are indicated. The named boreholes on the map related to those shown in Appendix B. Note that well BS031562 is a different name for the same well referred to as K2.

A separate database, NLOG (https://www.nlog.nl/en/welcome-nlog) exists for subsurface data that fall under the Dutch Mining Act (e.g. 2D and 3D seismic surveys and deep boreholes) and provides data that extends below -500 m NAP depth. This database will not be described in detail in the current report because of the limited use within the scope of this report.

2.1 Cone Penetration Tests

Geotechnical Cone Penetration Test (CPT) results for the Maasvlakte II site are available from several different sources. The main Dutch open access database from which subsurface data can be downloaded, DINOloket (https://www.dinoloket.nl/en/subsurface-data), provides .gef and .xml data files per CPT in a standardized format available through the Dutch National Key Registry of the Subsurface (BRO – https://basisregistratieondergrond.nl/english/). Within the site vicinity there are about 1590 CPTs available this way. Older, manually scanned CPT data are also available at DINOloket, but lack the possibility for easy digital manipulation of the data. These older CPT data do not cover the MV2 area, therefore they are not considered in the current report.

2.2 Borehole data

From DINOloket (https://www.dinoloket.nl/en/subsurface-data) borehole descriptions, geophysical well logs, core photographs and supporting analytical data (e.g. chemical and grain size) can be downloaded. Borehole descriptions are available as .gef and .xml data files and for some older localities also as scanned pictures of the hand-drawn logs. Boreholes have been described throughout the Netherlands according to a standardized borehole description method since 2000 AD (Bosch, 2000). Geophysical well log data are available as .las files and/or scanned pictures at DINOloket. While these data are provided in a standardized digital format, the type of analytical data that is provided may differ by location.

2.3 (Subsurface) Geological and Geohydrological models

The data stored in the open-source databases feed into geological mapping of the surface and subsurface by the Geological Survey of the Netherlands (TNO-GDN). These models can be visualized using DINOloket (https://www.dinoloket.nl/en/subsurface-models/map), or can be requested to view and use outside DINOloket (https://www.dinoloket.nl/en/request-model-files). Multiple subsurface models designed for specific purposes are available at DINOloket, explanations on the intended uses and data underlying the various models can be found at https://www.dinoloket.nl/en/explanation-subsurface-models. Stratigraphic units used in these models are described in the Stratigraphic Nomenclature of the Netherlands (Figure 2-2; https://www.dinoloket.nl/en/stratigraphic-nomenclature). The geohydrological model of the Netherlands (Hydrological Instrumentations of the Netherlands) or NHI is a collection of datasets, model codes, and tools to simulate the entire water cycle in the Netherlands. Data and models can be downloaded from https://nhi.nu/en/.

The relevant models in the current context will be briefly discussed in the following paragraphs.

2.3.1 Geological map of the Netherlands

In 2023 an update was made to the Geological map of the Netherlands (TNO-GDN, 2023). For the onshore area, previous geological mapping at a scale of 1:50.000 and the regional 3D subsurface models were used as basis. For a full background on the geological map of the Netherlands, see https://www.dinoloket.nl/en/geological-map.

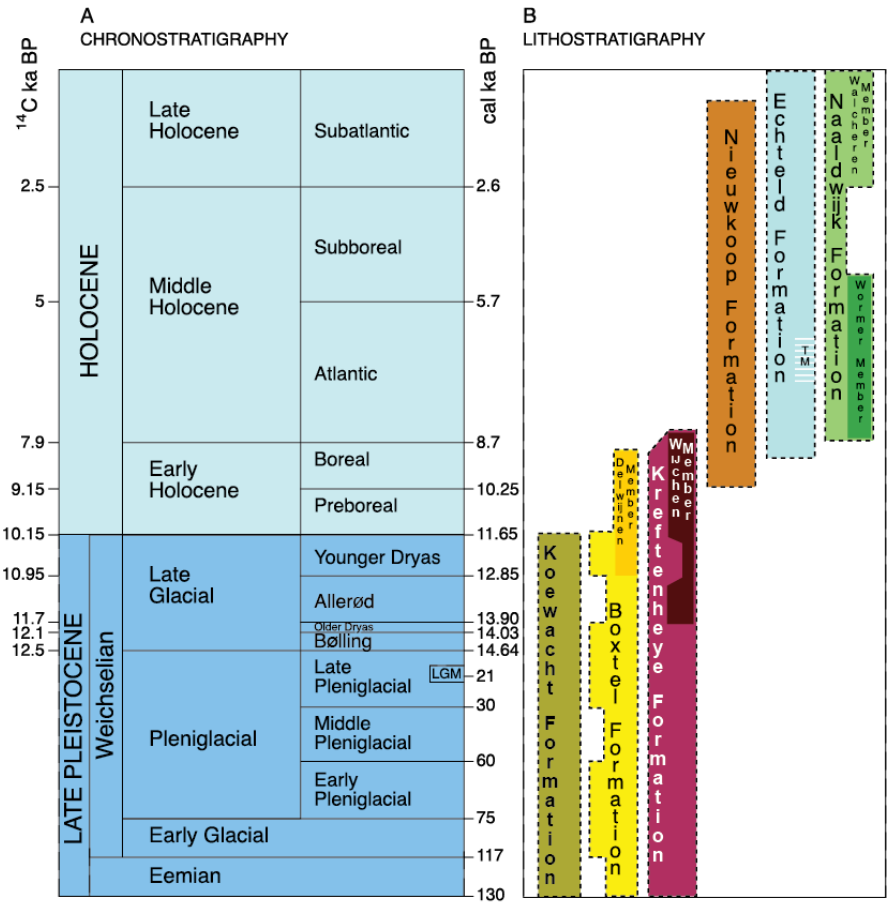

C

Chrono-stratigraphy (timescale non-linear)			Stratigraphic units of the Northsea Supergroup at formation level	
			Marine	Fluvial (Paleo-Rhine)
Quaternary	Holocene		Naaldwijk Formation	Echteld Formation
	Pleistocene	"Late"	Eem Formation	Kreftenheye Formation
		Chibanian		Urk Formation
				Sterksel Formation
		Calabrian		Waalre Formation
2,58 Ma		Gelasian	Maassluis Formation	
Neogene	Pliocene		Oosterhout Formation	Kiezeloöliet Formation
	Miocene		Breda sub-group	Inden Formation
23,03 Ma			Veldhoven Formation	
Paleogene	Oligocene		Rupel Formation	
			Tongeren Formation	
	Eocene		Dongen Formation	
	Paleocene		Landen Formation	
66 Ma				Adapted from: TNO-GDN 2019/12

Figure 2-2 (previous page). Dutch stratigraphic nomenclature as used in this report. A) Adapted from Hijma et al. (2009), ^{14}C ages and inferred calibrated ages for the Holocene follow Van Geel et al. (1980). Late Glacial ^{14}C ages follow Hoek (2001; 2008), while the Late Glacial calendar ages follow Rasmussen et al. (2006). Remaining Pleistocene chronostratigraphy according to Vandenberghe (1985) and Van Huissteden & Kasse (2001). B) Adapted from Hijma et al. (2009), lithostratigraphy for the southwestern coastal area of the Netherlands cf. De Mulder et al. (2003); Wijchen Member cf. Törnqvist et al. (1994); TM = Terbregge Member (Hijma et al. 2009, not officially part of the Dutch stratigraphic nomenclature). C) Adapted from Van Adrichem-Boogaert & Kouwe (1993) and updated by TNO-GDN 2019/12. Lithostratigraphy of the North Sea Supergroup at formation level, stratigraphic units are split in marine and fluvial facies. The fluvial units only represent those formations indicative for sediment supply from the southeast (e.g. Paleo-Rhine River). For a written description of these units at the scale of the Netherlands, see https://www.dinoloket.nl/en/stratigraphic-nomenclature.

2.3.2 GeoTOP

The GeoTOP model provides a detailed 3D model of the subsurface down to -50 m NAP to be used as a framework for groundwater management, (shallow) natural resources and infrastructure construction works. Voxels of 100 by 100 meters horizontally and 0.5 meter vertically provide lithology and lithostratigraphy including the probability of occurrence of each lithological class (sand, clay, peat etc.; Stafleu et al., 2013). The most recent version (v1.6) was released in 2023, but at present it does not include the part of MV2 that is the focus of this report. But since the boundary of the model lies only 1 km east of the study area, GeoTOP still provided useful information. For a full description see https://www.dinoloket.nl/en/detailing-the-upper-layers-with-geotop.

2.3.3 DGM/REGIS

The Digital Geological Model (DGM) and the regional geohydrological model (REGISII) that uses DGM as a framework provide regional-scale subsurface interpretations down to approximately -500 m NAP. DGM and REGIS are 3D layer models that classify lithostratigraphic units based on their lithology and other soil properties (hydraulic conductivity). These models do not cover the study area, but since also their boundaries lies just east of the study area, they still provide useful information. The horizontal and vertical resolution in the first 50 m in DGM/REGIS is lower than that of GeoTOP, which therefore should be preferred for interpretations in that depth interval. For more information see https://www.dinoloket.nl/ondergrondmodellen/kaart and https://www.dinoloket.nl/en/regis-ii-the-hydrogeological-model.

2.3.4 NHI/LHM

The "Nederlands Hydrologisch Instrumentarium" (Hydrological Instrumentations of the Netherlands) or NHI is a collection of datasets, model codes, and tools to simulate the entire water cycle in the Netherlands. The instrumentation tools consider groundwater flow and surface runoff as well as the interaction between the atmosphere, vegetation, soil moisture and salinization, which all play a role in certain areas of the Netherlands. The hydrological instrumentation can model both dry and wet conditions to predict where any problems may arise and the effects of interventions. This helps policymakers and land managers in making decisions that will limit damage from e.g. droughts and flooding. Hydrological models explore the possible effects of climate-change scenarios and can be used to substantiate and evaluate policy. The website (https://nhi.nu/en/) provides access to models, code, data and tools. Brief documentation is available for the various datasets and instrumentation and references are provided for the data portal or other online locations where the models, code, data and tools are available. The resolution of the data is 250 x 250 meter and it serves mainly for regional effects of measures. It also creates an efficient starting point for more

local geohydrological studies. The latest version (version 4.3.3) of the geohydrological model is described in Janssen et al. (2025).

2.4 Explanation of the GIS project

A table containing the explanation of the data sources used in the GIS project file is provided. See the attached file data_sources_GIS.xlsx. The GIS data is provided as a QGIS project file (.qgs). It is advised to open and visualize this in QGIS version 3.32.2 ‘Lima’.

3 Regional geological background

3.1 West Netherlands Basin

The study area lies on the southern edge of the tectonic West Netherlands Basin (WNB), a subregion of the wider North Sea Basin (Figure 3-1) that formed during the Late Mesozoic period (160-66 million years ago). For the vast majority of the Cenozoic, the current geological era that started 66 million years ago, it was part of a (shallow) marine depositional environment. The associated deposits start at depths of about 1100 m (Landen Formation; Figure 2-2) and consist of both clay and sand layers.

An important change occurred at the start of the Pleistocene, 2.58 million years ago, a period that is characterized by alternations between glacial and interglacial periods. During glacials, the formation of massive ice sheets resulted in lower sea levels and as a consequence the depositional environment at MV2 repeatedly shifted between shallow marine (interglacials) and terrestrial (glacials). Since the North Sea Basin hosts the Rhine and Meuse river systems, the terrestrial deposits mostly consist of fluvial sediment from these rivers. The oldest Pleistocene fluvial sediments in the study area are part of the Waalre Formation (Figure 2-2) and start at -80 to -90 m NAP.

The position on the southern flank of the sinking West Netherlands basin resulted in a northward dip of sediments. Tectonic movement is slow and hence the northward dip is especially clear for the older sediments, the younger sediments still lie more or less horizontally (Figure 3-1).

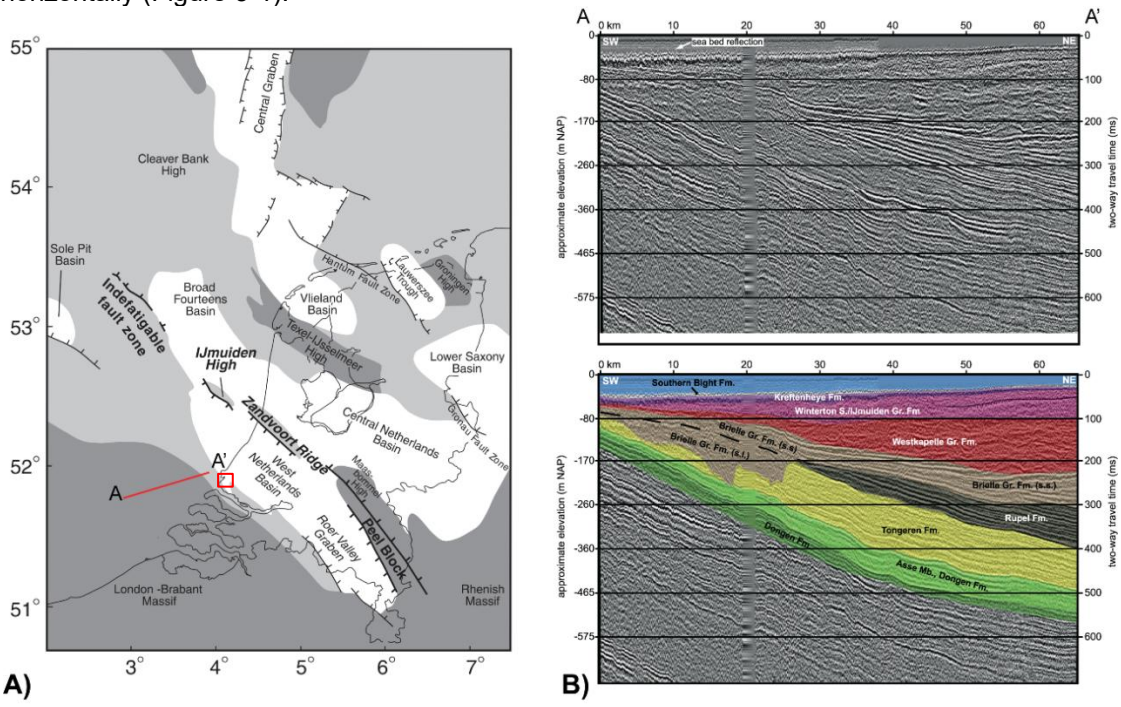

Figure 3-1 A) Generalized tectonic setting of the Netherlands (adapted from Michon et al., 2003). The MV2 area is indicated with the red box, it lies on the edge of the West Netherlands Basin (see also Chapter 7). B) Seismic cross-section showing processed (upper) and interpreted (lower panel) data (Hijma et al., 2012). Location indicated in panel A. The onshore equivalent for the Brielle Ground Formation is the Oosterhout Formation, for the Westkapelle/Winterton Shoal/IJmuiden Ground Formations the onshore equivalent is the Maassluis Formation.

3.2 Short description of the depositional history

In the following paragraphs the geological record at MV2 will be briefly described for five time-intervals. In each section the focus will be on the type of sediment that was deposited at these intervals and in which type of sedimentary environment these sediments were deposited. Afterwards, key characteristics of the geological units will be described individually per unit (Appendix A). The chosen units follow the Stratigraphic Nomenclature of the Netherlands (https://www.dinoloket.nl/en/stratigraphic-nomenclature) to enable easy comparison with existing subsurface models such as GeoTOP, REGISII and DGM-DEEP.

3.2.1 Mesozoic

Underneath the MV2 site, Mesozoic-aged deposits can be found at depths between approximately one and three kilometres (TNO-GDN, 2019). To illustrate this, we provide subsurface data from the nearby MSV-01 well (Figure 3-2). As stated above, the MV2 site is located along the southern margin of the West Netherlands Basin rift system (Van Balen et al., 2000; de Jager, 2003). Sedimentary rocks were formed in a half-graben basin and include limestones, sandstones and fine-grained siliciclastic deposits of the Upper Germanic Triassic Group. These include typical facies such as those of the Muschelkalk and Keuper formations.

The main pulse of rifting occurred during the Late Jurassic – Early Cretaceous, dividing the initially large basin into a series of smaller northwest-southeast striking subbasins. In these fault-bounded extensional subbasins argillaceous and marly marine formations were deposited. At the MV2 site these deposits have an approximate thickness of 400 m and are found at depths of 2100 – 2500 m. These deposits of the Schieland and Rijnland groups may contain (glauconitic) sandstone beds and intercalations; these may additionally be fluvial in nature. The synrift sequence is unconformably overlain by an approximately 900 m thick package of post-rift Chalk Group Cretaceous limestones. At well MSV-01, these limestones can be found at depths of 1200 to approximately 2100 m (Figure 3-2).

3.2.2 Cenozoic: Paleogene and Neogene

During the Paleogene and Neogene (Figure 2-2), sediments in the MV2 site vicinity were deposited in mostly shallow marine conditions. This includes both sand-dominant and clay-dominant intervals that are regionally recognizable and often separated by unconformable surfaces. The base of the Neogene deposits is formed by the Miocene Breda Formation and lies around -350 m NAP (TNO-GDN, 2025). Its top is formed by the Pliocene Oosterhout Formation and lies around -190 m NAP (TNO-GDN, 2025). This interval represents a gradual coarsening upwards sequence in which the fine-grained shallow marine deposits progressively get replaced by coarse-grained siliciclastic sediments deposited in coastal and delta-top depositional environments.

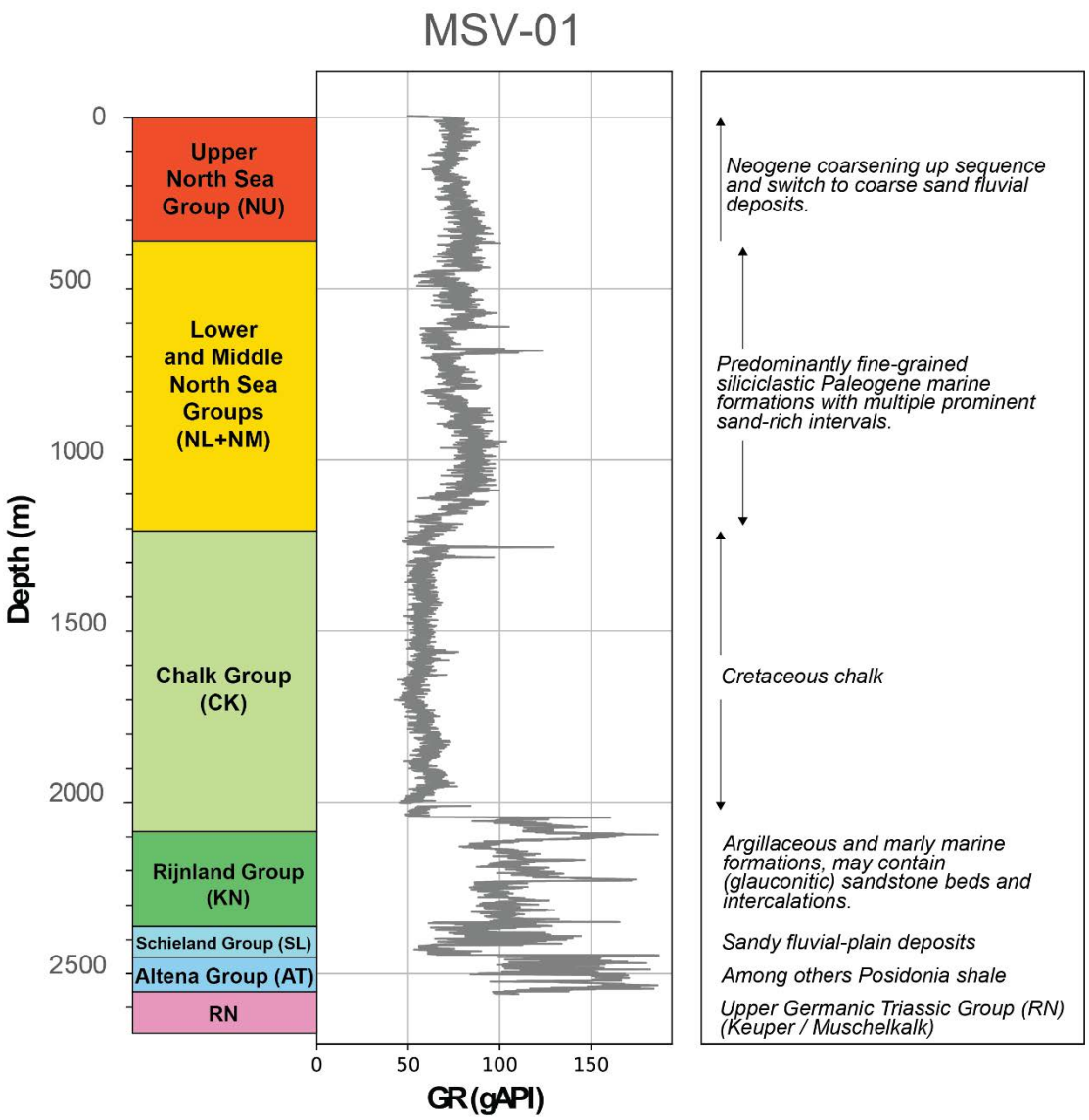

Figure 3-2 Gamma-ray well log of borehole MSV-01. This well is located to the east of the MV2 site, with the location indicated on Figure 1-1. On the left of the figure, the stratigraphy is shown at group level. On the right, brief descriptions of the typical lithologies and depositional environments that were encountered in the well. For more information on this well, see https://www.nlog.nl/nlog-mapviewer/brh/106518235?lang=en.

3.2.3 Cenozoic: Early and Middle Pleistocene

In the first part of the Pleistocene, depositional environments were still marine at MV2 and the mostly sandy deposits of the Maassluis Formation were deposited. According to the REGISII-model the upper part of the Maassluis Formation (depths between 80 to 90 m) is characterized by a ~5 m thick clay layer. This clay layer clearly stands out in the gamma-ray logs in two nearby wells at MV2 (Doornenbal, 2023), although in these wells the clay layer is interpreted to be part of the younger Waalre Formation (Figure 3-3).

Increasingly cold and longer lasting glacials during the Pleistocene resulted in long periods of lower sea level and the Rhine-Meuse system expanded into the North Sea Basin (Ten Veen et al., 2025). The associated estuarine and fluvial deposits of the Waalre Formation consist of alternations between more clayey and sandy units and has its top around -45 m NAP. The individual clayey units can have thicknesses of several meters (Figure 4-1).

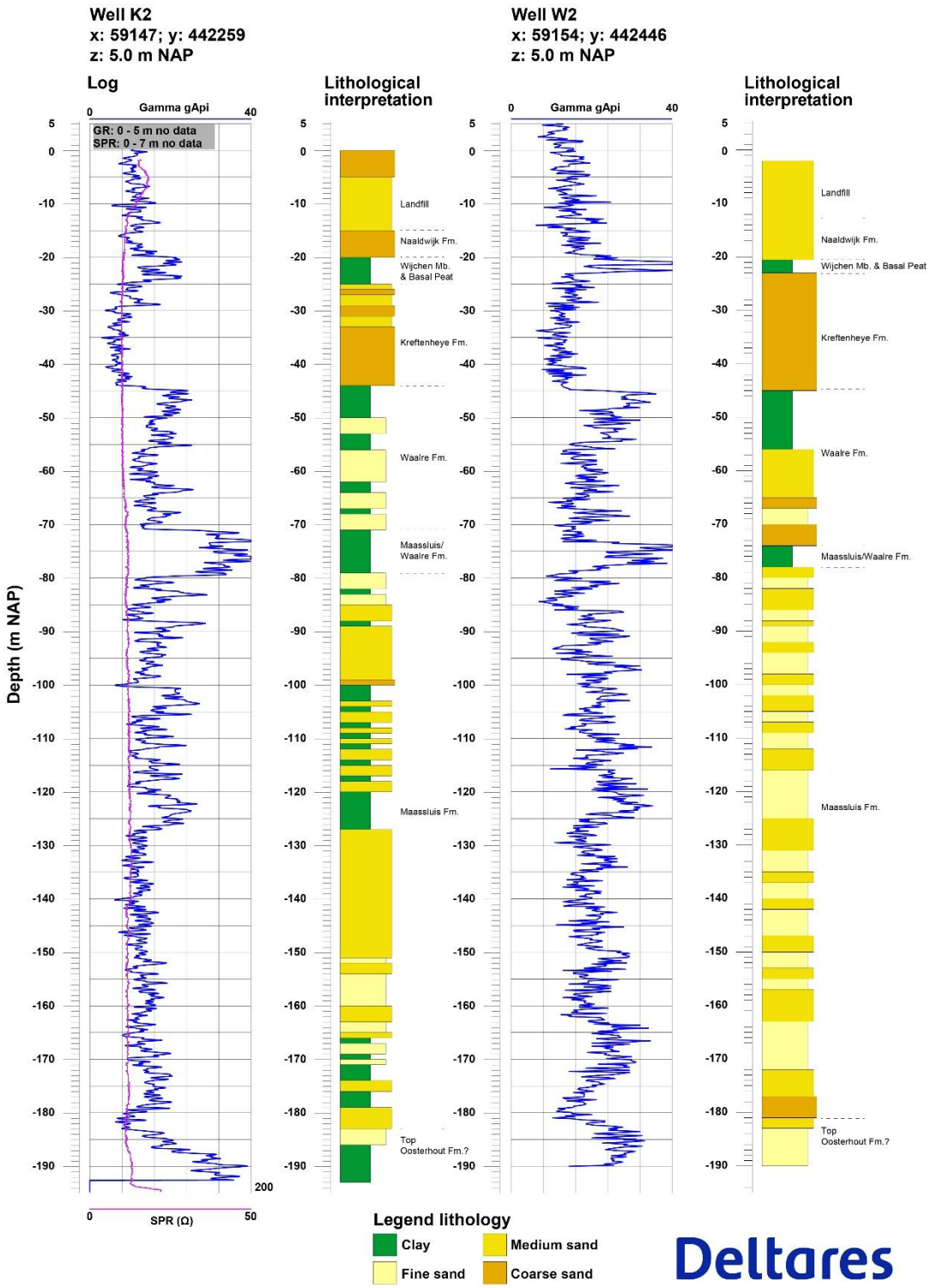

Figure 3-3 Gamma ray logs and lithological and geological interpretation (Doornenbal, 2023) for two boreholes about 200 m apart (K2, also referred to as BS031562 and W2, also known as BS031561) east of the study areas (see Figure 2-1 for location).

3.2.4 Late Pleistocene

A long hiatus of likely more than 1 million years exists between the Waalre Formation and the overlying Kreftenheye Formation. No sediments have been preserved that were deposited during this intermediate period. The Kreftenheye Formation predominantly consists of relatively coarse sand and was mostly deposited by braided rivers of both the Rhine and Meuse. Figure 3-4 shows that different units of the Kreftenheye Fm. are present below MV2 (see Figure 1-1 for location of cross sections), with the deepest unit potentially being part of the older Urk Fm.

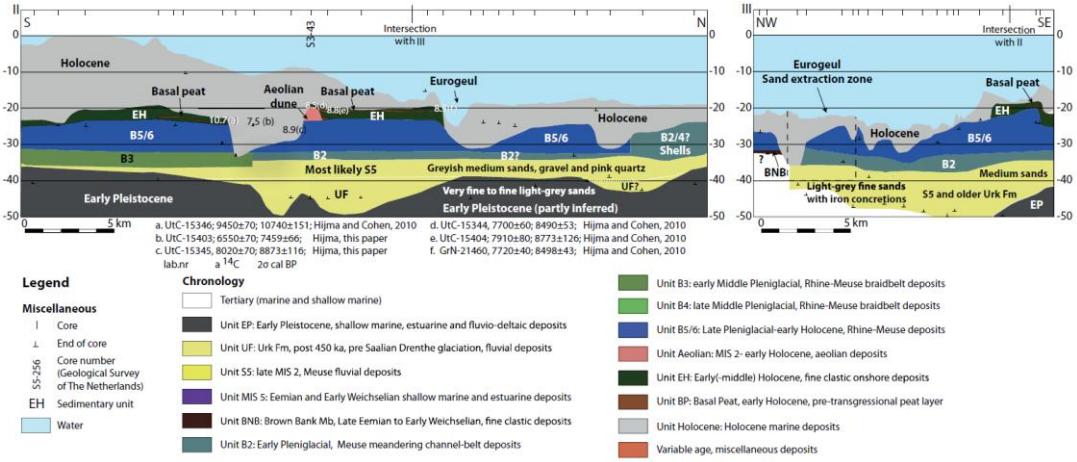

Figure 3-4 Geological cross-sections near MV2 (Hijma et al., 2012). Transect locations are shown in Figure 1-1, all depths are in metres relative to NAP.

3.2.5 Holocene

At the end of the last ice age, about 12,000 years ago, sea level was more than 60 meters lower than today, and the coastline was situated hundreds of kilometres downstream. The current MV2 site was part of a wide river plain of the combined Rhine and Meuse rivers, from which river dunes up to 15 meters high were blown up during dry periods. These dunes (Delwijnen Member of the Kreftenheye Formation) were attractive for people to live on because their higher location provided a good base for hunting. Around the MV2 site dune deposits occur widespread, with their base around -22/-23 m NAP (Vos, 2015; Vos et al., 2015; Moree et al., 2018). The deposits are mostly 1-2 m thick, but thicknesses up to 3 m are possible. Dune activity peaked around 11,000 years ago and lasted for a few hundred years (Vos et al., 2015). The dune deposits mostly rest on a thin layer of loamy and stiff overbank deposits (Wijchen Member of the Kreftenheye Formation). Also the lower parts of the dune deposits are covered by the Wijchen Member.

Between 12,000 and 6,000 years ago, the sea rose more than 50 meters, transforming the area from a river valley to an estuary with flanking tidal basins (Hijma et al., 2009; Hijma & Cohen, 2019; Hijma et al., 2025). Thick layers of clay, sand, and peat were formed, creating a complex subsurface structure (Figure 3-5 & Figure 3-6). As sea level rose, the MV2 site became wetter and large-scale peat formation commenced in between the channel systems after 9,500 years ago (Hijma & Cohen, 2010; Vos et al., 2015). Peat formation ended shortly after 8,500 when during a period of increased rates of sea-level rise the whole area drowned and turned into a freshwater tidal basin where initially gyttja and later clay of the Echteld Formation was deposited (Figure 3-7). With continued sea-level rise, the deposits became increasingly brackish in nature and are part of the Naaldwijk Fm.

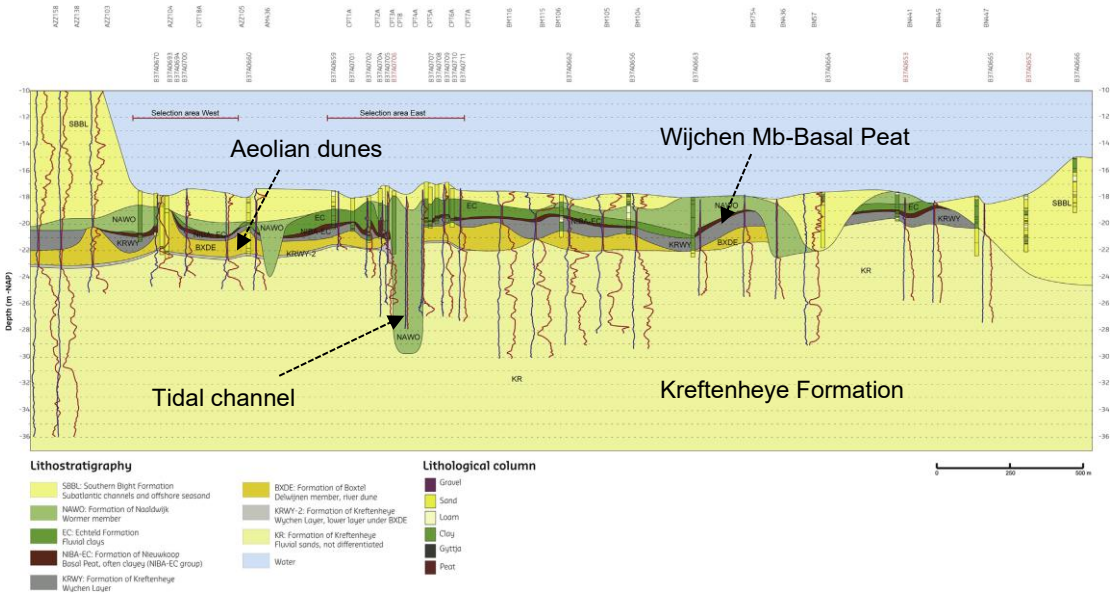

Figure 3-5 Geological cross-section (Vos et al., 2015) through the Late Pleistocene/early Holocene deposits of the study area in the Yangtze harbour, just a few kilometres east of the current study area. For location of the profile, see Figure 2-1. It shows that in most places the Kreftenheye Fm. is covered by a thin sheet of aeolian dune deposits (BXDE), that in its turn it commonly covered by a sequence of Wijchen Mb.-Basal Peat Bed. At some places tidal channels (Naaldwijk Fm.) were active and eroded deep into the Kreftenheye Fm.

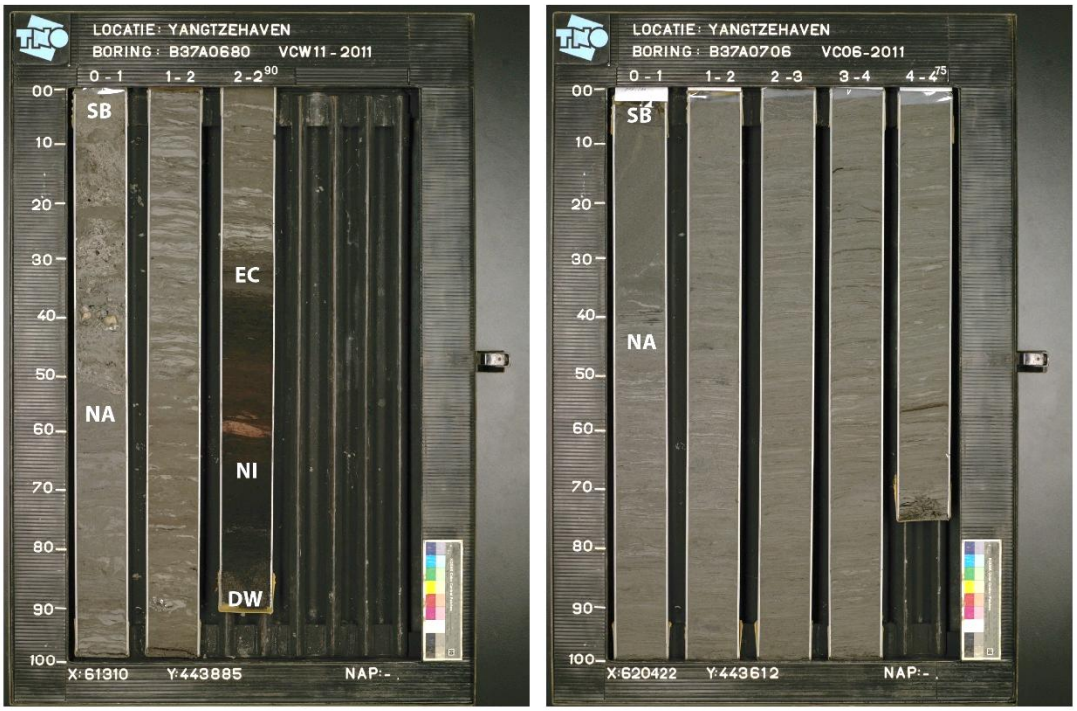

Figure 3-6 Examples of the deposits that can be expected at the study site (see also Figure 3-5). Borehole B37A0680 shows a sequence of sandy marine deposits (SB: Southern Bight Fm.), layered tidal deposits (NA: Naaldwijk Fm.), clayey fluvial deposits (EC, Echteld Fm.), a peat (NI, Nieuwkoop Formation) and sandy aeolian deposits (DW, Delwijnen Mb. of the Kreftenheye Fm). In nearby borehole B37A0702, the activity of a tidal channel has removed all older Holocene deposits.

Initially, the coast was still quite open, but from 6,000 years ago, the coast began to close, and peat formation in the hinterland increased significantly (Figure 3-7). This closure was mainly due to decreasing rates of sea-level rise: around 8,400 years ago, the rate was still over 1 meter per century, but around 6,000 years ago, this had decreased to 0.25 meters per century (Hijma & Cohen, 2019; Hijma et al., 2025). The discharge of the Rhine was now mainly towards Katwijk, but the Meuse still flowed out in the area of MV2. About 5,000 years ago, the coastline was already more or less in its current location, and until just before the Roman period, the situation remained fairly stable. The Meuse had its mouth near Hoek van Holland, the Rhine near Katwijk, and in between, the coastline was completely closed.

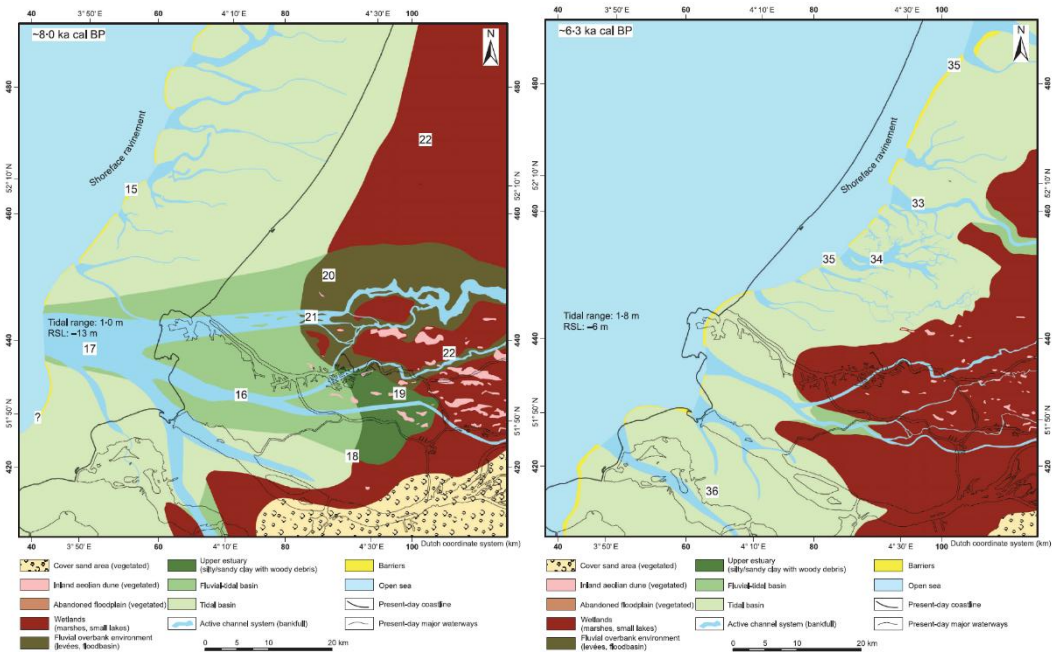

Figure 3-7 Paleogeographic maps of the area around MV2 (Hijma and Cohen, 2011). Left: 8,000 years ago with a large, combined mouth of the Rhine, Meuse, and Scheldt. The river dunes (pink spots) are clearly visible inland. Right: 6,300 years ago with a fairly open coast with several estuaries and many tidal basins around them.

A few centuries before the Roman period, several sea incursions occurred at the northern edge of the Meuse estuary, creating an opening into the peatlands. After this, the influence of the sea became rapidly greater, and an increasingly larger part of the hinterland peat area was affected and transformed into intertidal areas. The MV2 site remained in front of the estuary all this time. In the post-Roman period the estuary became increasingly dominated by the Rhine after the formation of the Lek and the Waal (Vos et al., 2011; Cohen et al., 2012). In the centuries after the 11th century large parts of the estuary and upstream rivers were embanked.

3.2.6 Anthropogenic influence: the creation of the Maasvlakte

At the start of the 19th century, the main mouth of the Rhine-Meuse estuary was the Haringvliet. North of it a smaller estuary was present (Figure 3-8, map of 1815), consisting of two outlets: the Brielse Maas and Het Scheur. In the 18th century this estuary had already become so shallow that larger ships had to go through the Haringvliet, which is a longer route towards the sea, and the first plans appeared to dredge a new outlet from Rotterdam to the sea. In 1858 extension of Het Scheur commenced and by 1872 the first ships went through the Nieuwe Waterweg (Figure 3-8, map of 1907).

The construction of the Nieuwe Waterweg also led to the first plans to close the Brielse Maas outlet, initially in order to get more water into the Nieuwe Waterweg, but later also to prevent floods and to decrease the speed of salinization. The Brielse Maas was closed by the Brielse Maasdam in 1958 (Figure 3-8, map of 1958). The resulting embayment was closed off in 1966 by the Brielse Gatdam, hereby creating the Oostvoornse Meer that was used as a sand-mining area for the first Maasvlakte (MV1; Figure 3-8, map of 1969).

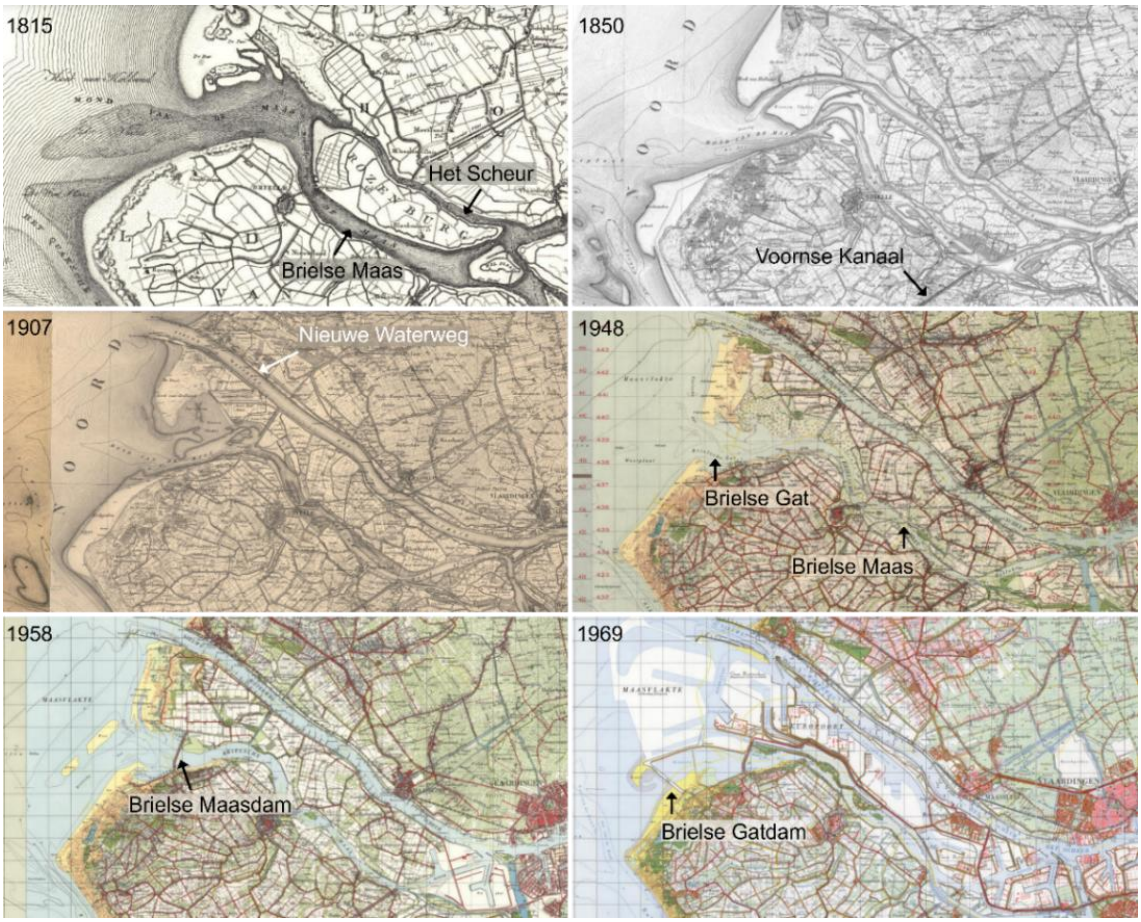

Figure 3-8 Topographical maps of the estuary of the Meuse from 1815 to 1969. Source: www.topotijdreis.nl; earlier published in Vermeer et al. (2025).

The MV1 was built because during the 1960's the number and size of ships going to Rotterdam increased steadily. This resulted in heavy traffic in the Nieuwe Waterweg and the Rotterdam-harbour was looking for ways to expand. It was decided to build a new harbour into the North Sea by first building a ring dike and fill the inner part with mined sand from the Oostvoornse Meer and the North Sea. The first ships were moored in 1973 and in 1974 the MV1 was officially opened (Figure 3-9, maps of 1968 and 1985).

The next step towards the current situation was taken in 1986 and 1987 when an extension of the southwestern part of MV1, the Slufter, was built to contain polluted dredged material (Figure 3-9, map of 2000).

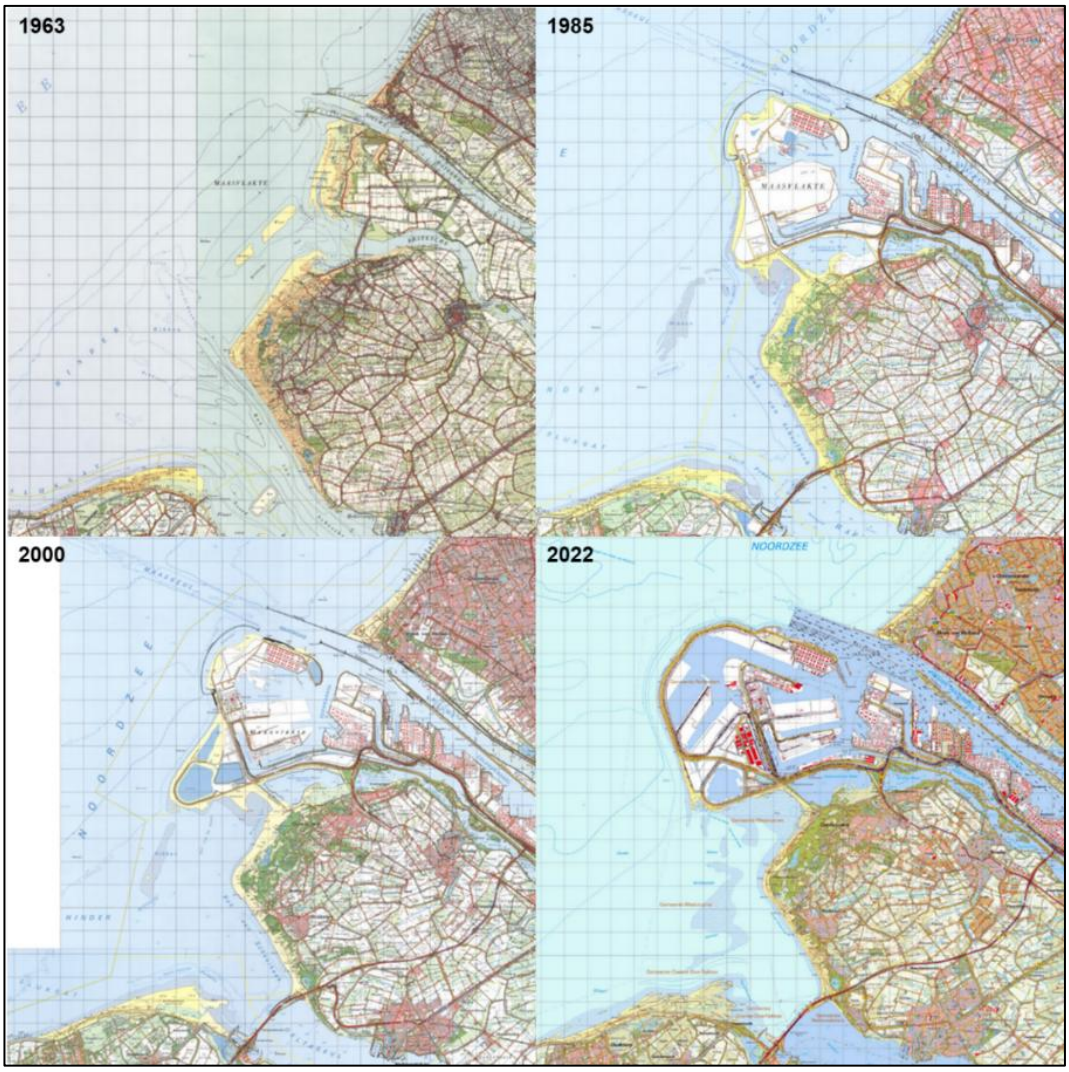

Figure 3-9 Topographical maps from before the construction of MV1 (1963), the MV1 (1985), the Slufter (2000) and MV2 (2022). Source: www.topotijdreis.nl; earlier published in Vermeer et al. (2025).

Construction of MV2

The building of MV2 started in 2008 and MV2 is in use since 2013. It extends about 6 km into the North Sea (Figure 3-9, map of 2022). The construction of MV2 is shown on satellite imagery in Figure 3-10, and a schematic overview of the construction periods is presented in Figure 3-11. Figure 3-11 highlights that MV2 was constructed in two phases. In the first phase, from 2008-2013, the flood-defence structures and the Prinses Amaliahaven were constructed. From 2018 onwards, phase 2, the Prinses Alexiahaven started to get shape, but not all plots have been finalized. All plots that are currently considered for the NPP at MV2 were built since or after 2018.

Figure 3-10 Satellite imagery of the construction of MV2. Source: https://luchtfototijdreis.nl/, which uses images from "Esri Nederland, Kadaster" (voor 2006-2008), "Esri Nederland, Cyclomedia/Aerodata (voor 2009-2011), "Esri Nederland, © aerodata, powered by CycloMedia" (voor 2012 t/m 2015), "Esri Nederland, Beeldmateriaal.nl" (voor 2016 t/m 2020), Beeldmateriaal.nl" (voor 2020 t/m 2024).

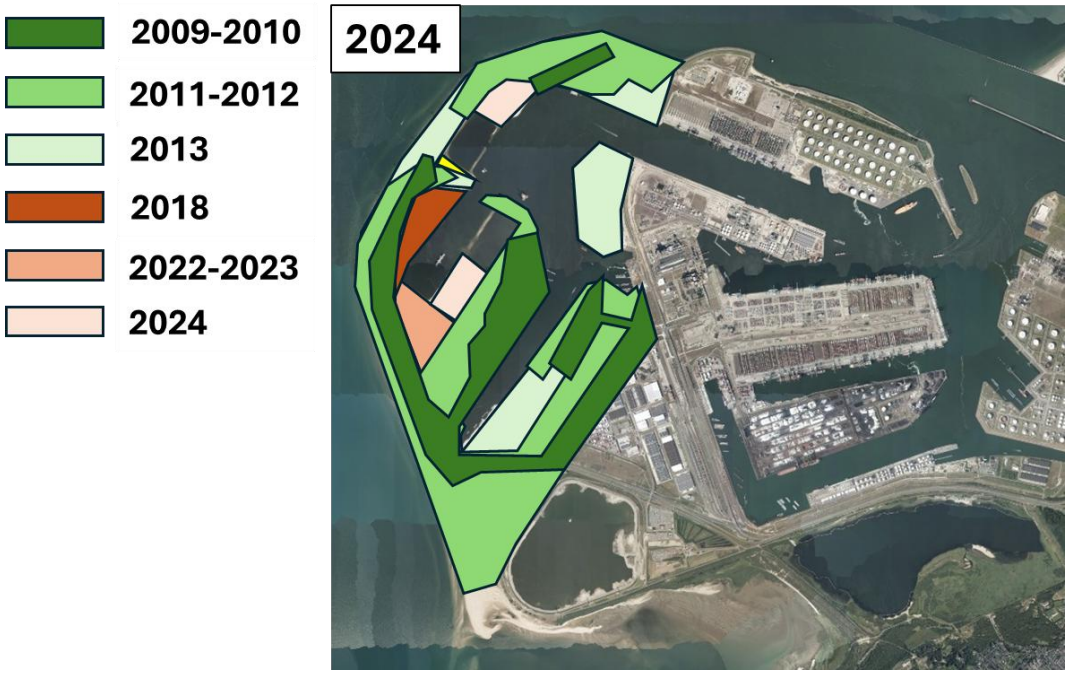

Figure 3-11 Schematic construction periods of MV2. Source satellite image: Source: https://luchtfototijdreis.nl/ - Beeldmateriaal.nl" (2024).

Since MV2 was built in much deeper water than MV1, building a ring dike first was no option. Therefore, bottom dumping was applied until about -7 m NAP (Figure 3-12a). When the sand is dumped it settles in elongated lenses of tens of meters wide and 1-2 m high with the coarsest grains at the bottom (Van Ginkel, 2019). This was followed by rainbowing from ships to bring the reclamation up to mean sea level (Figure 3-12b). In the last phase, sand was deposited by pipelines to heighten the landfill to the final level of 5.35 m NAP (Figure 3-12c).

All three types of sand deposition result in different degrees of heterogeneity, meaning that properties like grain size, hydraulic conductivity and consolidation are not constant throughout the landfill. According to Van Ginkel (2019), however, the heterogeneity is more predictable than that of natural soils.

Plans for Maasvlakte 3

In the last year the necessity for a third Maasvlakte is frequently mentioned and at present options for an extension of MV2 are investigated. There is support from both the province of South-Holland, the city of Rotterdam and the harbour of Rotterdam. Since it is not yet known where MV3 will be built, the impact on the potential NPP at MV2 is unclear. The largest impact may be expected on the design for cooling-water systems.

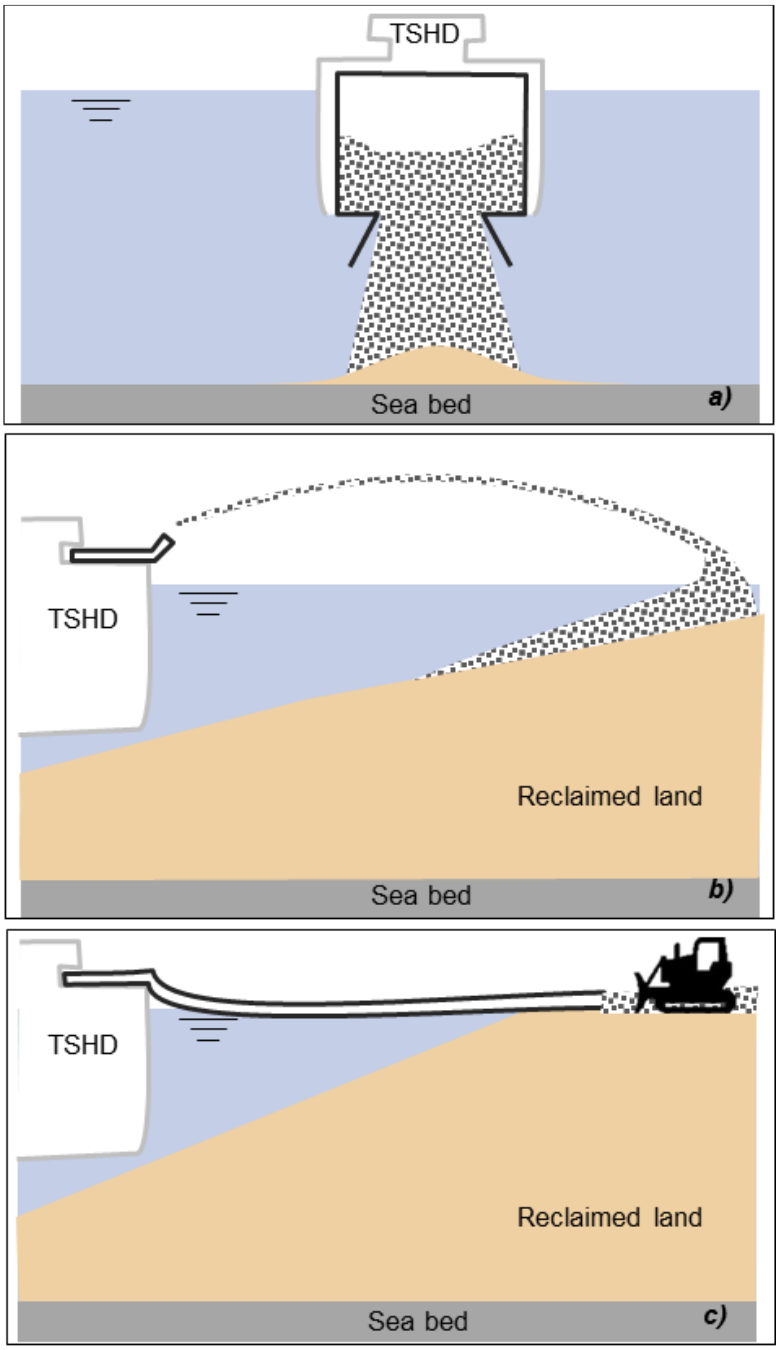

Figure 3-12 Applied land reclamation methods at MV2: bottom dumping (a), rainbowing (b) and pipeline discharge (c). Taken from Van Ginkel (2019).

4 Geological cross sections

The entire MV2 study site lay offshore until construction started in 2008, with water depths between 15 and 17 m. Since the current surface lies around 5 m NAP, this means a landfill thickness of 20-22 m. The base of the landfill is clearly marked in the CPT-data by a sudden increase in cone resistance and a drop in friction ratio and matches well with the pre-MV2 construction bathymetric data (Figure 4-1 and Figure 4-2). The two figures show only the interpreted formation, not the individual CPTs, boreholes and well logs. They can be found in Appendix B. In chapter 6 the geotechnical properties of the landfill are discussed in detail.

Below the landfill a mostly sandy unit is present, in general consisting of shoreface deposits from the Southern Bight Formation on top of tidal deposits from the Naaldwijk Formation. The shoreface deposit is 0.5-1.0 m thick (Figure 3-6), relatively coarse, contains shells and has low percentages of clay and silt. The Naaldwijk Formation is more heterogenous, relatively fine and shows frequent alternations between clay/silt and sand (Figure 3-6). At locations of former tidal channels the Naaldwijk Formation is thickest and lies incised into the Kreftenheye Formation, locally to depths of nearly -30 m NAP (Figure 3-5, Figure 4-2).

The Naaldwijk Formation is underlain by a complex sequence of clayey freshwater-tidal fluvial deposits (Echteld Formation), a peat layer (Basal Peat Bed of Nieuwkoop Formation) and a loamy and stiff overbank deposits from the Kreftenheye Formation (Wijchen Member). The freshwater-tidal deposits are often organic, contain wood remains and reed roots and consist of gyttja at the base. The thickness of the peat bed is mostly between 5-20 cm (Hijma et al., 2009; Vos et al., 2015). The Wijchen Member below the peat is absent on the higher parts of the underlying aeolian river dunes.

The aeolian river dune deposits are well sorted sands with medium grain sizes between 150-210 µm (Delwijnen Member of the Kreftenheye Formation). Mostly present as a blanket of ~1 m thick, but higher dunes reach thicknesses of 3 m and are often cut off at the top by tidal deposits. In the central part of the MV2-site the dunes seem absent due to the presence of incised tidal channels (Figure 4-2). The dunes were blown out of dry river banks of the Rhine-Meuse system (Kreftenheye Formation) of which the top consists of medium fine to coarse sand (150-300 µm). In between the dunes and the sandy fluvial deposit, a thin second layer of the Wijchen Member is often present. At the MV2-site this second layer seems absent (Figure 4-2). The dunes are known for their archaeological importance (Moree & Sier, 2015).

The Kreftenheye Formation is 20-25 m thick and consists of stacked sandy deposits from both meandering and braiding rivers. Alternations between very coarse, gravelly sand with finer sand layers can be expected over short distances and an occasional clay layer can be present.

Between the Kreftenheye Formation and Waalre Formation a hiatus exists of at least one and perhaps two million years. The boreholes and gamma logs clearly show that the Waalre Formation consists of a mix of sand and clay layers. The transition towards the Maassluis Formation is formed by a regionally traceable clay layer at a depth between -70 and -75 m NAP. Also the Maassluis Formation consists of a mixture of sand and clay layers (Figure 4-1).

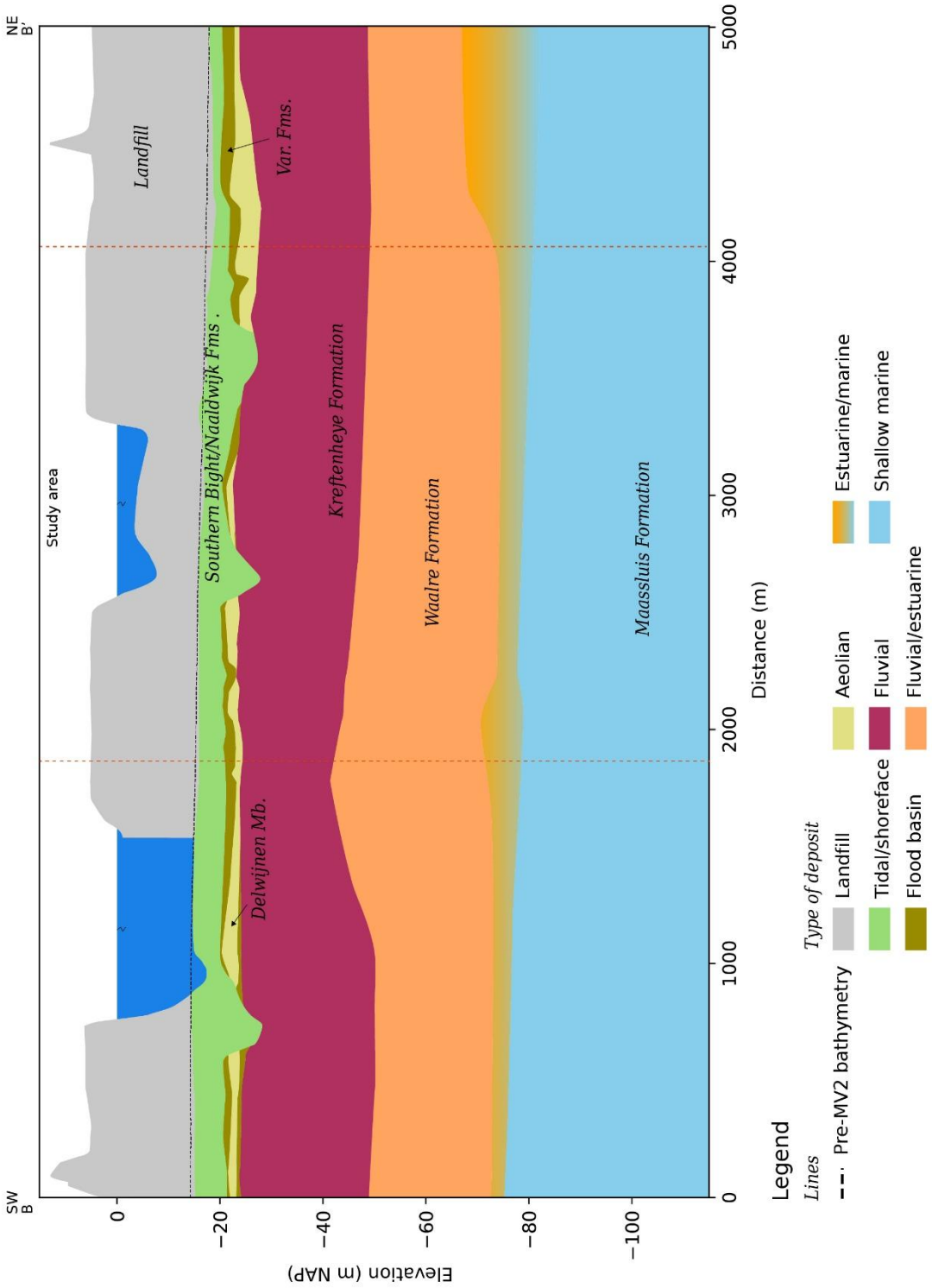

Figure 4-1 Southwest-northeast interpreted cross-section (B-B') for the wider MV2 site (for location see Figure 2-1; red dash lines indicate the part that will potentially host a NPP. The cross-section is based on the available CPTs, boreholes and gamma logs, in combination with expert knowledge about the local geological setting. Note that the provided cross-sections are based on an interpretation of the currently available data. When new data becomes available, these cross-sections should be updated. The top of the landfill lies around 5 m NAP. For unknown reasons some CPT's start at nearly 10 m NAP, suggesting those CPT's should be treated with caution. A version including all lithologies from CPTs, boreholes and gamma logs is provided in Appendix B.1.

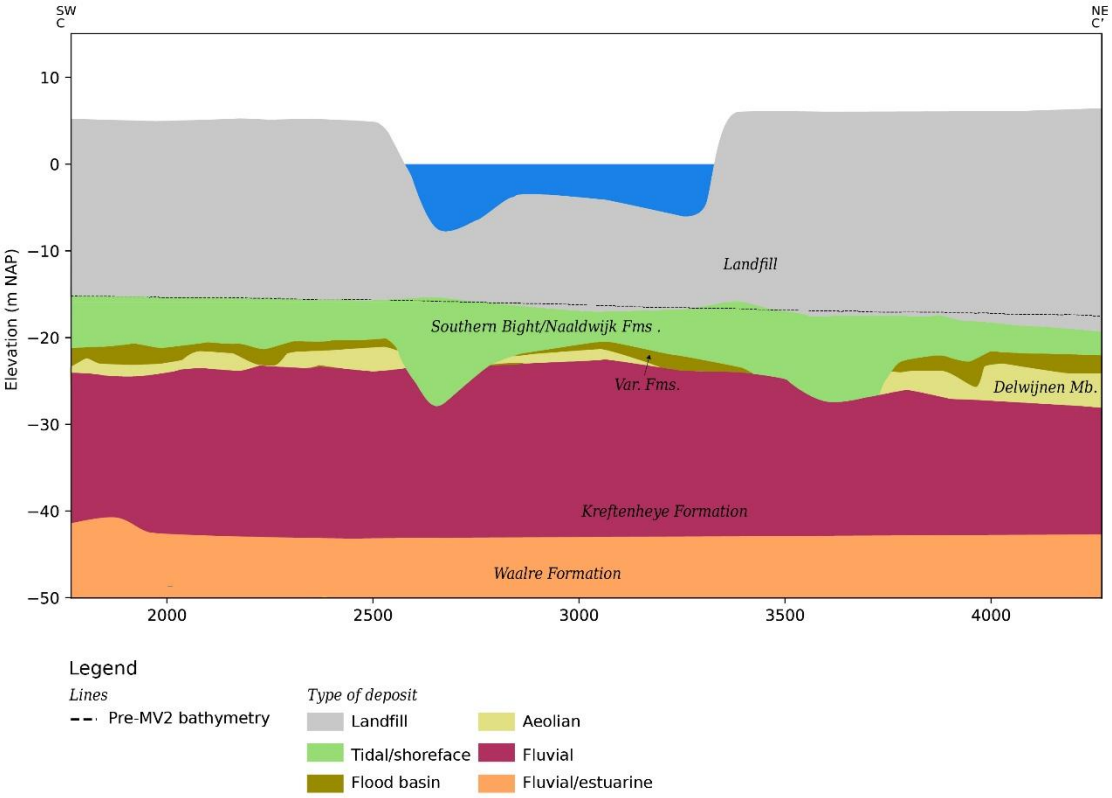

Figure 4-2 Southwest-northeast interpreted cross-section (C-C'), showing the build-up of the subsurface at the MV2 site location in more detail (see Figure 2-1 for location). The cross-section is based on the shown CPT's and boreholes, as well as gamma logs K2 and W2, in combination with expert knowledge about the local geological setting. Note that the provided cross-sections are based on an interpretation of the currently available data. When new data becomes available, these cross-sections should be updated. A version including all lithologies from CPTs, boreholes and gamma logs is provided in Appendix B.2.

5 Geohydrological site characterization

5.1 Geohydrological characterization based on REGISII

The Dutch national geohydrological model REGISII is used to provide a basic overview of the geohydrological conditions at the near surroundings of the project area. In Figure 5-1 a northeast-southwest geohydrological REGIII cross-section is shown. Note that the naming of the geological formations in REGISII differ for the upper part since in REGISII all Holocene deposits are grouped into one “complex” unit (NUHlc).

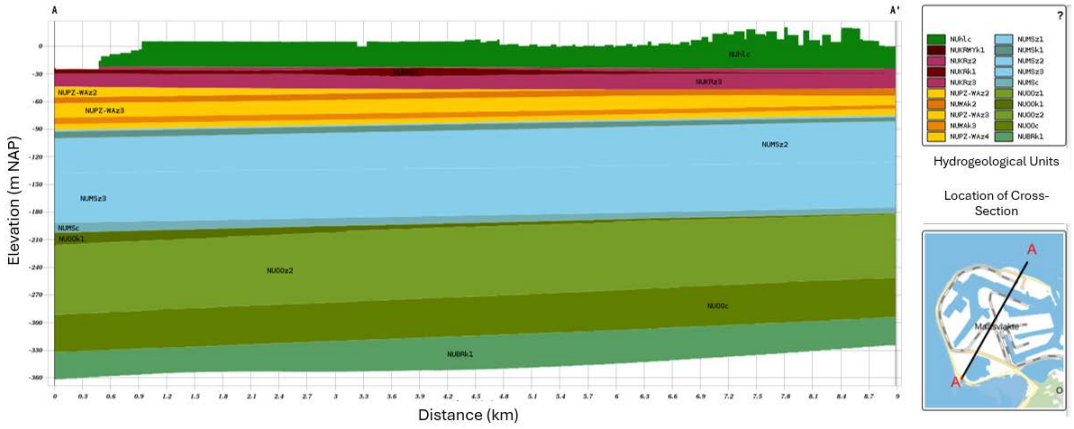

Figure 5-1. Northeast-southwest geohydrological profile based on the model REGISII, it closely represents the geohydrological characterization at the project area, as the area of interest is 2km west of the line A-A'.

As chapters 3 and 4 show, the Holocene unit is approximately 25 m thick and consists of an anthropogenic landfill on top of sand, clay and peat layers. REGISII doesn’t provide any information about permeability for this whole unit, but since it consists of a complex mix of different lithologies, the permeability will vary considerably in both lateral and vertical direction. Below this unit, the coarse sandy layers of the Kreftenheye formation (NUKR* in Figure 5-1) are present that include a single clayey layer at the top, at most places separating aeolian dune deposits from the fluvial deposits. The Kreftenheye formation is approximately 20 meters thick in total and horizontal permeability values are estimated to lie between 25-100 m/d. The anisotropy of this layer has been studied on a national scale, with a median value of 3 and an estimated range of 1.2-4.5 (Fugro et al., 2020). The transmissivity for this aquifer is 625-1300 m^2/d and the intermediate clayey layer has a vertical resistance of 100-500 days and can be assigned to be the first significant aquitard. In REGISII this aquitard has an average thickness of 5 meters, but Figure 4-2 shows its thickness has a maximum of 1-2 m and that it is locally dissected by younger tidal channels.

The underlying Waalre Formation (labelled as NUPZ-WA* in REGISII) is characterized by three aquifers separated by aquitards with vertical resistances of 100-1000 days. These aquitards are also visible in Figure 4-1 and Appendix B.1, but the boreholes seem to suggest more variation in thickness and depth than the REGISII-model indicates. The aquifers have intermediate permeability values of 5-10 m/d whereas the lowest part of the aquifers has slightly higher values of 10-25 m/d. The transmissivity of this aquifer is 100-200 m^2/d.

Around -80 m NAP a several meter thick aquitard separates the aquifers from the Waalre and the Maassluis Formations. The Maassluis aquifer (NUMS*) is around 100 m thick and has a maximum overall permeability of 10 m/d. The transmissivity is estimated to 350-700 m^2/d.

The lower part of the aquifer is a complex mix of sand, clay and organic materials that introduces a vertical resistance of 100-500 days. Underneath this complex, there is thin glauconite sandy layer (less than 0.5 meter) of the Oosterhout formation (NUOO*) before a significant aquitard emerges from that same formation with a vertical resistance of 100-500 days. Below this aquitard the lower most aquifer starts with a thickness of maximal 125 meters up to –320 meters NAP. The lower part of this aquifer is a complex of different materials that generates 500-1000 days resistance and a horizontal permeability of 1m/d. The geohydrological base is set at a depth of –320 meters NAP as the low permeable Breda Formation (NUBRk1) begins.

In Table 5-1, the overall geohydrological representation of the Maasvlakte site is shown, representing the center of the cross-sectional line in Figure 5-1.

5.2 Available data for geohydrological site characterization

The Dutch Geohydrological Model (LHM) simulates groundwater levels from 1970 up to 2022 on a daily base. The resolution is 250 x 250 meter and it serves therefore to simulate regional conditions rather than local ones. Nevertheless, the LHM is suitable to give insights in regional geohydrological conditions that might initiate local studies in the future that also take the presence of aspects like sheet piles and quay walls into account. There are two major modifications necessary to simulate MV2 correctly. The first is to include the latest topography of the Maasvlakte and the second is to add the effects of density differences between fresh and salt water.

The latest LHM version represents the Maasvlakte as present in 2000 (Slufter phase). The project area is therefore not yet an active part of the groundwater-flow model. The model has been adjusted to represent the current situation at the Maasvlakte. Therefore, the latest Digital Terrain Model of The Netherlands (https://www.ahn.nl/) was used to modify the upper boundary of the LHM, see Figure 5-2.

Table 5-1 Overall geohydrological representation of the Maasvlakte at x=60232; y=443353 (RD). Kh=horizontal permeability and Kv=vertical permeability.

Layer	Geohydrological unit	Lithology	Formation name	Top [m NAP]	Bottom [m NAP]	Kh [m/d]	Kv [m/d]
1	Phreatic aquifer	Variable	NUHlc	5	-22	-	
2	Aquifer	Fluvial sand	NUKRz2	-22	-24	25-50	8.3-16.5[$]
3	Aquitard	Clay	NUKRk2	-25	-30		0.01-0.05
4	Aquifer	Fluvial Sand	NUKRz3	-30	-46	50-100	16.5-33.5[$]
		Sand	NUPZ-WAz2	-46	-50	5-10	
5	Aquitard	Clay	NUPZ-WAk2	-50	-57		0.01-0.05
6	Aquifer	Sand	NUPZ-WAz3	-57	-72	5-10	
7	Aquitard	Clay	NUPZ-Wak3	-72	-79		0.01-0.05
8	Aquifer	Sand	NUPZ-Waz4	-79	-84	10-25	
		Glauconite Sand	NUMSz1	-84	-86	5-10	
9	Aquitard	Sandy Clay	NUMSk1	-86	-93		0.001-0.005
10	Aquifer	Coarse sand	NUMSz2	-93	-130	5-10	
		Coarse sand	NUMSz2	-130	-185	5-10	
11	Aquitard	Complex	NUMSc	-185	-192	2.5-5	0.001-0.005
		Glauconite Sand	NUOOz1	-192	-193	5-10	
		Clay	NUOOk1	-193	-198		0.001-0.005
12	Aquifer	Glauconite Sand	NUOOz2	-198	-275	5-10	
13	Aquitard	Glauconite complex	NUOOc	-275	-317	1	0.005-0.01
		Glauconite sand/clay	NUBRk1	-317	-354		0.001-0.005

[$]Kv is estimated using anisotropy factors of 1.4 for aeolian sand and 3 for fluvial sand of the Kreftenheye Formation, rounded to halves. The anisotropy factors are taken from Fugro et al. (2020).

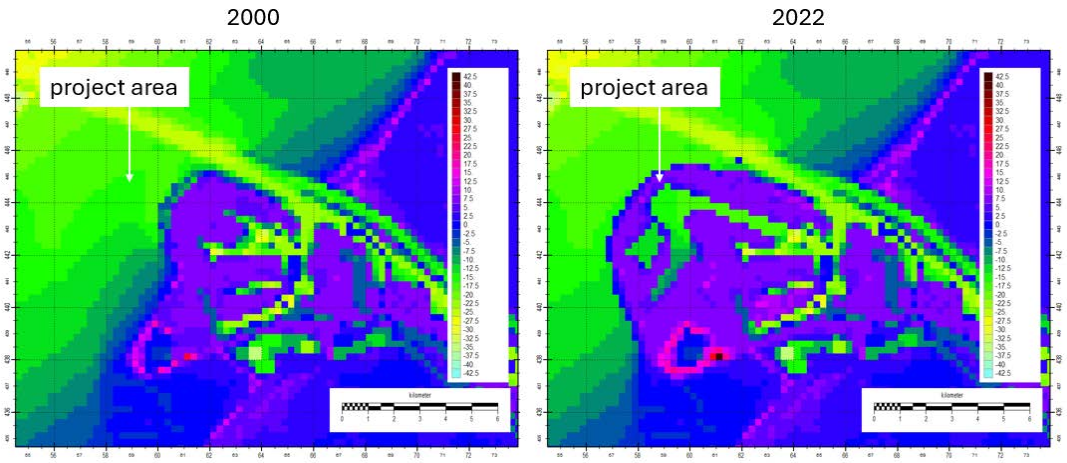

Figure 5-2 The upper boundary (elevation in metres above NAP) of the situation in 2000 as represented in the current LHM (left), and this boundary after adjustment to reflect the current situation (right)

The landfill itself is a complex mixture of sand, sandy-clay, clayey-sand and clay. As the landfill is discretized as a single layer in the LHM, it is common to compute a harmonic mean (natural-logarithm) for permeability, instead of an arithmetic mean. The permeability of this reclaimed land was therefore set to the average value of sand (Kh=100 m/d) and clay (Kh=0.01 m/d), yielding ½LN(100)+½LN(0.01) yielding an average permeability for the landfill of ~1.0 m/d, see Figure 5-3. The surrounding North-Sea and harbours are modelled with a fixed water level of 0 m NAP. The existence of sheet piles along MV2 is not present in the model. They can have an effect in case they completely block the landfill in all directions toward the sea and have a significant resistance. Currently, both of these are unknown. The groundwater recharge is set to 0.55 mm/d and is derived as average value from a long-term simulation with the LHM including unsaturated flow. It depends on the actual paved and built-up areas which might increase or decrease the nett recharge. Drainage is absent as it is not active due to low groundwater levels of more than 3 meter below surface level.

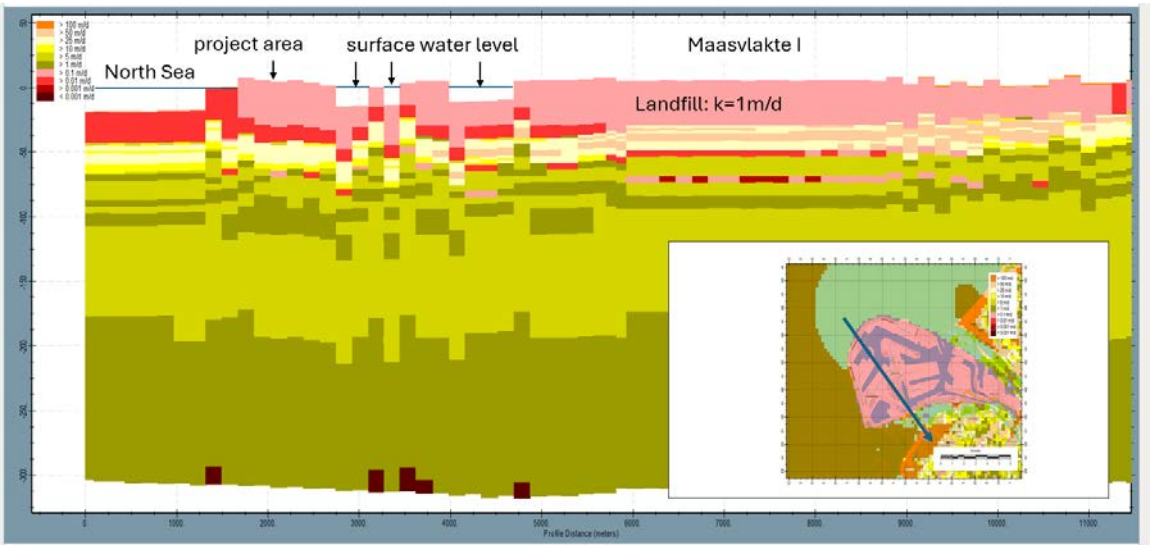

Figure 5-3 Cross-section of the conceptual model adapted from the LHM 4.3.3

5.3 Hydraulic conductivities based on the pumping tests

Nearby MV2, a pumping test was conducted (Rijksinstituut voor Drinkwatervoorziening, 1969), see Figure 5-4. The pumping test was carried out to determine the required dewatering capacity for draining an excavation pit in preparation for the construction of a

dock. The excavation pit needed to be dewatered to a depth of -16 m NAP. It was decided to conduct two separate pumping tests: one in a connected Holocene/top Pleistocene aquifer unit until -26 m NAP (analogous to Various Formations, see Figure 4-1) and one in the Pleistocene aquifer unit below (Kreftenheye Formation). A total of nine observation wells were installed. The borehole logs clearly indicate the presence of a first and second aquifer, separated by layers of clay and peat. Based on current knowledge of the subsurface structure, the pumping test involves dewatering from aquifer units NUHlc/KRz1 and KRz2, which are separated by the clayey deposits of KRk1. This confining layer is schematized at a depth of approximately -26 m NAP during the pumping test. The hydraulic soil parameters were determined based on two pumping tests. The transmissivity of the first aquifer was determined to be 90 m^2/day, and that of the second aquifer was 690 m^2/day. According to REGISII these values should lie between 75-150 m^2/d and 800-1600 m^2/d for the first and second aquifer, respectively. The pumping test also provided the leakage factor, which is a parameter determined by the vertical resistance above and below the aquifer. It is expressed as $\lambda = \sqrt{(k \cdot c)}$, where *k* is the hydraulic conductivity and *c* is the vertical resistance. The leakage factor (λ) was calculated to be 140 m for the first aquifer and 300 m for the second aquifer. When converted back to vertical resistance (c), this corresponds to approximately 130 and 217 days, respectively. From REGISII these values are in between 100-500 days and 140-700 days for the first and second aquifer. The results from the pumping test thus match reasonably well with the parameter values from REGISII.

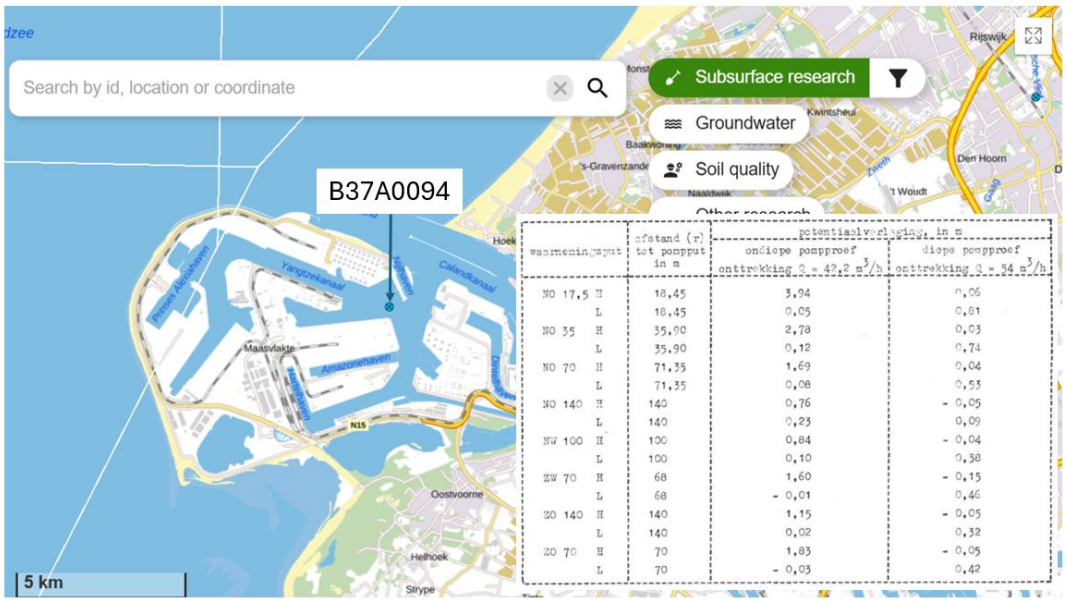

waarnemingput	afstand (r) tot pompput in m	potentiaalverlaging, in m: ondiepe pompproef onttrekking Q = 42,2 m³/h	diepe pompproef onttrekking Q = 54 m³/h
NO 17,5 H	18,45	3,94	0,06
L	18,45	0,05	0,81
NO 35 H	35,90	2,78	0,03
L	35,90	0,12	0,74
NO 70 H	71,35	1,69	0,04
L	71,35	0,08	0,53
NO 140 H	140	0,76	- 0,05
L	140	0,23	0,09
NW 100 H	100	0,84	- 0,04
L	100	0,10	0,38
ZW 70 H	68	1,60	- 0,15
L	68	- 0,01	0,46
ZO 140 H	140	1,15	- 0,05
L	140	0,02	0,32
ZO 70 H	70	1,83	- 0,05
L	70	- 0,03	0,42

Figure 5-4 Location of the pumping test near MV2.

5.4 Groundwater level monitoring

Public available information on measured piezometric levels is available through www.DINOloket.nl and https://www.grondwatertools.nl/gwsinbeeld/. The closest monitoring well is located at respectively 4.0 km southeast from the project area (GMW000000038090), see Figure 5-5 and Table 5-2. The most recent hydraulic head data for GMW000000038090 is from January 2025. The data is split into two separate timeseries (GLD000000082379 from February 16th 2019 until December 7th 2020, and GLD000000082380 FROM January 4th 2021 until January 29th 2025).

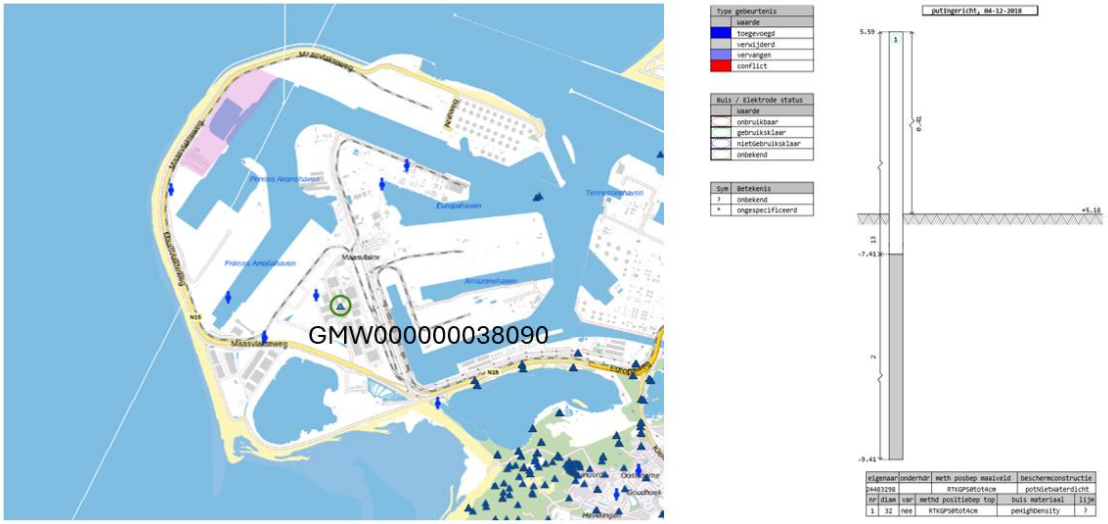

Figure 5-5. Locations of the monitoring well near MV2.

Table 5-2. Locations of the monitoring well near MV2.

Monitoring well	RD-X	RD-Y	Elevation Top well	Number	Top filter	Bottom filter	Data range	
	[m]	[m]	[m NAP]		[m NAP]	[m NAP]	Start measurement	End measurement
GLD82379	60726	440276	5.59	001	-7.41	-9.41	16-02-2019	07-12-2020
GLD82380	60726	440276	5.59	001	-7.41	-9.41	04-01-2021	29-01-2025

At a monitoring depth of -7.41 m NAP in GLD000000082379, the hydraulic head fluctuates seasonally between values of approximately 1.2 and 1.6 m NAP (Figure 5-6). Some significantly lower values of less than 0.8 m NAP appear in the beginning of 2021. Possibly this is caused by temporary extraction activities for construction purposes. The surface level is 5.59 m NAP, which means that the groundwater level (1.3 m NAP) is on average 4.3 m below surface level.

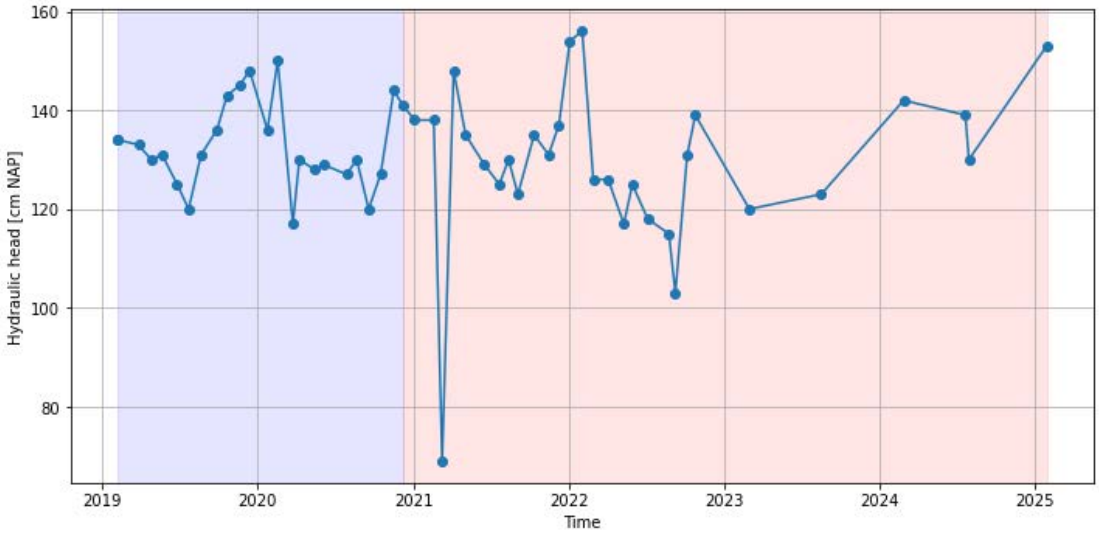

Figure 5-6. Measured piezometric head southeast of project area in GMW000000038090. The heads are measured from depths of 741 cm -NAP (purple=GLD000000082379 and red=GLD000000082380).

Based on the dataset of GMW000000038090, the measurement intervals are too low to compute reliable average highest, lowest and spring groundwater levels. From the Dutch National Groundwater Flow model (LHM) an indication is computed at this location, see next section.

5.5 Modeled Groundwater situation

Groundwater levels at MV2 are largely influenced by density contrasts in the groundwater, as fresh water (<1g/l) floats on top of salt/brackish water (>1g/l). These effect are not accounted for in the LHM model. At present, the surface water at MV2 has a density of 16 g/L (saline). A comparison of LHM output with the actual measurements at the nearest monitoring well (GMW000000038090) shows that the LHM underestimates the groundwater level by 1 m and LHM-results need to be corrected. The result of this correction is presented in Figure .

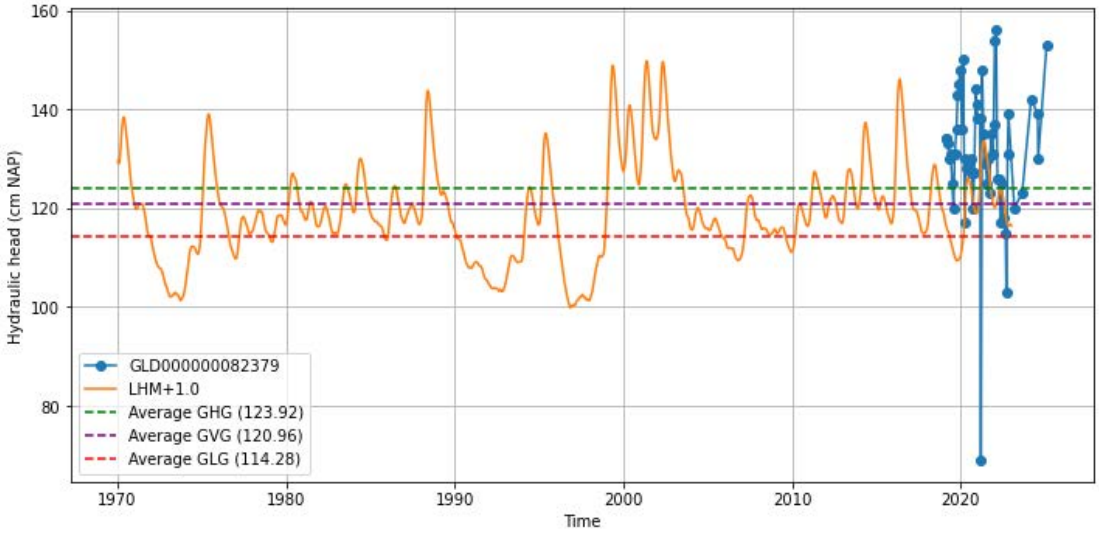

Figure 5-7 Timeseries of the corrected results from the LHM for density compared to the monitoring well GMW000000038090. The dotted lines are the mean average high (GHG) and low (GLG) levels.

LHM simulations suggest that the groundwater level at GMW000000038090 fluctuated between ~0.5 and 1.0 m NAP. The first reclamation part of the Maasvlakte started in the

1970s. The model results give a valuable insight in the groundwater-level fluctuations that have occurred since the 1970s. An average highest and lowest groundwater level is estimated for this period at 1.24 and 1.14 m NAP, respectively. The spring groundwater level (GVG) lies at 1.21 m NAP (spring groundwater level is defined as the average at 14th of March, 28th of March and 14th of April). The simulation results clearly show known wet (1999-2001) and dry periods (parts of the 1970s and especially the 1990s). On top of these large-scale fluctuations, a yearly cycle with 0.1-0.2 fluctuations is present. This means that the average groundwater fluctuation between seasons is about 0.15 m, but over the years groundwater level can fluctuate up to values of 0.5 m.

The project area is ~4 km from the above mentioned monitoring well. The computed average groundwater level (including the effect of density) is given in Figure 5-8. At the project area the average groundwater level is ~0.8 m NAP and thus ~0.8 m lower than at the monitoring well GMW000000038090. This is i) a logical consequence of the fact that the sea is more nearby than at the location of the monitoring well and ii) it can be caused by higher permeable material in the subsurface. Since surface levels are approximately 5 m NAP, the average groundwater level lies well below the surface and there is not a direct risk for groundwater flooding and/or groundwater disturbance. A more detailed modelling of the subsurface would improve the predicted groundwater level as local phenomena as continuous clayey deposits might interrupt vertical groundwater flow and cause higher groundwater levels than in cases in which those deposits are interrupted or absent.

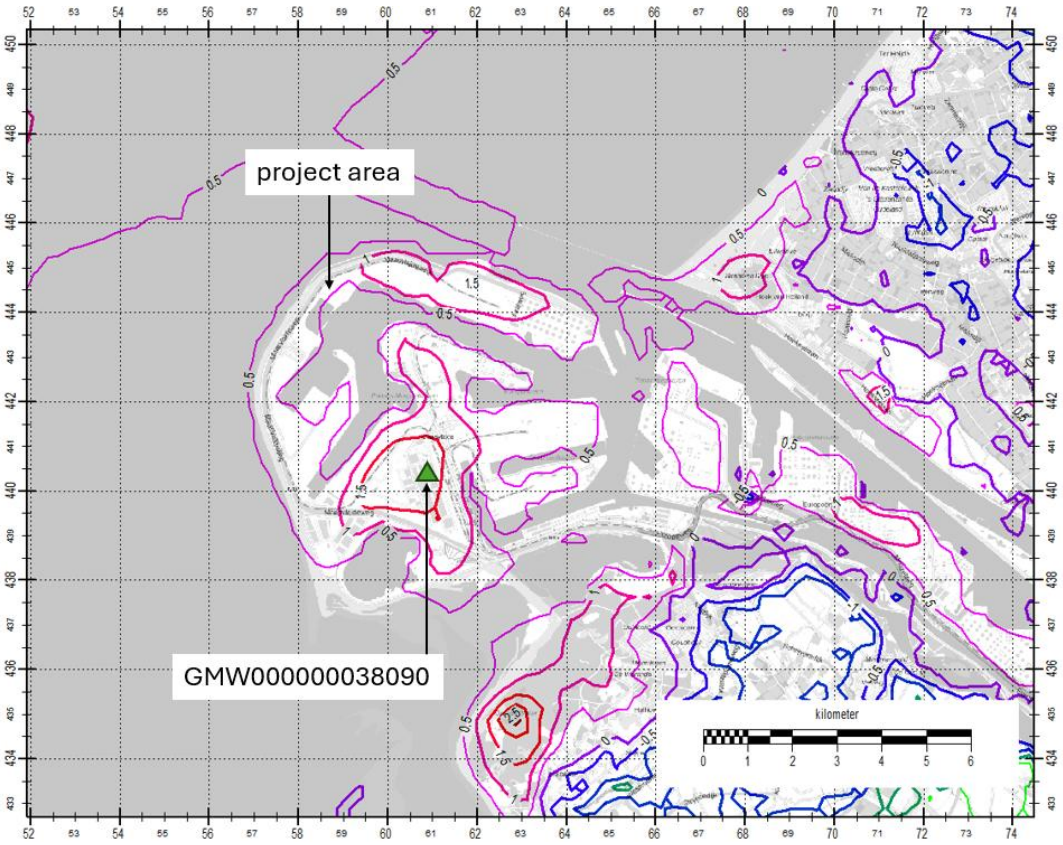

Figure 5-8 Computed average groundwater level (m NAP) with the modifed LHM model and including effects of density.

Since the land reclamation the subsuface has been saturated with this high-density saline water. Over time, groundwater recharge from excess precipitation can gradually displace this saline water, and form a freshwater lens. Whether this occurs depends on the type of land use which allows groundwater to recharge. Also, local drainage systems and/or permeability

of the subsurface influence this process. The higher the groundwater level is allowed to raise, the larger this freshwater lens can develop. As freshwater has a density of 1000 kg/m^3 and salt water 1024 kg/m^3, according to the Ghyben-Herzberg-principle the ratio between both specifies the depth of the fresh-salt interface, thus the interface should be at 1000/(1025-1000)=40 m depth. This is a statistical approach and does not accommodate for local distortions of this relationship such as permeability distributions, boundary conditions etc. Also it does not quantify how this freshwater lens evolves in time, a model is needed to do that. Generally it takes 10-20 years to freshen the first 5 meter of the subsurface, another 20-30 years to freshen the next 5 meter and an additional 50 years to double the fresh water lens. For the Maasvlakte, which was reclaimed in 1970 and was initially saline, it took approximately 50 years for a well-developed freshwater lens to form in some areas. As of 2020, the core of the island in many locations was still brackish to saline (>1 g/l). For the current adjusted model of the LHM, that includes density, the development of a freshwater lens is computed for the entire Maasvlakte as it is nowadays. The simulation starts at 2020 to indicate the start of MV2. The subsurface is at that stage completely saturated with salt water (16g/l). From that moment onwards the model ran up to 2045 (25 years of simulation). It has been assumed there is a constant average surplus of precipitation (1 mm/d) that recharges the landfill with fresh water. The development of the freshwater lens underneath the project area is given in Figure 5-10. The current situation (2025) after 5 years of refreshing the subsurface at the project area is still brackish (1.5 g/l). In 2035 it becomes fresh and in 2045 the upper part of the groundwater body in the entire Maasvlakte area could be fresh.

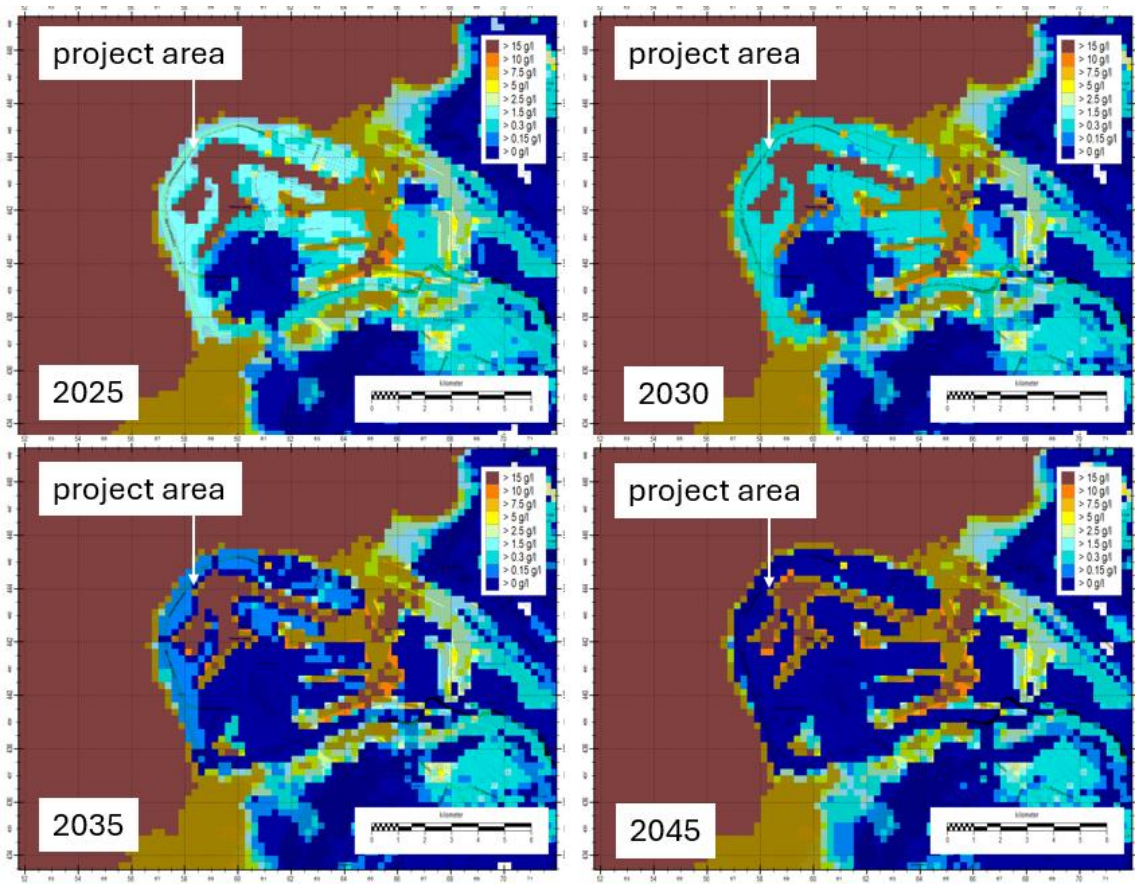

Figure 5-9 Simulated salt concentration of the groundwater level for 2025, 2030, 2035 and 2045 in autonomeous conditions.

The depth over time of this freshwater lens for different salt concentrations is shown for a location at the project area in Figure 5-10. The southern part of the Maasvlakte, that was developed in the 70s, is fresh already up to greater depth, see the cross-section in that figure.

The computed thickness is ~60 meter and coincides more-or-less with an average groundwater level of 1.5 m NAP. At the project area, the depth of the fresh water interface (0.15 g/l) is at ~6 m-NAP in 2045. The increase of depth seems a linear process but will flatten to an equilibrium when times continues. The estimated maximal depth of the freshwater lens is ~30 – 40 m based on the Ghyben-Herzberg-principle. This takes into consideration a groundwater level of 0.5 – 1.0 m NAP, as simulated with the LHM with density. It depends on the rate of recharge, subsurface heterogeneity, construction activities with or without drainage whether this freshwater lens declines or increases.

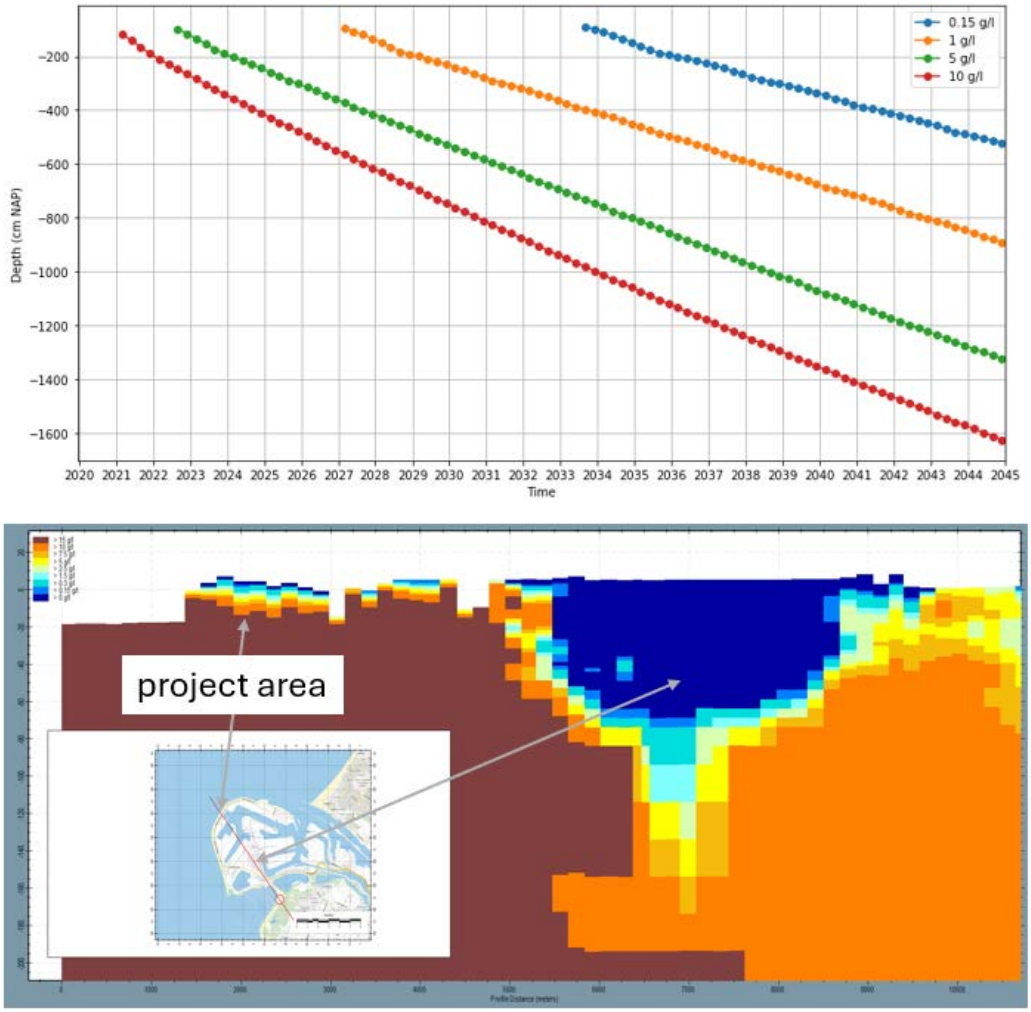

Figure 5-10 (top) Computed increase of the depth of different salt concentrations at the project area; (bottom) cross-section of the Maasvlakte showing the salt-concentration in depth for 2045.

6 Geotechnical parameters

6.1 Subdivision project area

For the geotechnical analysis, the geological model (as explained in Chapter 4) has been divided into three subareas. In the southwestern and northeastern parts the landfill have been raised to a level of approximately NAP +5 m. The centre section is not yet fully filled in. Figure 6-1 repeats the previously shown cross section highlighting the subareas. Section 6.1.1 to 6.1.3 describe the three subareas and section 6.1.4 provides an overview of the representative cross sections.

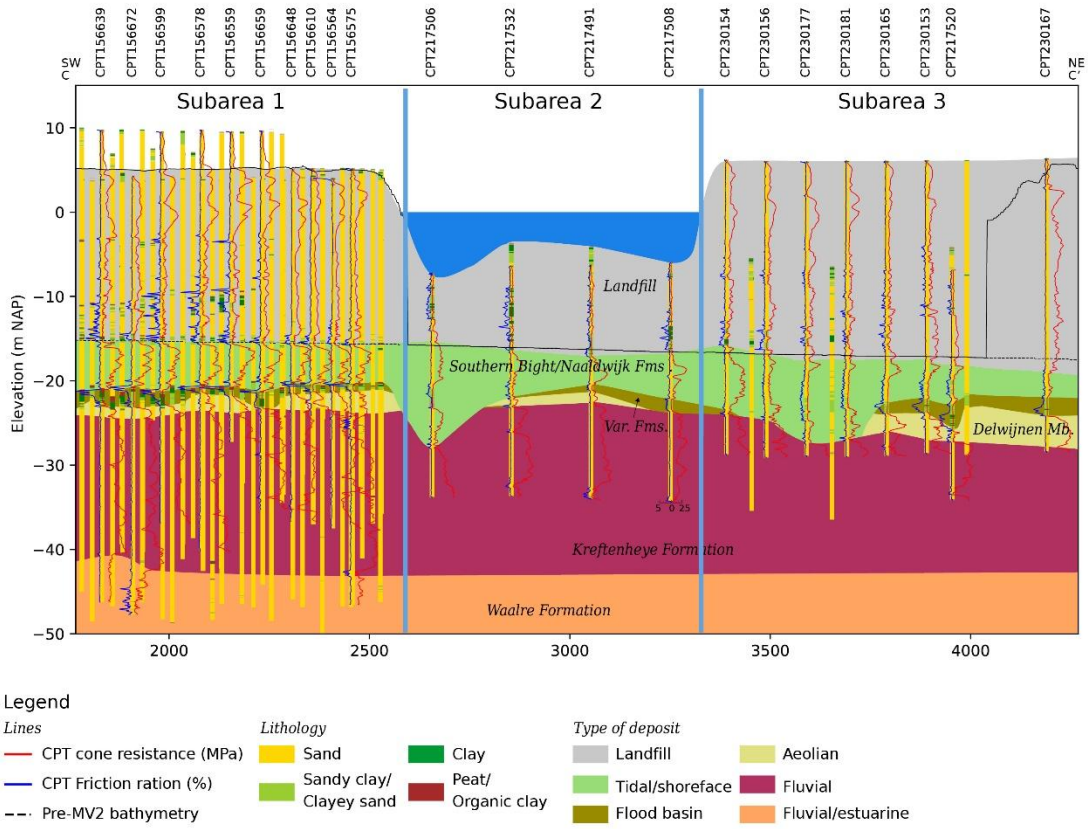

Figure 6-1 Geological cross-section (Figure 4-2) highlighting the three subareas used for geotechnical characterisation.

In Figure 6-2 the locations of the CPTs used to determine the geotechnical properties are highlighted relative to the position of the cross section, indicating that the southwestern corner lacks CPT data. Based on the variance in the CPT profiles, it can be expected that the described subsurface profile also represents this southwestern corner, but additional investigation is needed to validate this. Figure 6-3 highlights the ground level and final penetration depth of the CPTs.

Figure 6-2 The cross section line and the location of the used CPT's relative to the cross section.

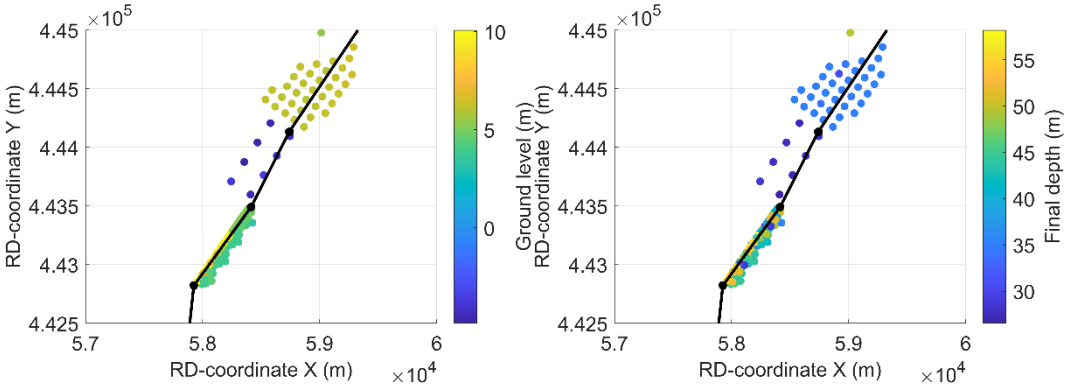

Figure 6-3 The ground level and final penetration depth of CPT's.

Figure 6-4 highlights the geotechnical composition along the entire cross section. The soil classification is based on the classification by Robertson (1990), which has been adjusted by Fugro to the Dutch conditions. The lithologies are determined separately for each CPT in 10 cm depth interval based on (normalized) cone resistance and friction ratio. The automatic procedure then divides the CPTs in intervals with a length of 25 m along the cross section. Within each interval the lithologies over depth are grouped and a distribution of the present lithologies at each depth within each 25 m interval is computed. The profile is coloured according to these percentages. The subareas are described in further detail in the following paragraphs. The used CPTs may be further from the cross section in the perpendicular direction, and the cross section therefore provides an overview of the geotechnical properties of the area.

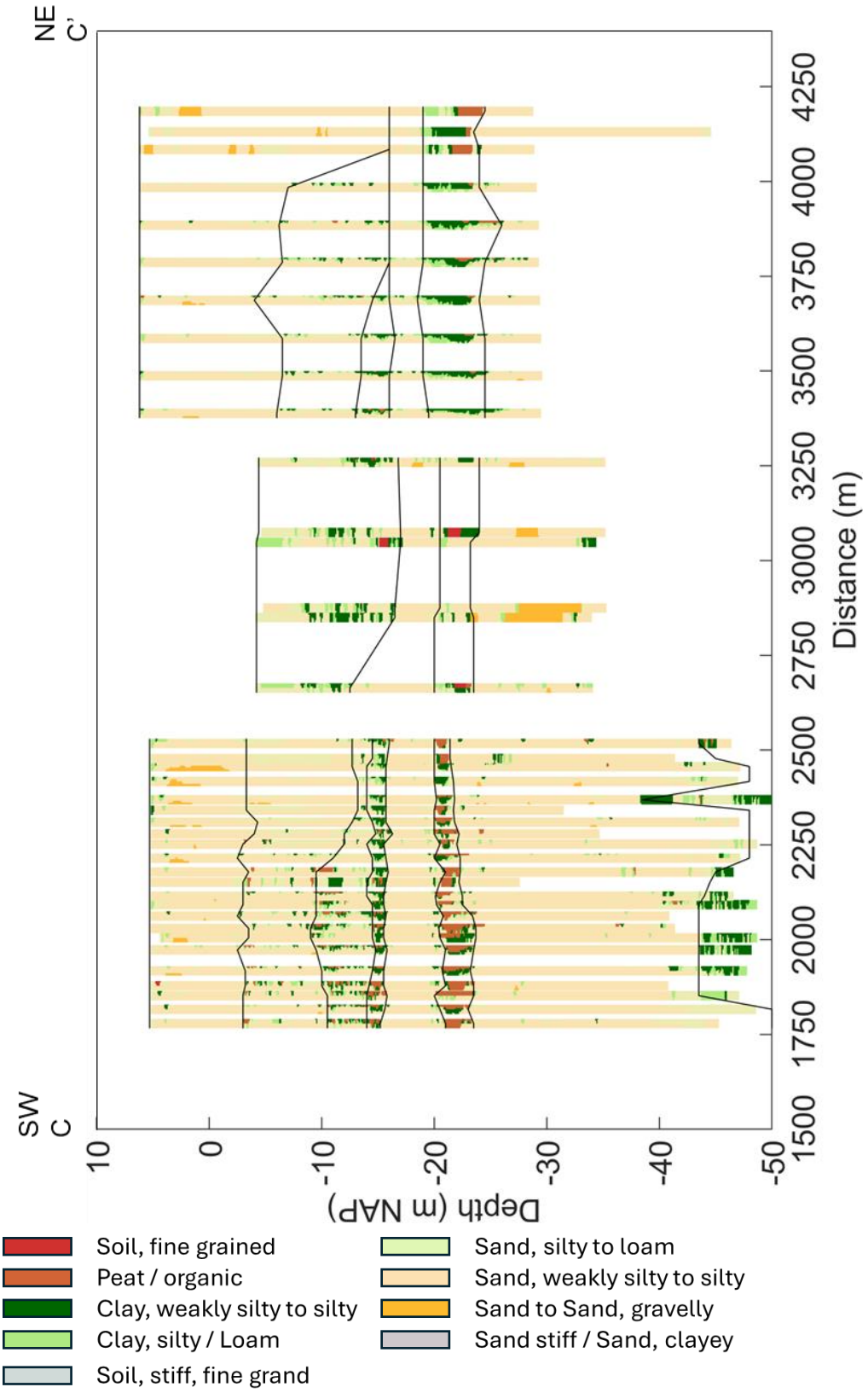

Figure 6-4 The geotechnical lithological classification according to automatic CPT classification. The black lines provide interpreted geotechnical layer boundaries.

6.1.1 Subarea 1 Southwestern landfill

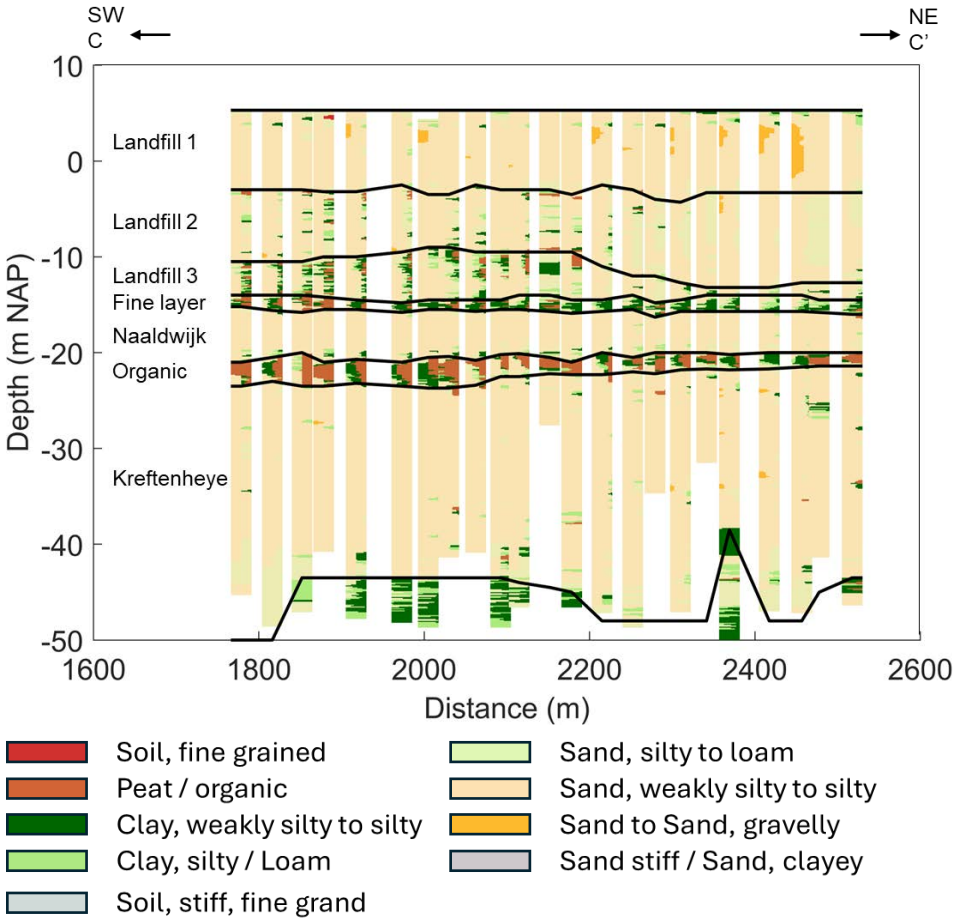

Figure 6-5 The geotechnical lithological classification of Subarea 1 according to automatic CPT classification. The black lines provide interpreted layer boundaries.

Figure 6-5 present the geotechnical cross section for Subarea 1. Figure 6-6 and Figure 6-7 highlight the cone resistance of the CPTs closest to the cross-sectional line. The contour plots are created by assigning the values of the closest CPTs at their position along the cross section and interpolating in between the CPTs. Figure 6-6 and Figure 6-7 provide an indication of the resistance of each layer, and indicate stronger and weaker zones. These plots also provide an overview of the local variation within layers.

Subarea 1 has a landfill layer consisting of sand and silty sand. Some CPTs present a ground level of ~10 m NAP for the landfill, while the height of the area according to LiDAR information is approximately 5 m NAP. There is no offset within the subsurface, indicating that the CPT-data are not shifted. The cause for this discrepancy is unclear. The cone resistance varies significantly throughout the landfill. Halfway through the layer the presence of silt and clay layers increases, and the cone resistance reduces. Therefore the landfill has been subdivided into three layers: a top layer (landfill 1) consisting mainly of sand with a higher cone resistance, a middle layer (landfill 2) with some small clay and sand layers and a reduced cone resistance, and a bottom layer (landfill 3) with a low cone resistance and more fine layers. The amount of fine layers is higher on the left side of the cross section. At approximately -14.5 to -16.0 m NAP the fine-grained sediments become dominant. This fine layer may contain small sand layers.

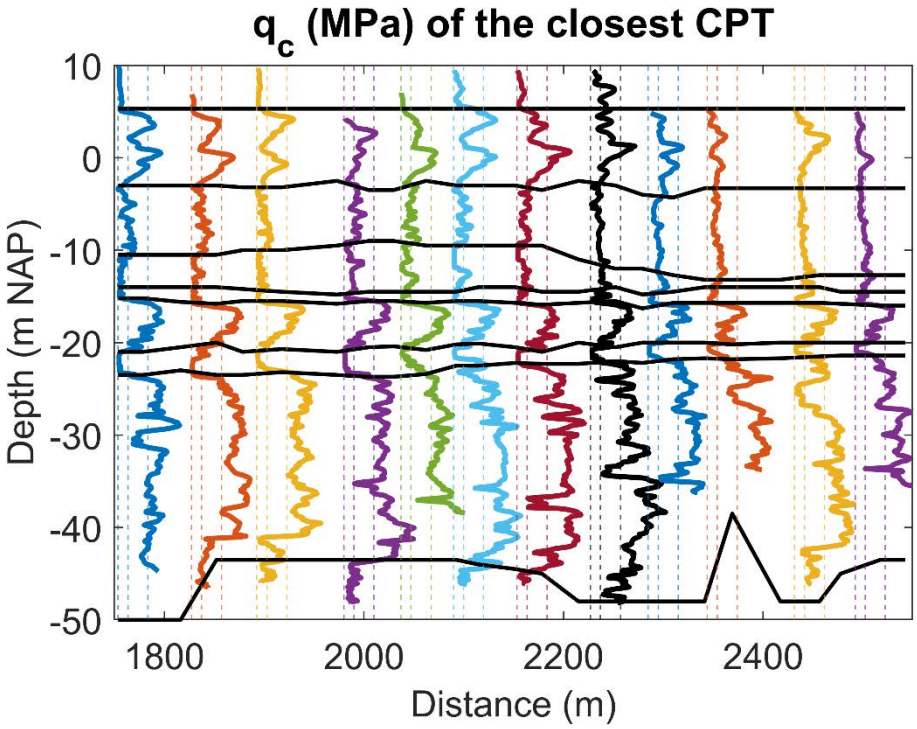

Figure 6-6 The cone resistance of the closest CPT to the cross section line for Subarea 1. For each CPT the dotted lines indicate a cone resistance of 0, 10 and 30 MPa. Due to the large number of CPTs in this subarea only halve of the CPT groups have been shown.

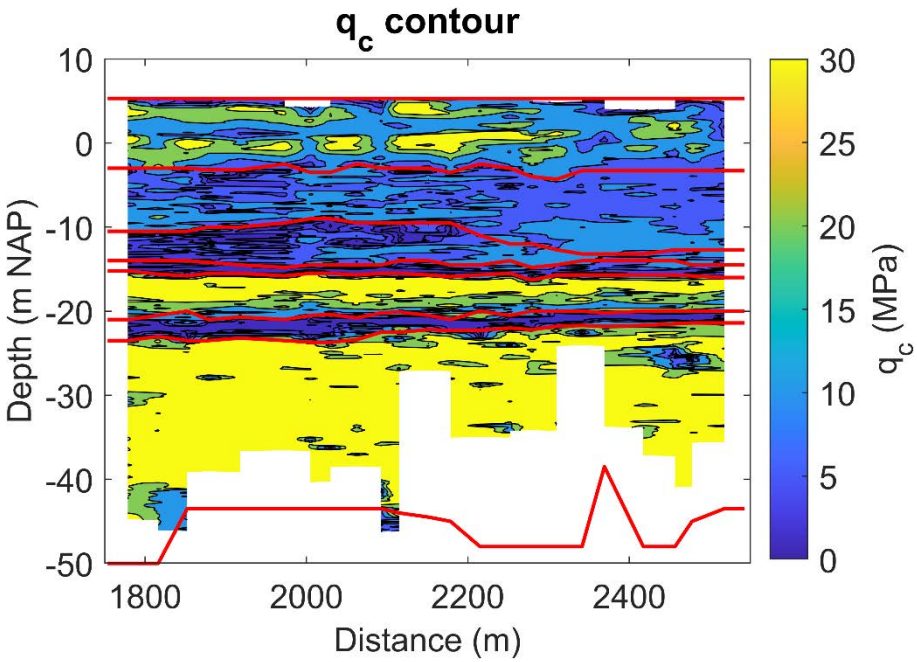

Figure 6-7 A contour plot of the cone resistance of the closest CPT to the cross section line for Subarea 1.

The top of the Naaldwijk Formation is located at a relatively constant depth of approximately NAP -16.0 m. It is a fine sand layer which ends at approximately -20.5 m NAP. The top of the layer has a high cone resistance, which reduces with depth. The sand layer lies on top of a layer of clay/peat layer of approximately 2 meters thick until approximately -23.6 m NAP. The thickness of this clay/peat layer can vary significantly.

The clay/peat layer lies on top of the 20-25 m thick sandy Kreftenheye Formation (that includes the aeolian dunes from the Delwijnen Member). This formation consists of well compacted sands according to the CPTs. The thickness of the Kreftenheye Formation is difficult to judge from the CPTs, but Figure 4-2 indicates its base lies around -42 m NAP.

6.1.2 Subarea 2 Central submerged

Figure 6-8 presents the detailed view of the cross sectional layering of Subarea 2, and Figure 6-9 and Figure 6-10 highlight the cone resistance of the CPTs closest to cross-section line. Compared to the top layer of Subarea 1, the submerged top layer (landfill) of Subarea 2 has a much higher fines content and consist mainly of a mixture of loose silty sand and clay layers. The cone resistance of this layer is low, especially for a sandy layer. Below this top layer at approximately -15 m NAP, the Naaldwijk Formation consists mainly of sand. This is similar to Subarea 1 with a cone resistance of approximately 10 to 20 MPa. The fine layer below the Naaldwijk Formation contains more sandy layers, and is absent in some of the CPTs, which based on Chapter 4 is likely caused by the presence of incised tidal-channel deposits. An impermeable layer might therefore be absent in some parts of this subarea. Similar to Subarea 1, the Kreftenheye Formation starts at a depth of approximately -23.5 m NAP, with somewhat lower cone-resistance values than in subarea 1.

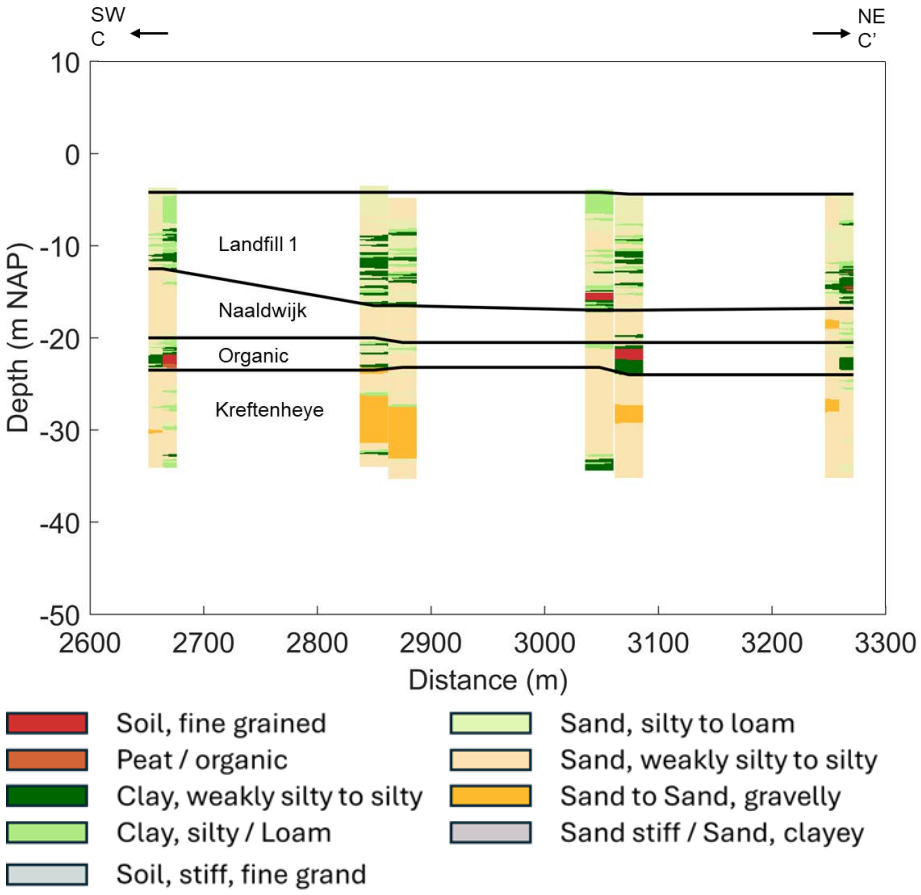

Figure 6-8 The geotechnical soil classification of Subarea 2 according to automatic CPT classification. The black lines provide interpreted layer boundaries.

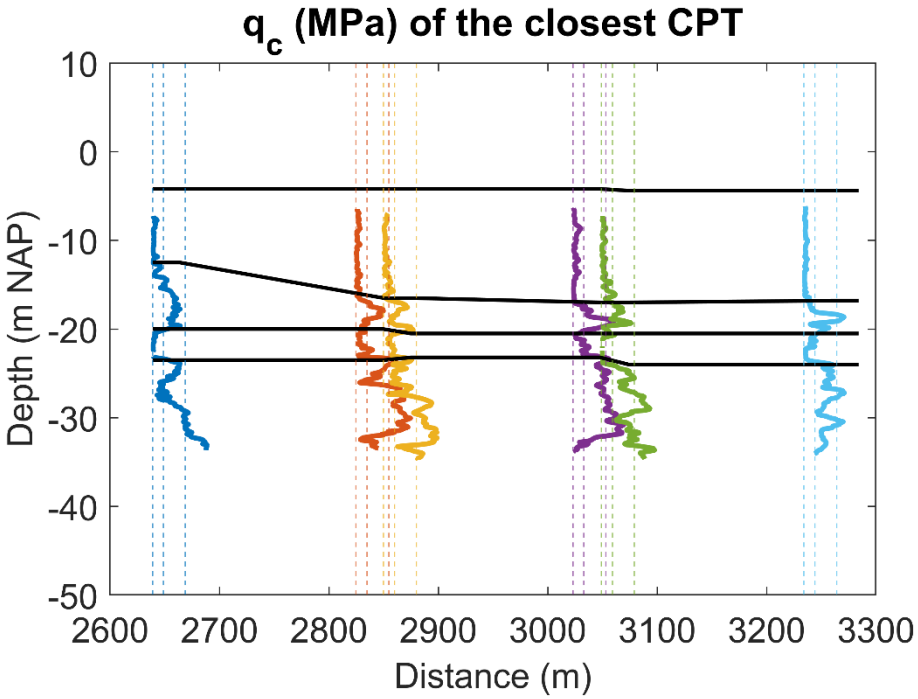

Figure 6-9 The cone resistance of the closest CPT to the cross section line for Subarea 2. For each CPT the dotted lines indicate a cone resistance of 0, 10 and 30 MPa.

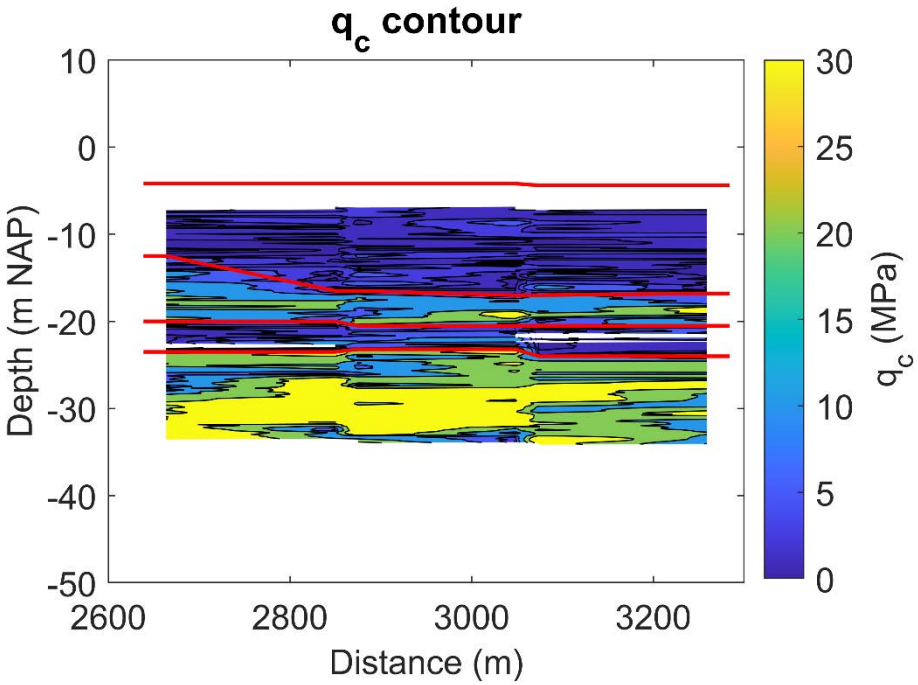

Figure 6-10 A contour plot of the cone resistance of the closest CPT to the cross section line for Subarea 2.

6.1.3 Subarea 3 Northeastern landfill

Figure 6-11 presents the detailed view of the cross sectional layering of Subarea 3, and Figure 6-12 and Figure 6-13 highlight the cone resistance of the CPTs closest to the cross sectional line.

Similar to Subarea 1, the land fill consists of sand and silty sand, with some small clay/silt layers. This landfill has a lower cone resistance compared to Subarea 1. The landfill may be divided into 1 to 3 layers depending on the fine content. A higher fine content is observed on the southwest end of the cross section. On the northeast side of the cross section the thin fine layers are absent, and the cone resistance is relatively high. This indicates a relatively high compaction of the land fill, likely due to the earlier construction, as is evident in the aerial photographs Section 3.2.6. At -13 m NAP a predominantly fine layer is found on the left hand side on top of the Naaldwijk Formation. This is similar to the succession found in Subarea 1. On the right hand side this fine layer is absent, and the landfill is difficult to distinguish from the Naaldwijk Formation.

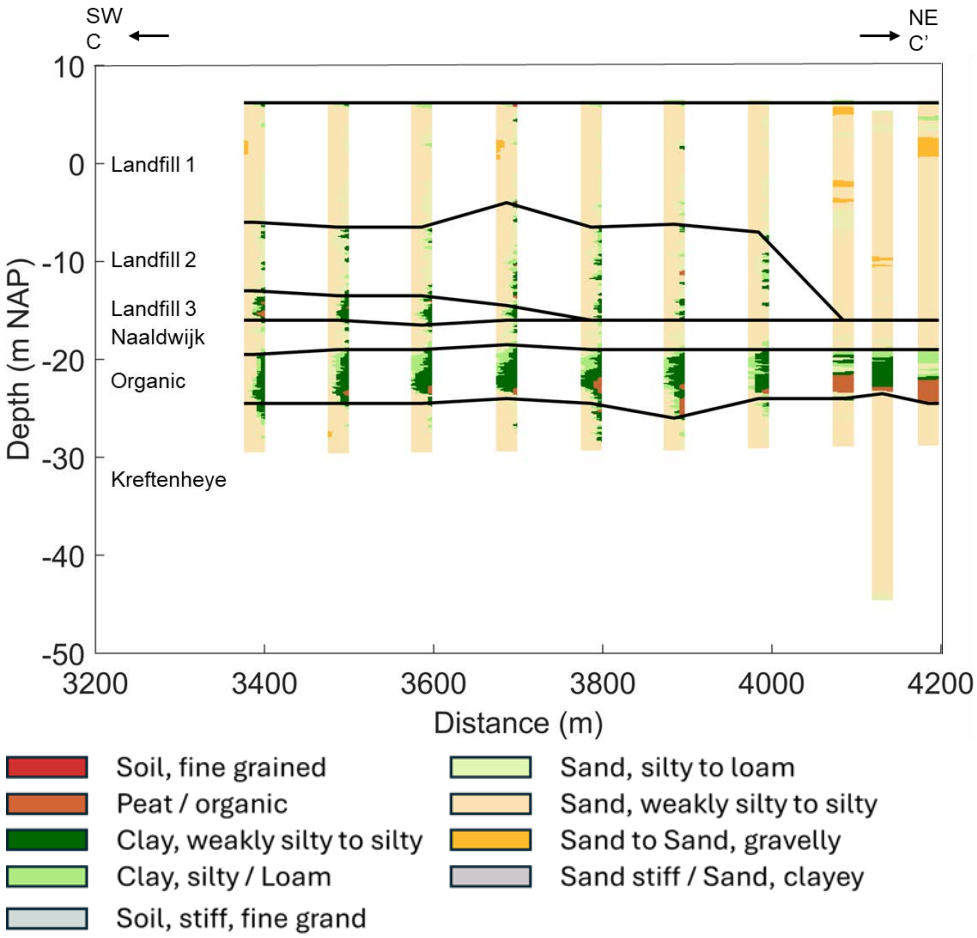

Figure 6-11 The geotechnical soil classification of Subarea 3 according to automatic CPT classification. The black lines provide interpreted layer boundaries.

The sandy Naaldwijk Formation mostly ends higher than in the other subareas at approximately -19 m NAP, and has a lower cone resistance. The thickness of the layer below the Naaldwijk Formation varies significantly, and the fine layer contains many thin sand layers. In some CPTs the fine layer is absent. For the geotechnical profile, the layer divisions indicate the depths where the fine layer may be expected.

Finally, the properties of the sandy Kreftenheye Formation cannot be clearly determined, due to the fact that limited data is available. However, based on the available information at the top of the layer, it is expected that the cone resistance of the layer is comparable to subareas 1 and 2, i.e. between 20 and 50 MPa.

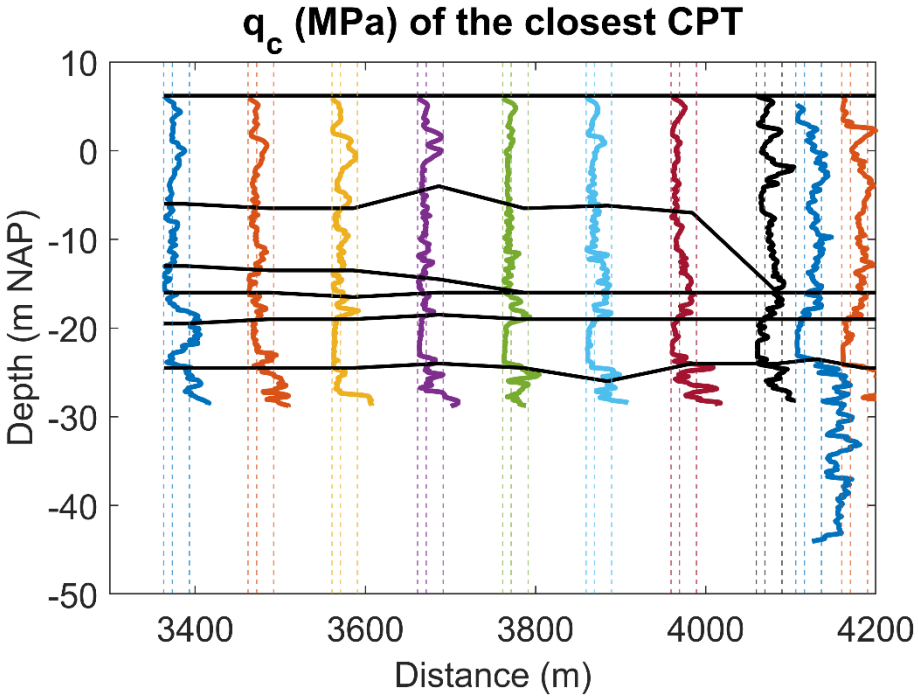

Figure 6-12 The cone resistance of the closest CPT to the cross section line for Subarea 3. For each CPT the dotted lines indicate a cone resistance of 0, 10 and 30 MPa.

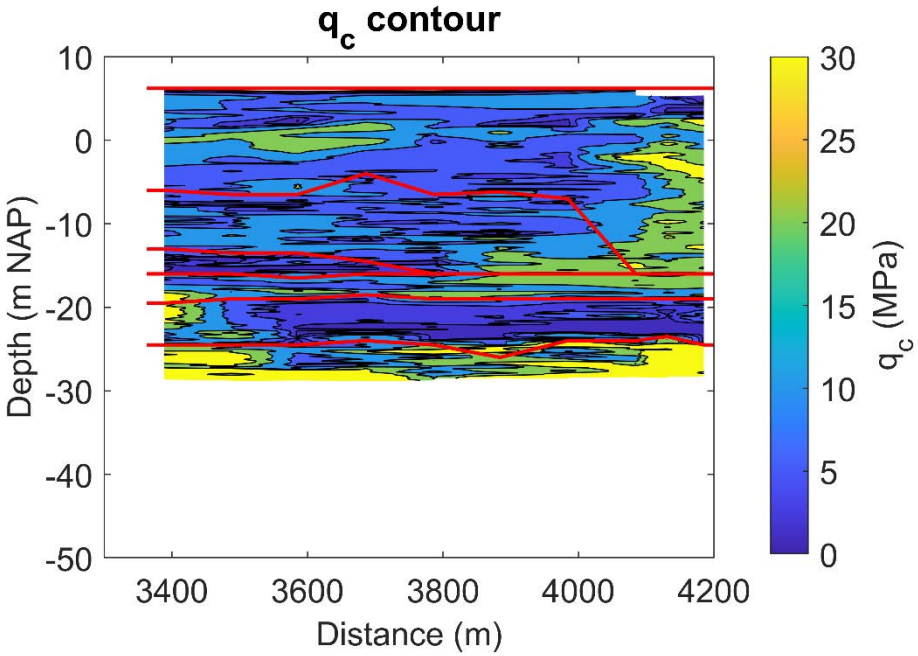

Figure 6-13 A contour plot of the cone resistance of the closest CPT to the cross section line for Subarea 3.

6.1.4 Representative cross sections

Figure 6-14, 6-15 and Figure 6-16 provide schematic representations of the subarea cross sections, providing an indication of the different layers, which can be used in the current design phase. Note that the layer boundaries of the land fill are vague, and that the organic layer may be absent in specific locations. This must be further quantified in later stages of the design process. The used layer boundaries have been provided in Appendix C.1.

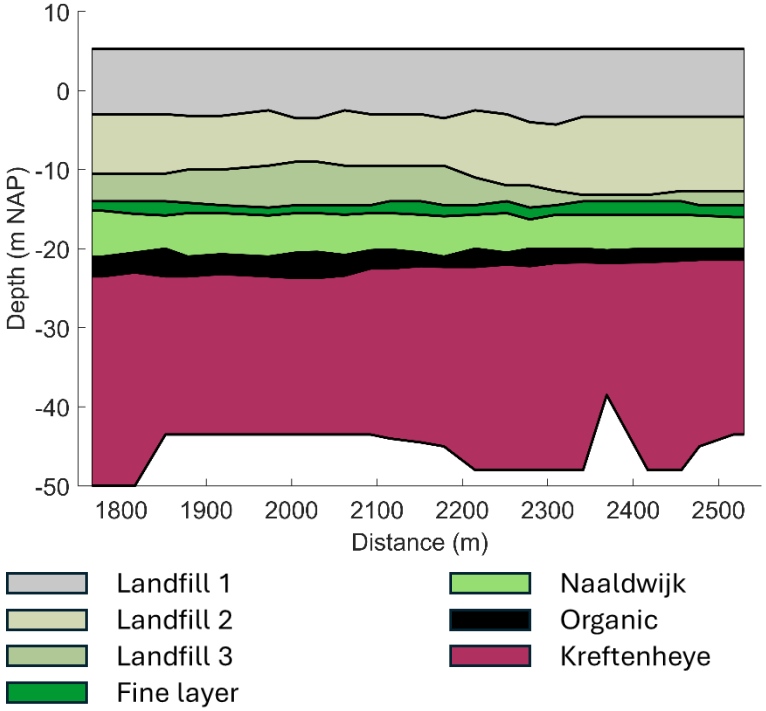

Figure 6-14 Representative geotechnical cross section for Subarea 1

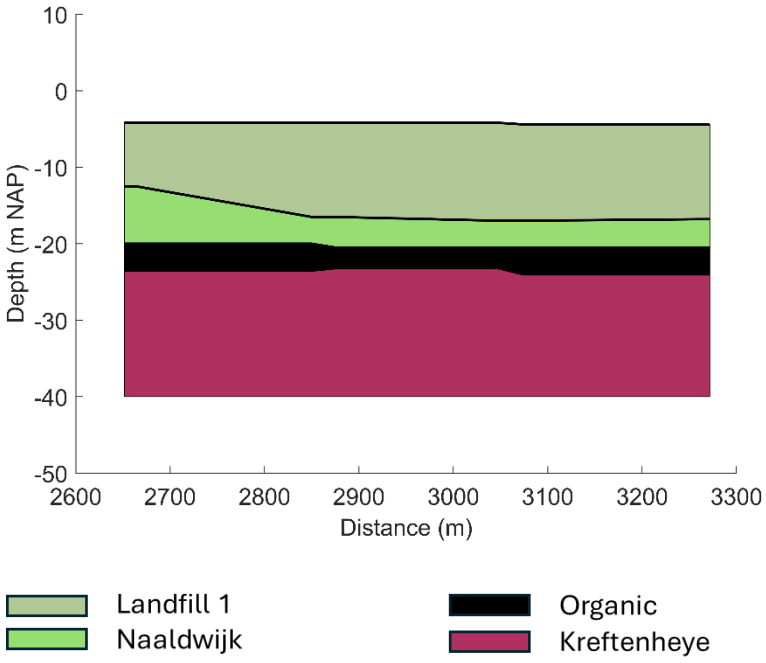

6-15 Representative geotechnical cross section for Subarea 2

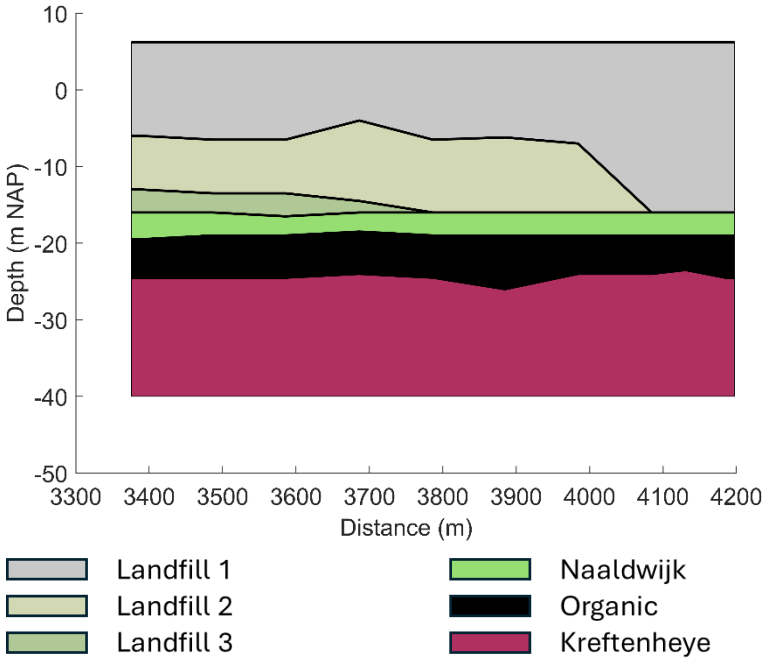

Figure 6-16 Representative geotechnical cross section for Subarea 3

6.2 Selection of soil parameters

6.2.1 Unit weight

The unit weight of the soil layers is determined based on a Netherlands-specific correlation between the cone resistance and the unit weight (Lengkeek et al., 2018). The unit weight is presented for the closest CPTs, which is in good agreement with the average unit weight over the CPTs per group.

Figure 6-17 to Figure 6-22 present the unit weight of subareas 1, 2 and 3. Note that the groundwater level is assumed to be at 0 m NAP, resulting in a lower unit weight above the water level. The saturated unit weight of the sand in the top layer for the two landfills of subareas 1 and 3 range from 19 to 21 kN/m^3. The fine layers in the landfills are estimated to have a unit weight of 16-18 kN/m^3. The loose top layer in Subarea 2 is variable (see Figure 6-19 and Figure 6-20), with a saturated unit weight ranging from 16 to 20 kN/m^3

The Naaldwijk Formation is consistent along the entire cross section. It has a heavier top layer of ~20.5 kN/m^3 (partly from the Southern Bight Formation) and decreases in weight with depth to ~19.5 kN/m^3. For the organic layer below the Naaldwijk Formation the unit weight of the fine material is estimated to range from 14 to 16 kN/m^3. However, the Naaldwijk Formation crosses the organic layer in some locations (resulting in a unit weight ranging from 19.5 to 20.5 kN/m^3). The unit weight of the Kreftenheye Formation varies from 19.5 to 20.5 kN/m^3 (similar to the Naaldwijk Formation).

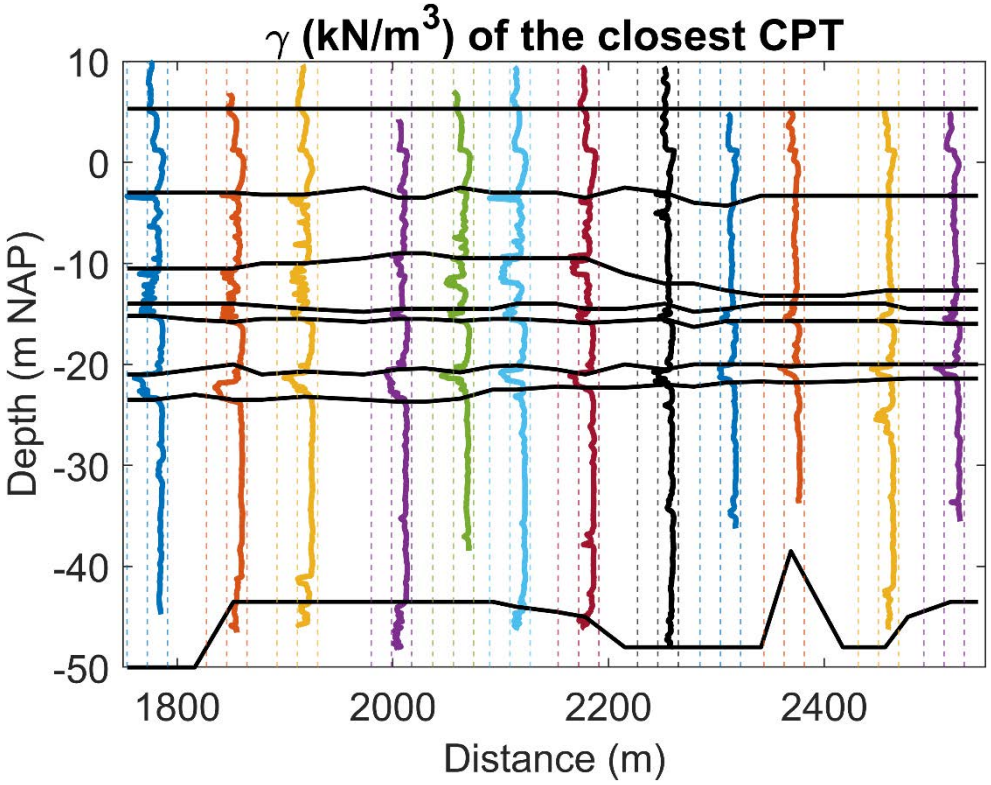

Figure 6-17 The estimated unit weight according to Lengkeek et al. (2018) based on the closest CPT to the cross section line for Subarea 1. For each CPT the dotted lines indicate a unit weight of 10, 16 and 22 kN/m³.

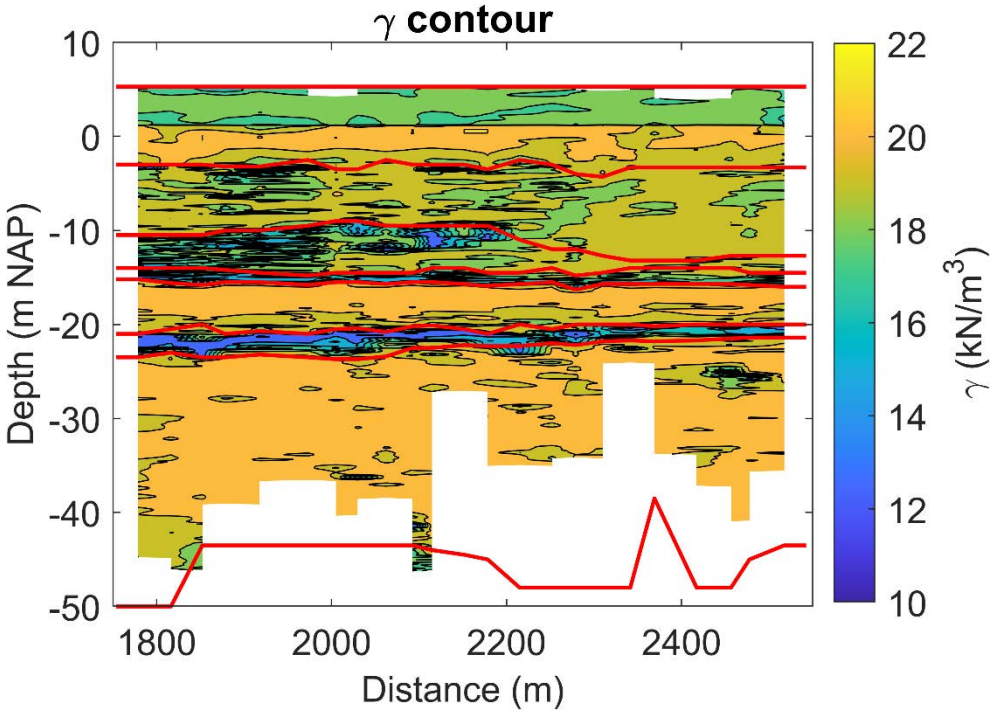

Figure 6-18 Contours of the estimated unit weight according to Lengkeek et al. (2018) based on the closest CPT to the cross section line for Subarea 1.

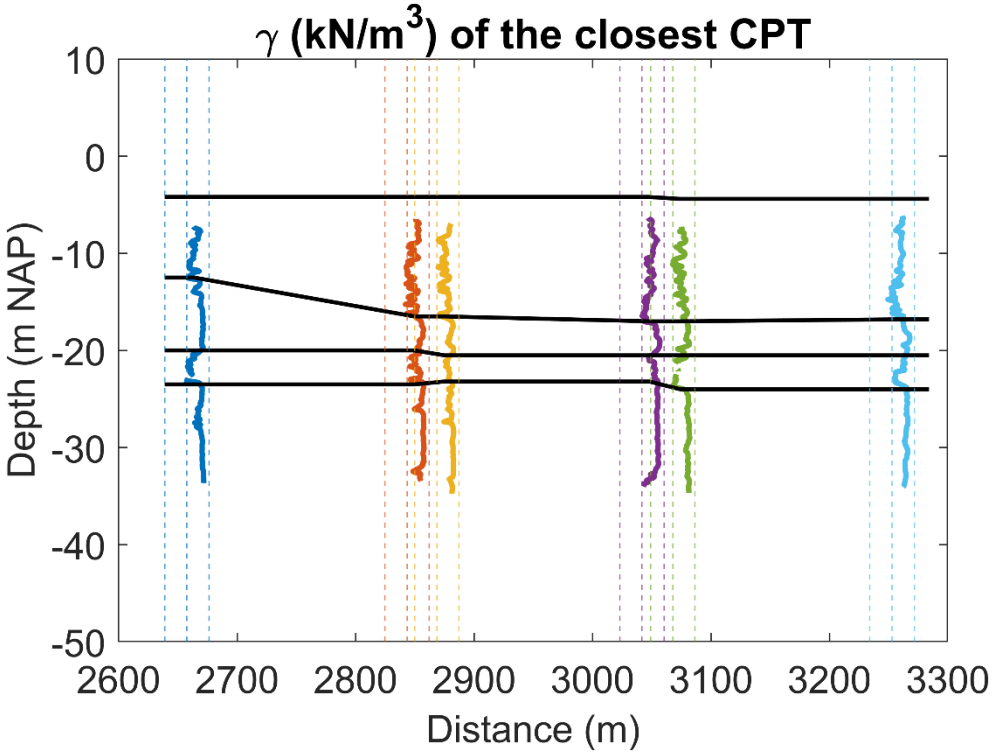

Figure 6-19 The estimated unit weight according to Lengkeek et al. (2018) based on the closest CPT to the cross section line for Subarea 2. For each CPT the dotted lines indicate a unit weight of 10, 16 and 22 kN/m³.

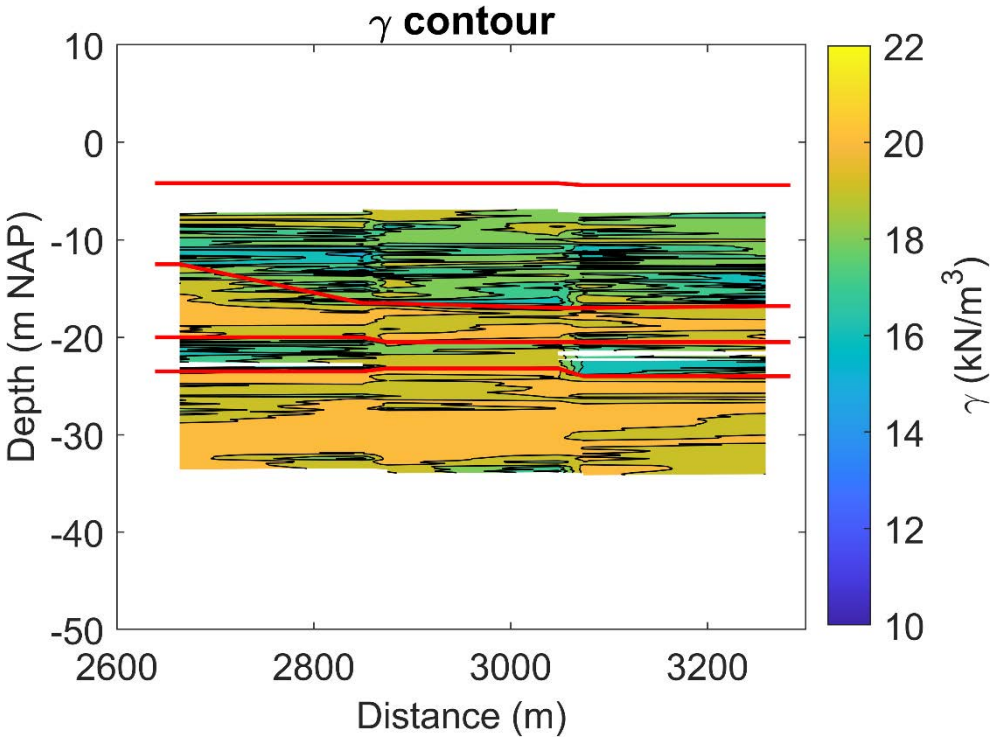

Figure 6-20 Contours of the estimated unit weight according to Lengkeek et al. (2018) based on the closest CPT to the cross section line for Subarea 2.

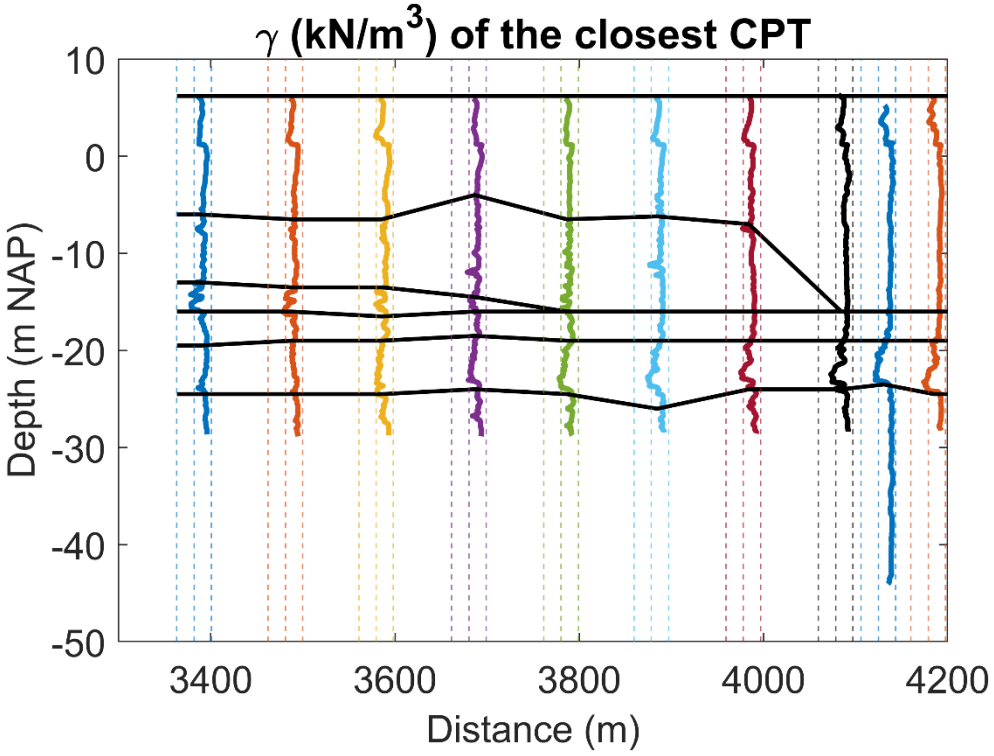

Figure 6-21 The estimated unit weight according to Lengkeek et al. (2018) based on the closest CPT to the cross section line for Subarea 3. For each CPT the dotted lines indicate a unit weight of 10, 16 and 22 kN/m³.

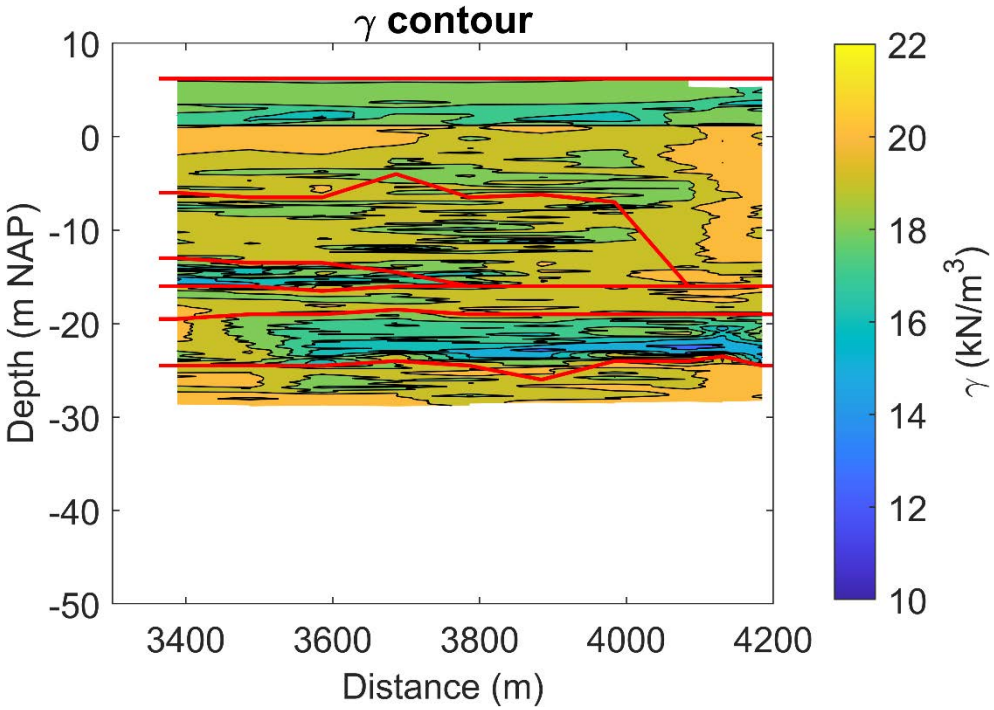

Figure 6-22 Contours of the estimated unit weight according to Lengkeek et al. (2018) based on the closest CPT to the cross section line for Subarea 3.

6.2.2 Minimum/maximum unit weight

The minimum and maximum unit weight have not been derived from CPT data. Laboratory testing on soil samples will be required to estimate these properties.

6.2.3 Relative density sand layers

The relative density of the sand layers is assessed using the correlation of Lunne and Christoffersen (1983). This correlation was not designed for landfills, and further investigation might therefore be required. In the next figures the correlation results are shown for subareas 1, 2 and 3, and they are summarized in section 6.4. For each area, the average relative density per group is presented. To indicate potential liquefaction risks, also the minimum relative density per group is shown. It should be noted that for the cone resistance no thin layer correction or any other correction for layer boundaries is applied. This results in a conservative estimate of the relative density.

Subarea 1 is denser than Subarea 3 (especially the left side of Subarea 3 is quite loosely packed). As the landfill settles, the relative density is expected to increase. For both landfills (subareas 1 and 3) the correlation gives a high relative density for the first sand layer. The sand layers with intermediate fine layers are loose (20-50% relative density). Due to the thin layer effect, caused by the interbedded clay layers in this unit, the measured cone resistance may underestimate the homogeneous clean sand cone resistance.

The sand in the submerged top layer of Subarea 2 is estimated to be very loose. The Naaldwijk and Kreftenheye formations are medium dense to dense (50-80% relative density).

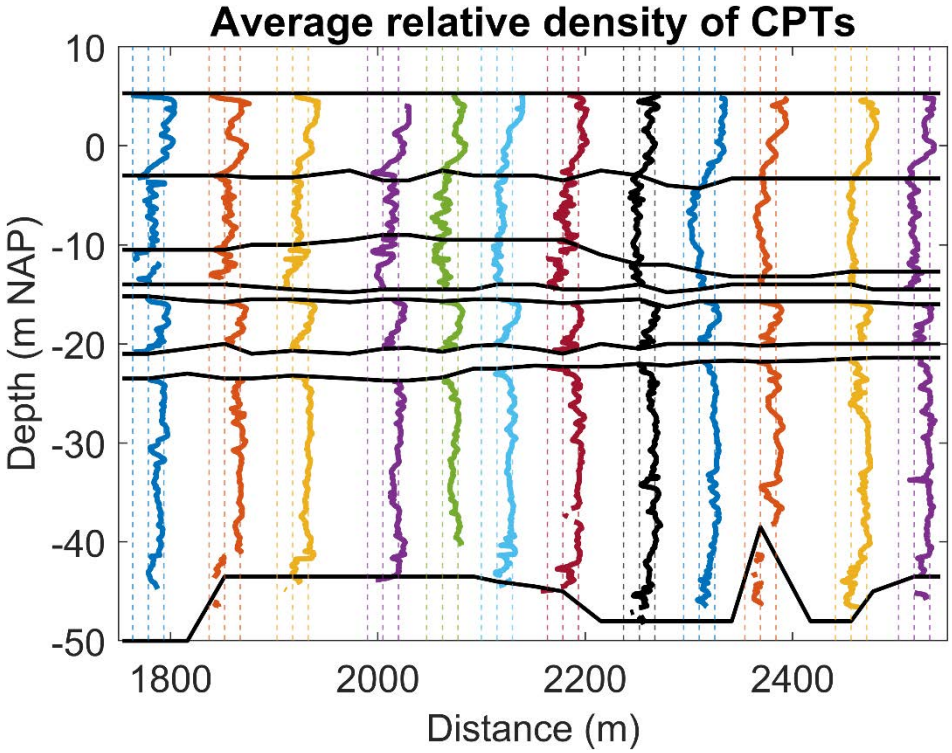

Figure 6-23 The estimated average relative density according to Lunne & Christoffersen (1983) based on all CPTs near the cross section line for Subarea 1. For each CPT the dotted lines indicate a relative density of 0.2, 0.5 and 0.8.

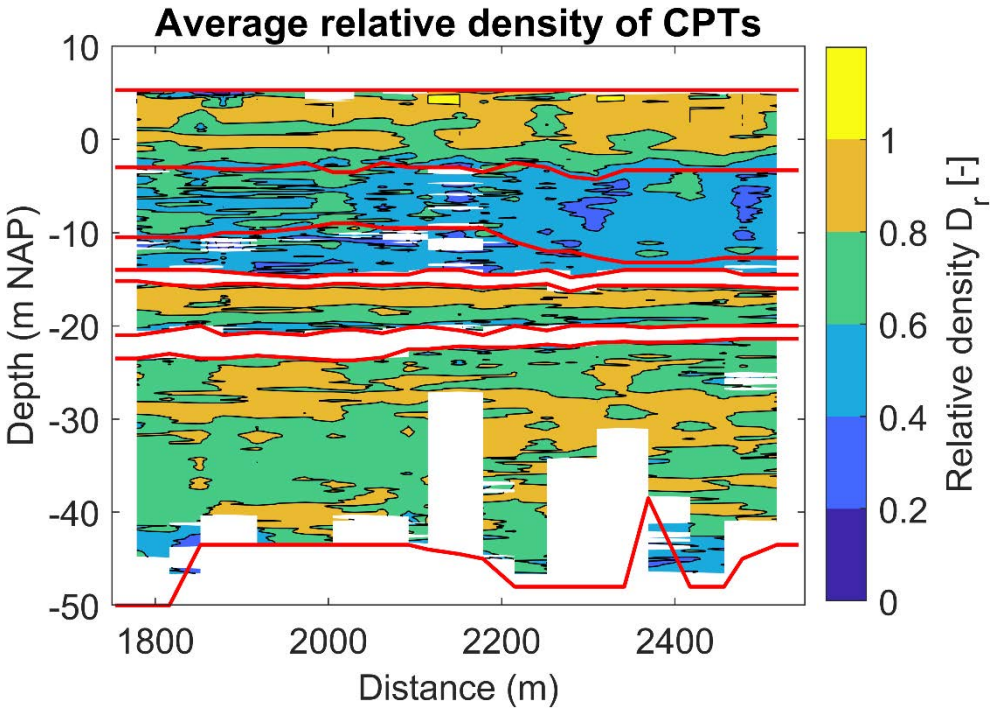

Figure 6-24 Contours of the estimated average relative density according to Lunne & Christoffersen (1983) based on all CPTs near the cross section line for Subarea 1. The red lines provide interpreted layer boundaries.

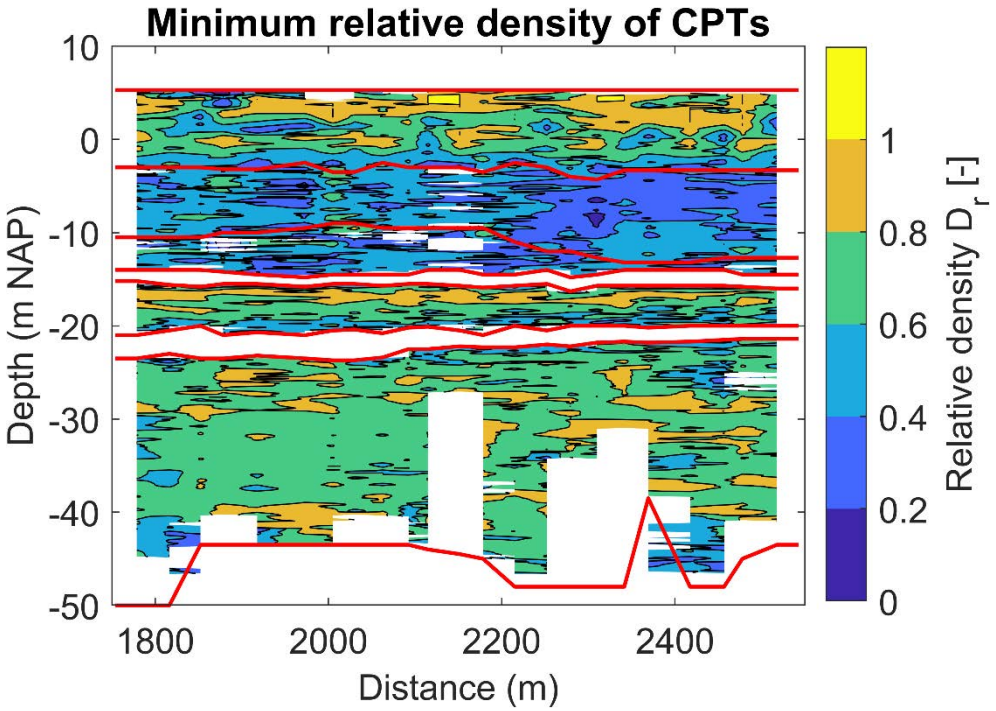

Figure 6-25 Contours of the estimated minimum relative density according to Lunne & Christoffersen (1983) based on all CPTs near the cross section line for Subarea 1. The red lines provide interpreted layer boundaries.

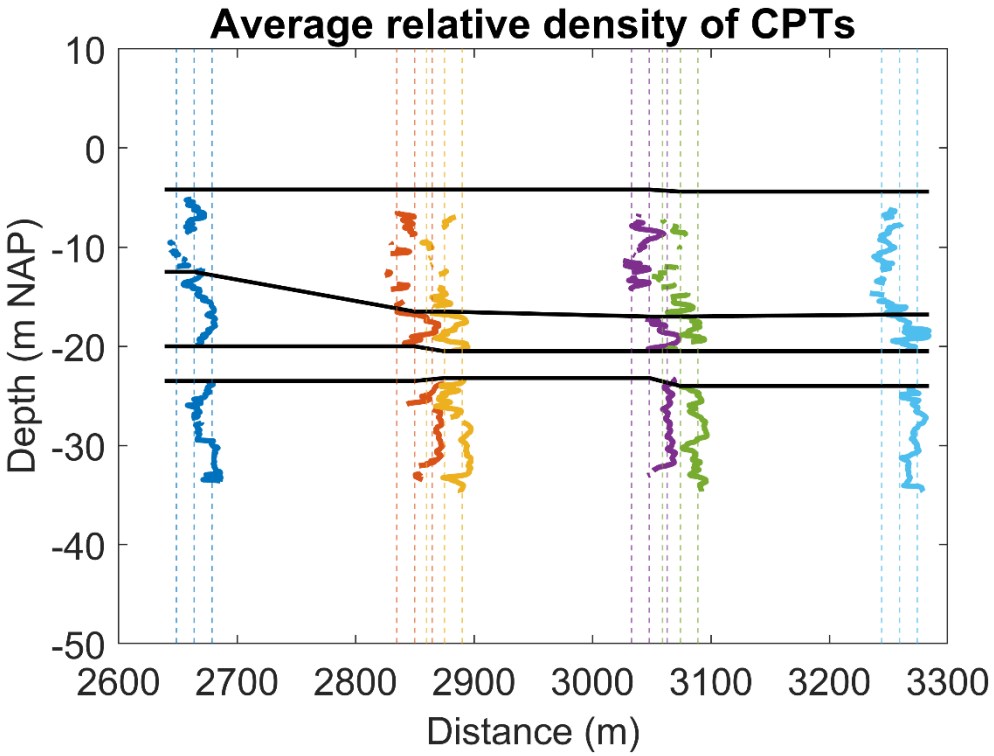

Figure 6-26 The estimated average relative density according to Lunne & Christoffersen (1983) based on all CPTs near the cross section line for Subarea 2. For each CPT the dotted lines indicate a relative density of 0.2, 0.5 and 0.8.

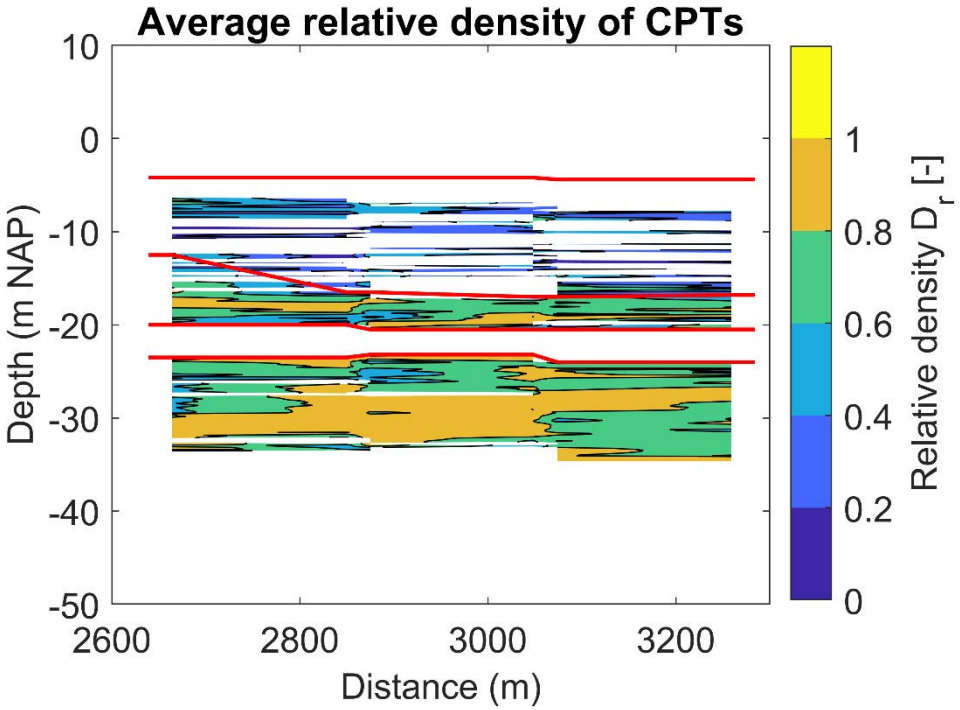

Figure 6-27 Contours of the estimated average relative density according to Lunne & Christoffersen (1983) based on all CPTs near the cross section line for Subarea 2. The red lines provide interpreted layer boundaries.

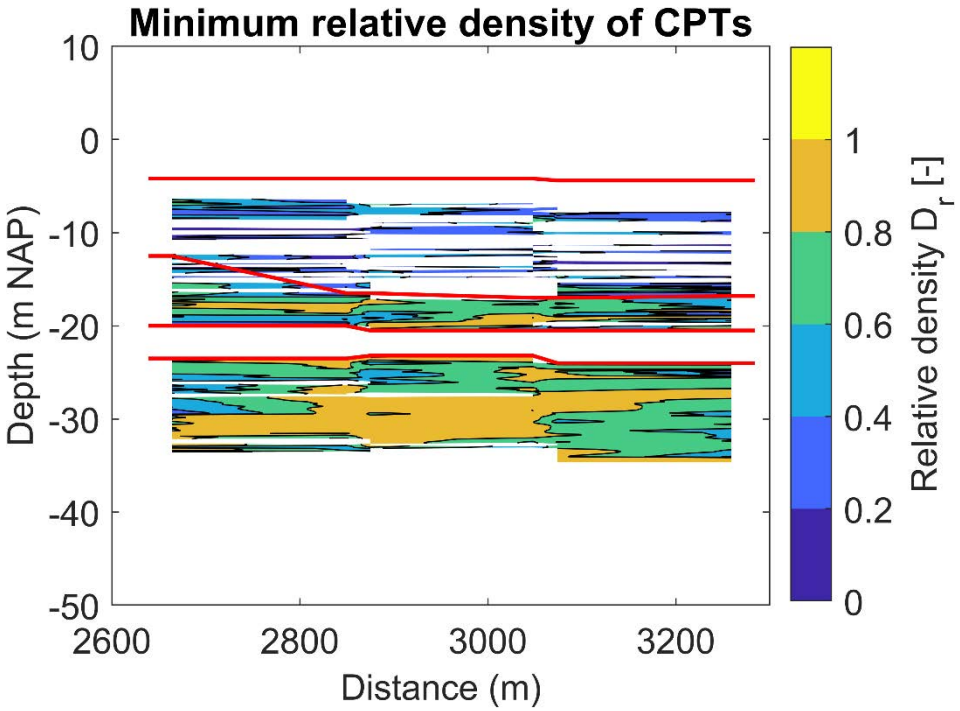

Figure 6-28 Contours of the estimated minimum relative density according to Lunne & Christoffersen (1983) based on all CPTs near the cross section line for Subarea 2. The red lines provide interpreted layer boundaries.

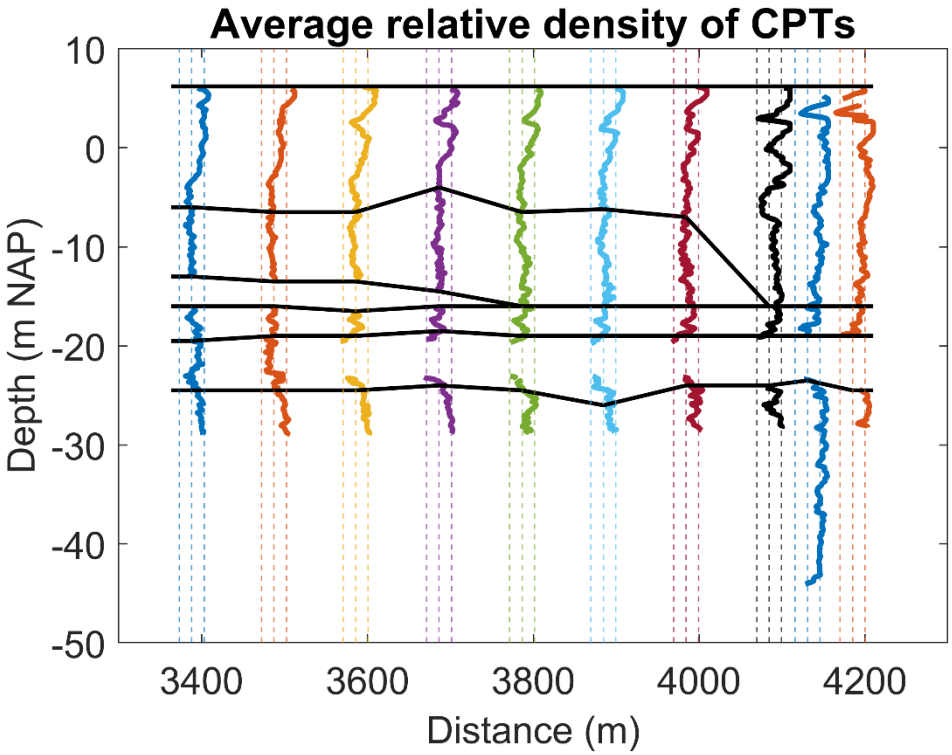

Figure 6-29 The estimated average relative density according to Lunne & Christoffersen (1983) based on all CPTs near the cross section line for Subarea 3. For each CPT the dotted lines indicate a relative density of 0.2, 0.5 and 0.8.

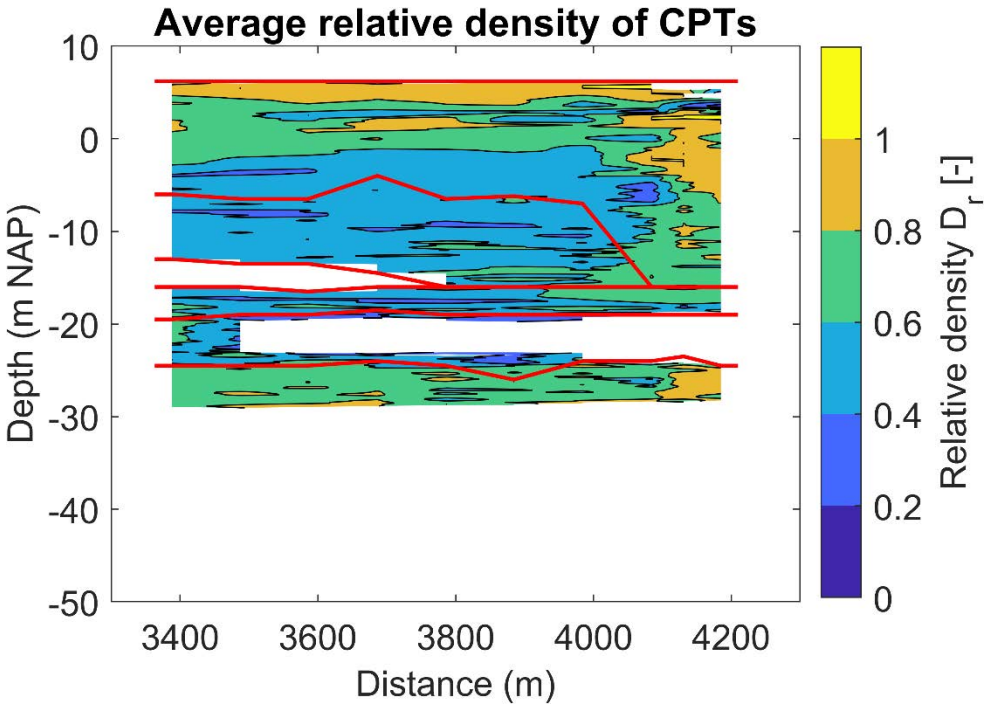

Figure 6-30 Contours of the estimated average relative density according to Lunne & Christoffersen (1983) based on all CPTs near the cross section line for Subarea 3. The red lines provide interpreted layer boundaries.

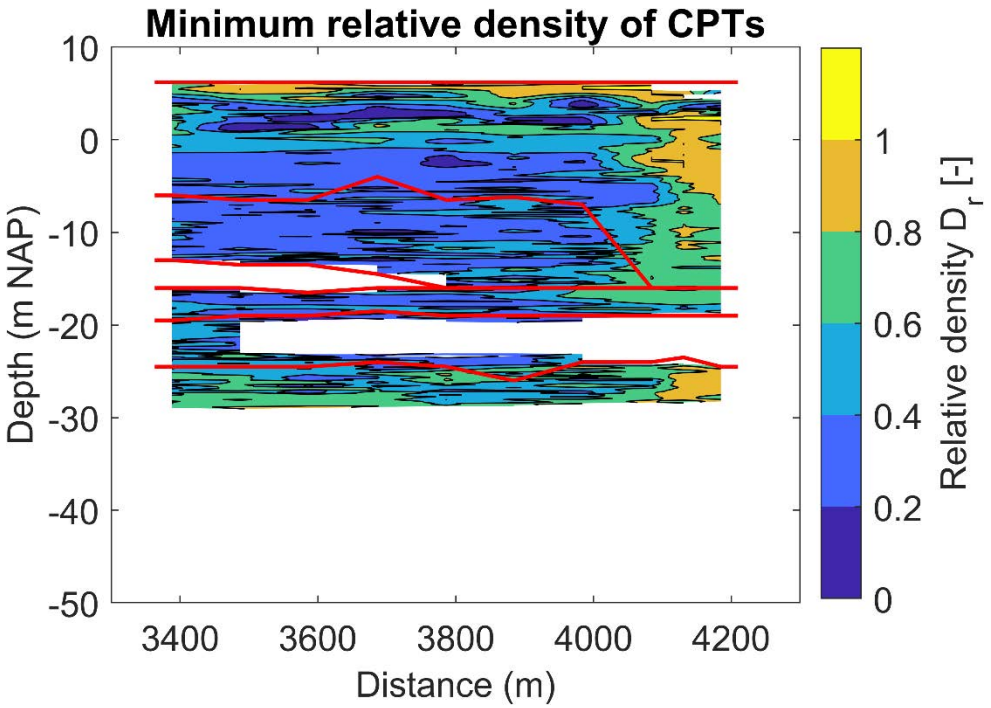

Figure 6-31 Contours of the estimated minimum relative density according to Lunne & Christoffersen (1983) based on all CPTs near the cross section line for Subarea 3. The red lines provide interpreted layer boundaries.

6.2.4 Strength parameters

6.2.4.1 Friction angle ϕ

The friction angle has been estimated based on the normalized cone resistance and an interpolation on Table 2.b of NEN9997. The data used for the interpolation is provided in Appendix C.2. The normalization procedure overestimates the cone resistance for the top of the cross section. The friction angle in the denser sand layers (top of the land fill, the Naaldwijk Formation and the Kreftenheye Formation) is estimated between 31° and 33°. In the looser sand zones of the landfill the friction angle is estimated at 29° and 31°. In the clayey zones and organic layer the friction angle decreases to 15°. These estimates must be confirmed with element testing.

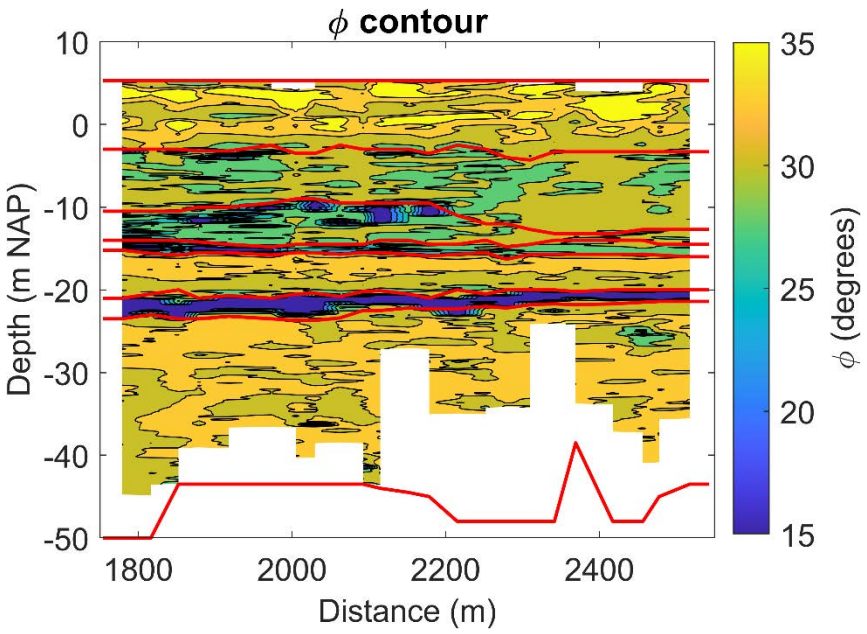

Figure 6-32 Contours of the estimated ϕ according to an interpolation of NEN-9997 based on the closest CPTs near the cross section line for Subarea 1.

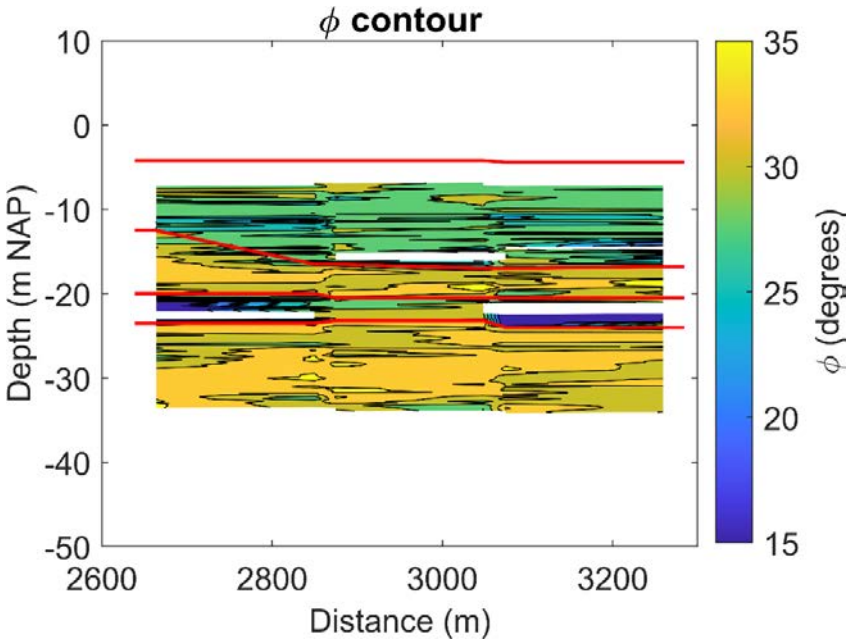

Figure 6-33 Contours of the estimated ϕ according to an interpolation of NEN-9997 based on the closest CPTs near the cross section line for subarea 2.

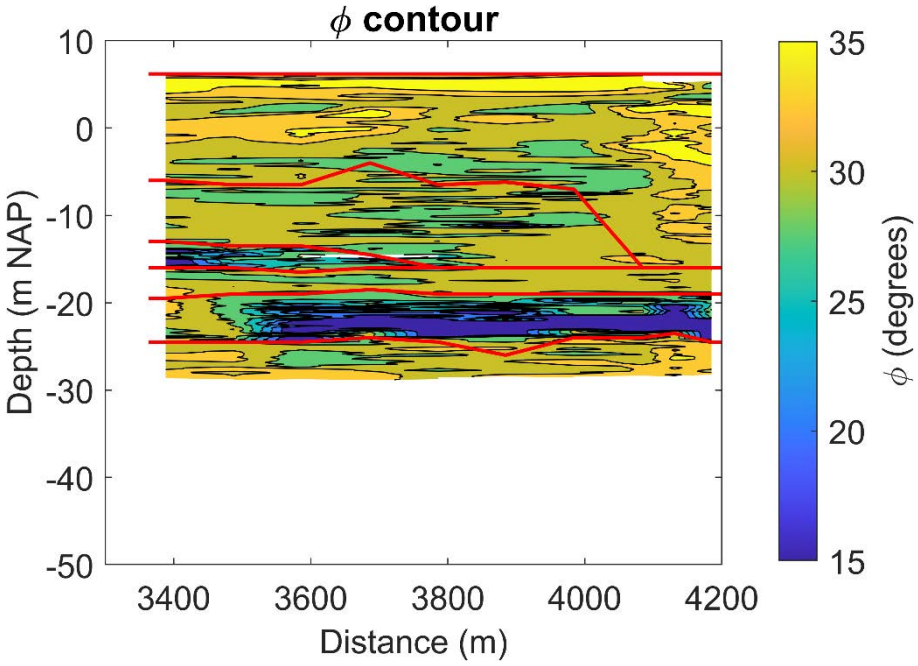

Figure 6-34 Contours of the estimated ϕ according to an interpolation of NEN-9997 based on the closest CPTs near the cross section line for Subarea 3.

6.2.4.2 Cohesion c

Interpolation on the NEN9997 table does not provide a consistent effective cohesion. Therefore the following estimates are suggested:

- Sand layers: c = 0 kPa
- Clay zones: c = 1 kPa
- Peat/organic clay: c = 1 kPa

6.2.5 Stiffness parameters

The stiffness of granular materials found in the subsurface varies with the confining stress level and thus with the depth of the material. An efficient way to account for this variation of stiffness with depth within an otherwise uniform soil formation is by relating the stiffness parameter (E) to a reference stiffness (E_{ref}) at an effective confining stress (σ_c') that is equal to a reference stress (p_{ref}), typically taken as 100 kPa (atmospheric pressure). This models the stiffness as a stress dependent parameter. The relation between stiffness and effective confining soil stress is for cohesionless soil:

$$E = E_{ref} \cdot \left(\frac{\sigma_c'}{p_{ref}} \right)^m$$

With:

- E stiffness [kN/m^2].
- E_{ref} stiffness at reference stress level p_{ref} [kN/m^2].
- p_{ref} reference stress level, commonly p_{ref} = 100 kPa is used.
- m power defining the change of E with changing σ_c' [-], commonly m = 2/3 is used.

As an initial estimate the E_{100} has again been determined from interpolation (using Appendix C.2 which is based on the NEN-9997 Table 2.B). Fixed suggestions for ‘m’ are provided in NEN-9997. The normalization procedure overestimates the cone resistance in at the top of the profile. The reference stiffness in the denser sand layers (top of the land fill, the Naaldwijk Formation and the Kreftenheye Formation) is estimated between 30 and 70 MPa. In the looser sand zones of the landfill the reference stiffness drops to 15 to 30 MPa. In the clayey

zones and organic layer the reference stiffness is estimate between 1 and 3 MPa, corresponding to a moderately stiff organic clay.

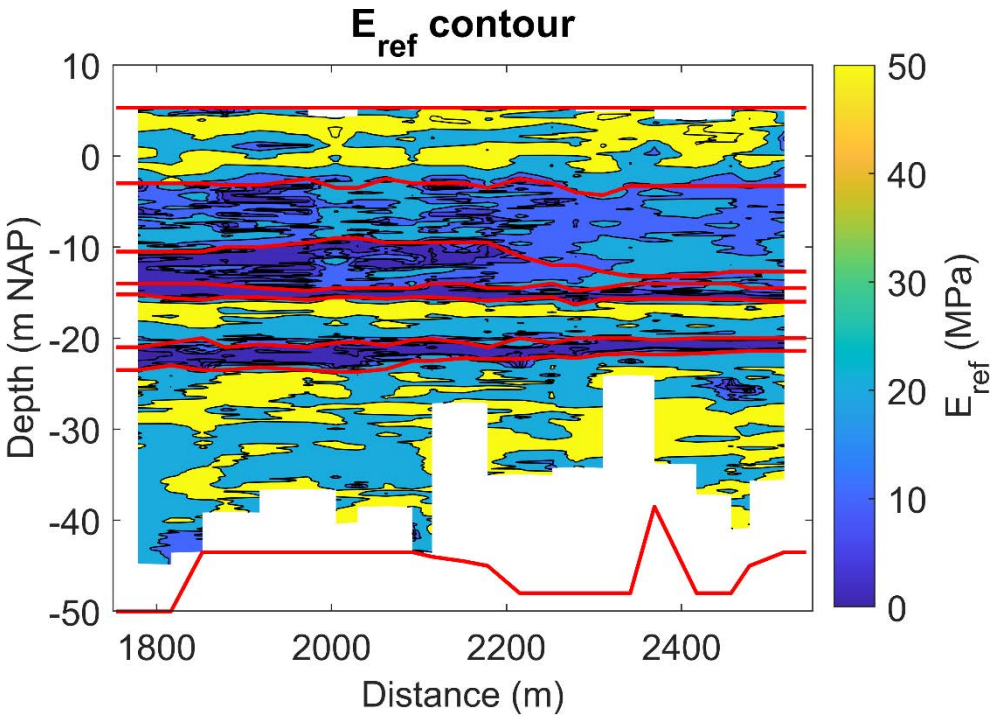

Figure 6-35 Contours of the estimated E_{100} according to an interpolation of NEN-9997 based on the closest CPTs near the cross section line for Subarea 1.

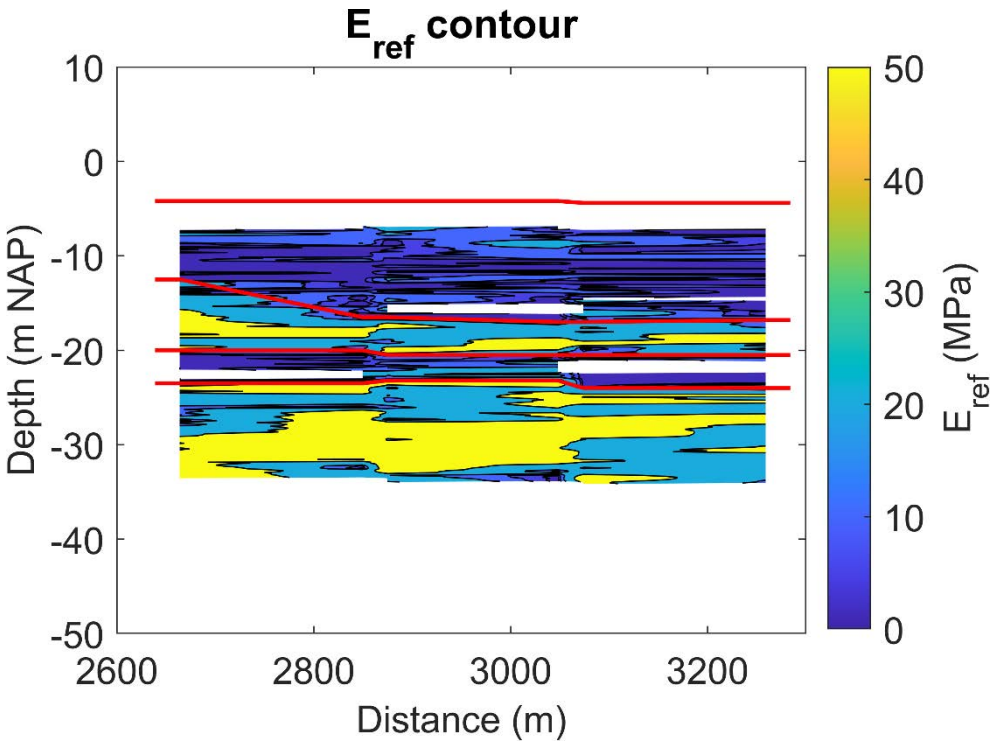

Figure 6-36 Contours of the estimated E_{100} according to an interpolation of NEN-9997 based on the closest CPTs near the cross section line for subarea 2.

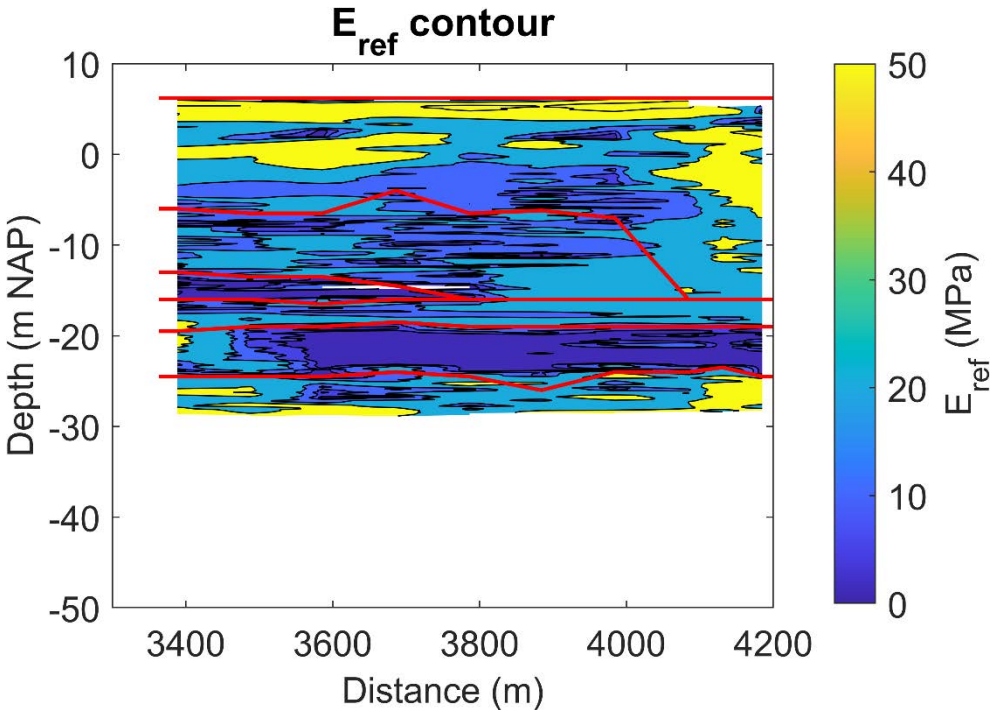

Figure 6-37 Contours of the estimated E_{100} according to an interpolation of NEN-9997 based on the closest CPTs near the cross section line for Subarea 3.

6.3 Settlement parameters

The settlement parameters are based on Dutch experience based on table 2.b of NEN 9997, the Dutch version of EC7. Again the results have been interpolated based on the normalized cone resistance. The settlement parameters are summarized per section in this section

6.3.1 Subarea 1

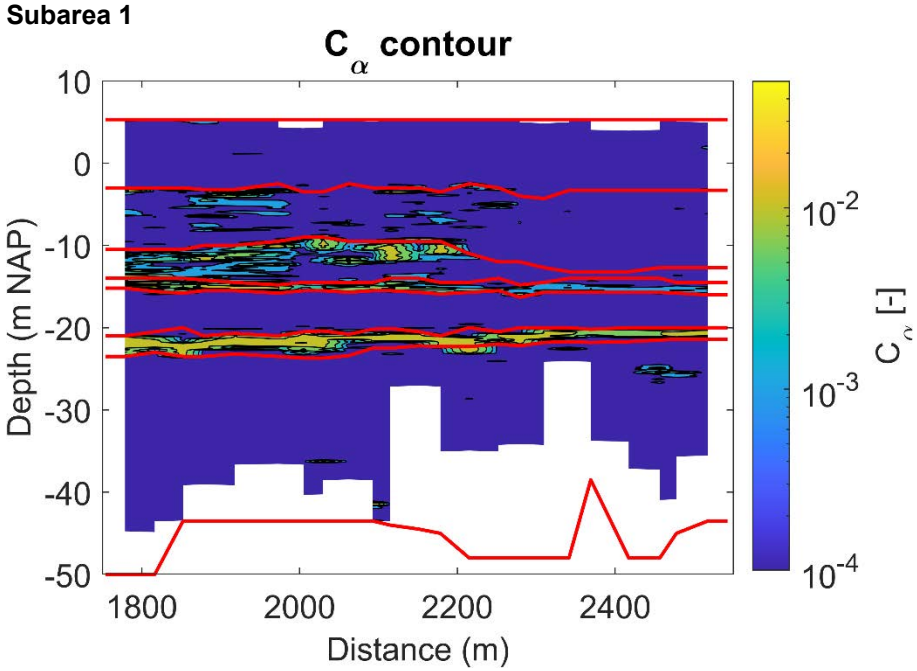

Figure 6-38 Contours of the estimated C_α according to an interpolation of NEN-9997 based on the closest CPTs near the cross section line for Subarea 1. Note that in the sand layer C_α = 0

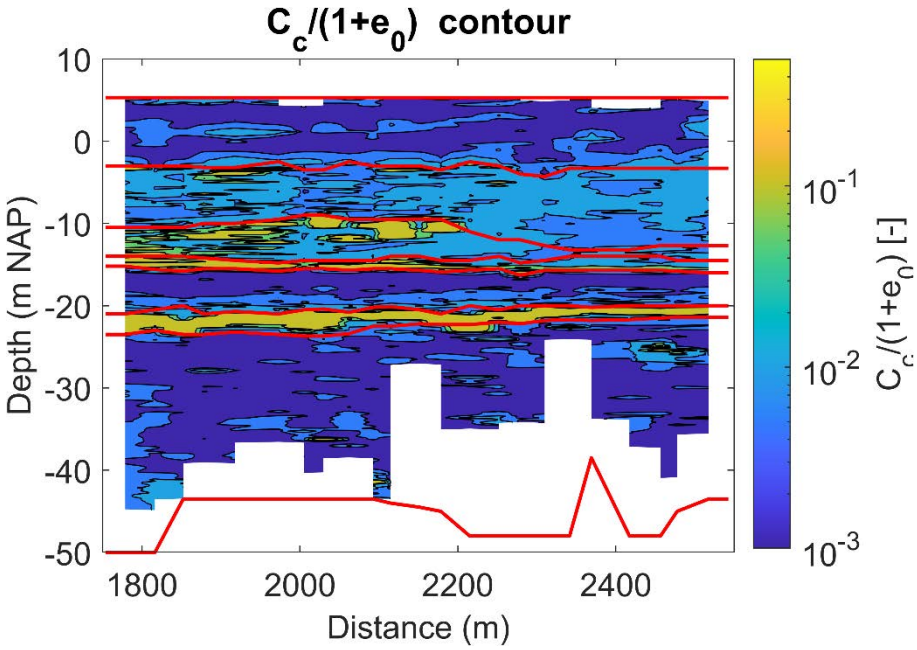

Figure 6-39 Contours of the estimated $C_c/(1+e_0)$ according to an interpolation of NEN-9997 based on the closest CPTs near the cross section line for Subarea 1.

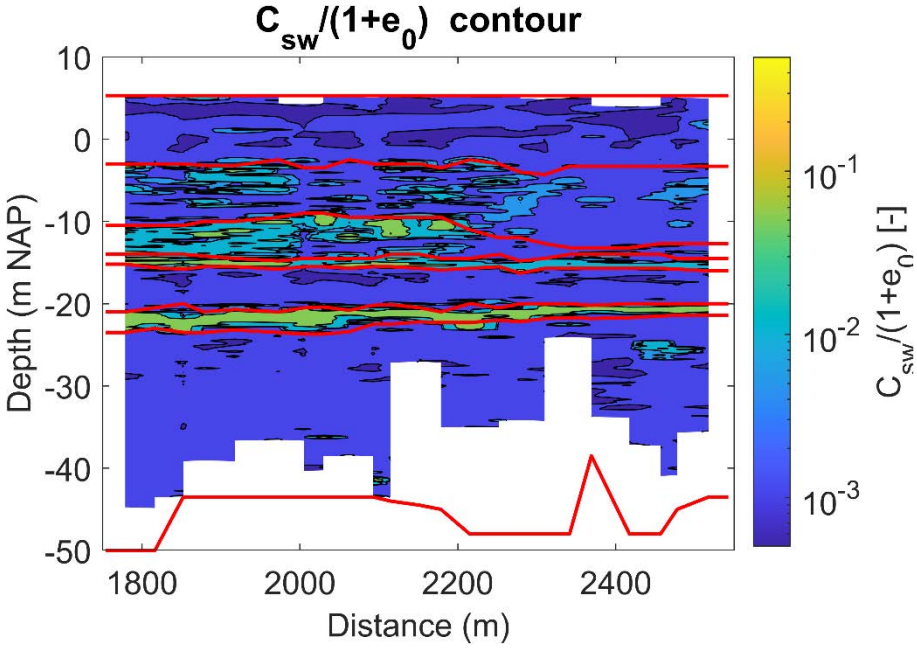

Figure 6-40 Contours of the estimated $C_{sw}/(1+e_0)$ according to an interpolation of NEN-9997 based on the closest CPTs near the cross section line for Subarea 1.

6.3.2 Subarea 2

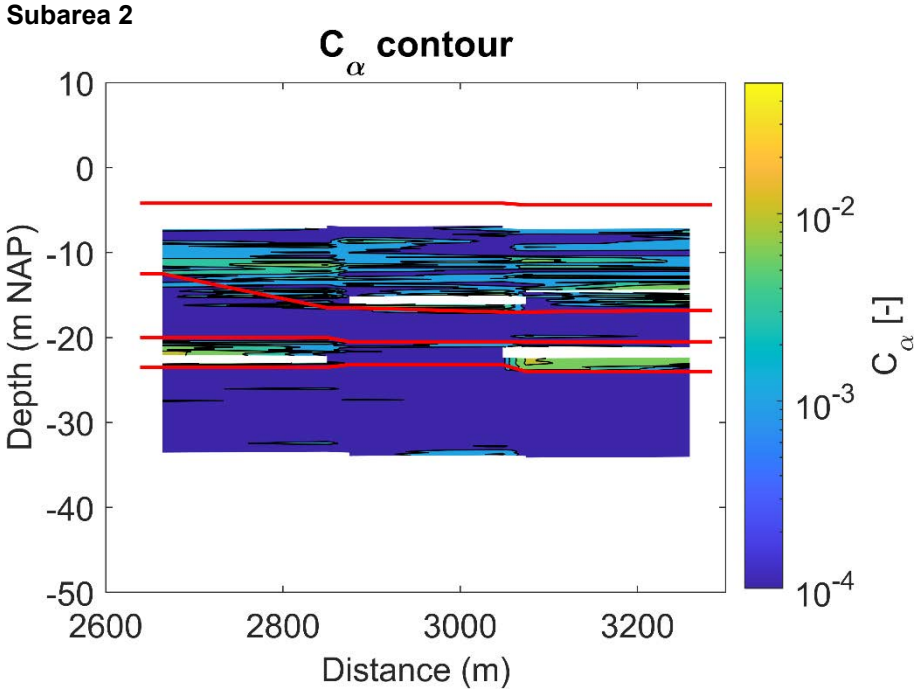

Figure 6-41 Contours of the estimated C_α according to an interpolation of NEN-9997 based on the closest CPTs near the cross section line for Subarea 2. Note that in the sand layer $C_\alpha = 0$

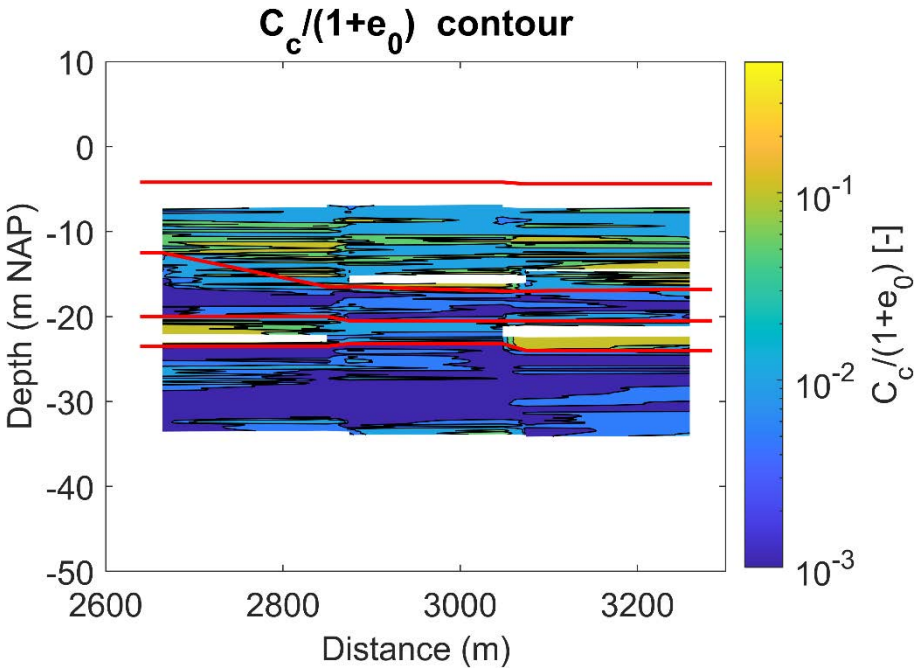

Figure 6-42 Contours of the estimated $C_c/(1+e_0)$ according to an interpolation of NEN-9997 based on the closest CPTs near the cross section line for Subarea 2.

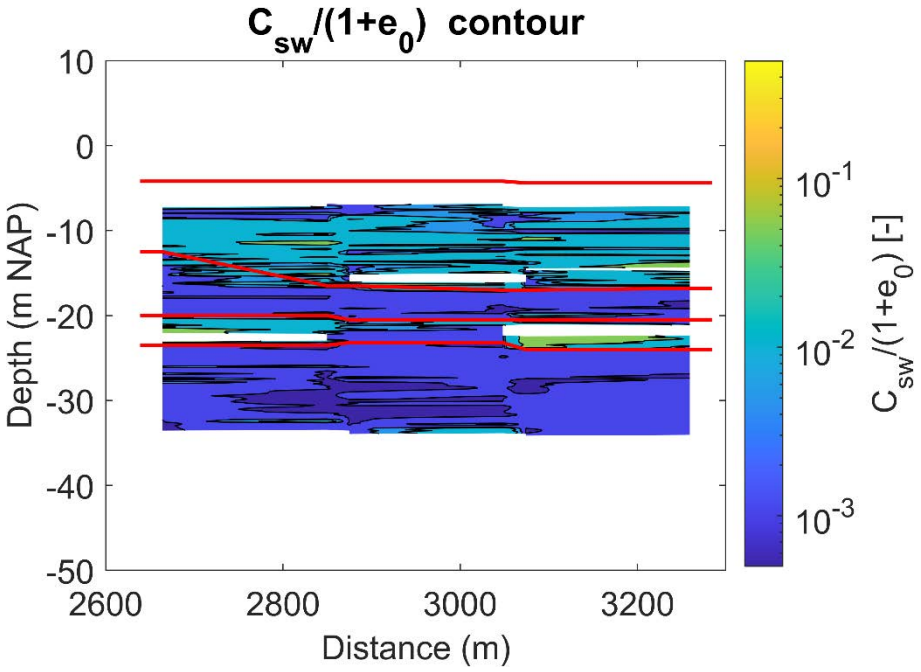

Figure 6-43 Contours of the estimated $C_{sw}/(1+e_0)$ according to an interpolation of NEN-9997 based on the closest CPTs near the cross section line for Subarea 2.

6.3.3 Subarea 3

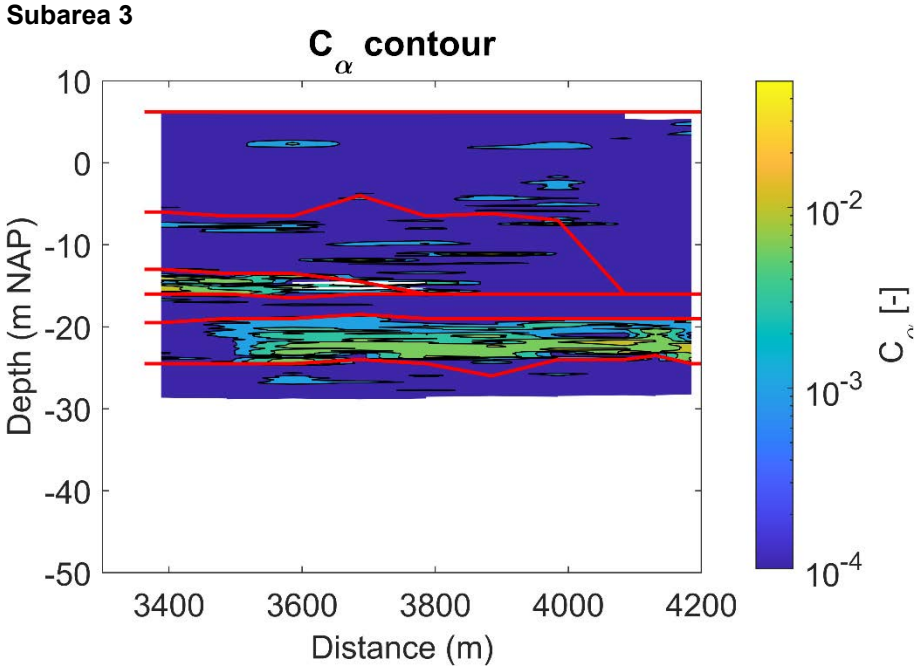

Figure 6-44 Contours of the estimated C_α according to an interpolation of NEN-9997 based on the closest CPTs near the cross section line for Subarea 3. Note that in the sand layer $C_\alpha = 0$

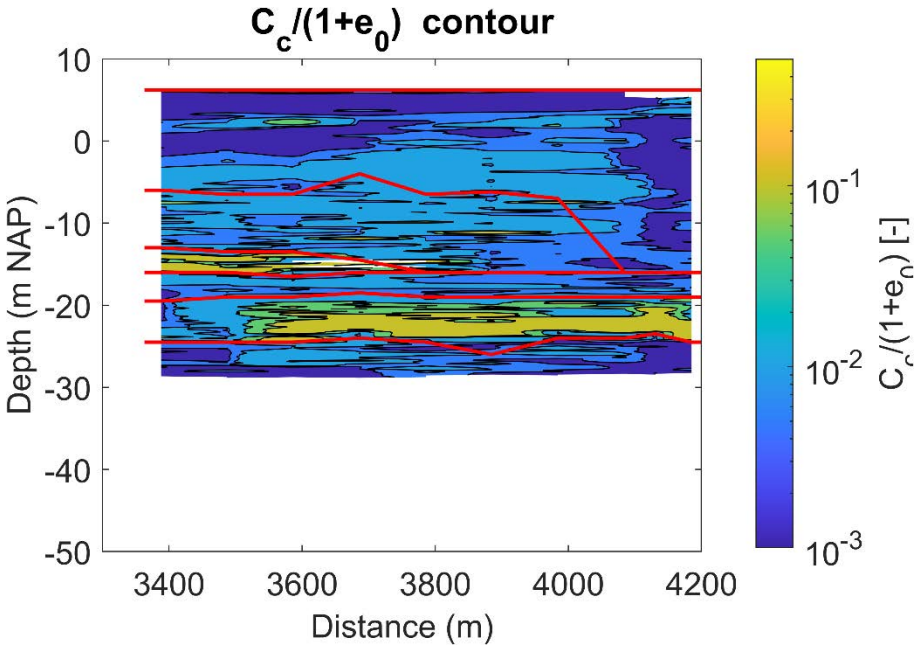

Figure 6-45 Contours of the estimated $C_c/(1+e_0)$ according to an interpolation of NEN-9997 based on the closest CPTs near the cross section line for Subarea 3.

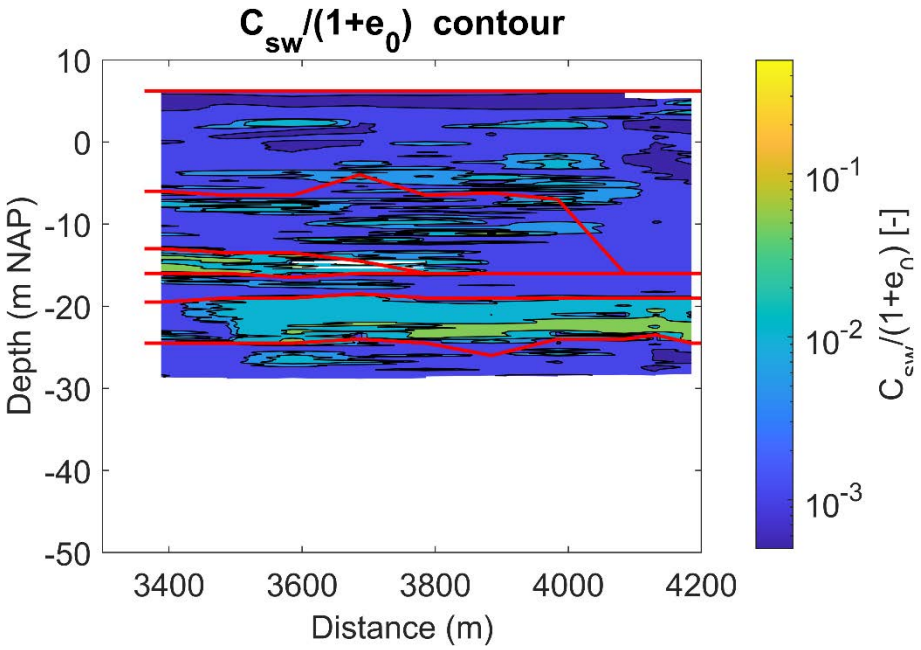

Figure 6-46 Contours of the estimated $C_{sw}/(1+e_0)$ according to an interpolation of NEN-9997 based on the closest CPTs near the cross section line for Subarea 3.

6.4 Summary of geotechnical parameters

Section 6.1.4 provides a schematic representations of the subareas. A summary of the material properties for these representations is provided in Table 6-1 to Table 6-3. Note that significant variation is present in the layers as was highlighted in the previous sections, and that for the landfill this variation is higher than typical in Dutch soil conditions. Therefore, when fines are present in the landfill layers both the weaker and stronger material is presented in the following tables. The organic layer is not continuously present in subareas 1 and 2, but this has not been included in the tables, and should be further investigated in the design stage.

Table 6-1 Summary of the material properties for Subarea 1.

layer	Top of layer	Relative density	Unit weight	Strength parameters		Stifness	Settlement parameters		
	m + NAP		γ kN/m^3	c kPa	ϕ degr	E100 MPa	$C_c/(1+e_0)$	$C_{sw}/(1+e_0)$	C_a
Landfill 1	5.0	Medium dense	16 - 20 (moist) 19 - 21 (wet)	0	33 – 36	30 – 70	0.0025 – 0.0075	0.001-0.003	0
Landfill 2 – Sand	-3.0 – -4.5	Loose – medium dense	19 - 21	0	29 – 31	15 – 30	0.0075 – 0.05	0.003-0.01	0
Landfill 2 – Silty sands	-3.0 – -4.5		16 - 18	0-1	20 – 25	1 – 3	0.05 – 0.25	0.01-0.075	0.001 – 0.015
Landfill 3 – Sand	-9.5 – -13.2	Loose – medium dense	19 - 21	0	29 – 31	15 – 30	0.0075 – 0.05	0.003-0.01	0
Landfill 3 – Silty sands	-9.5 – -13.2		16 - 18	0-1	15 – 25	1 – 3	0.05 – 0.25	0.01-0.075	0.001 – 0.015
Silty sand layer	-14.0 – -14.8		16 - 18	1	15 – 25	1 – 3	0.15 – 0.25	0.05-0.075	0.001 – 0.015
Naaldwijk (sand)	-15.2 – -16.3	Medium dense – dense	19.5 - 20.5	0	31 – 33	30 – 70	0.0025 – 0.0075	0.001-0.003	0
Organic (organic clays and peat)	-20.0 – 21.0		14 - 16	1	15	1 – 3	0.15 – 0.25	0.05-0.075	0.01 – 0.015
Kreftenheye (sand)	-21.4 – -23.5	Medium dense	19.5 - 20.5	0	31 – 33	30 – 70	0.0025 – 0.0075	0.001-0.003	0

Table 6-2 Summary of the material properties for subarea 2.

layer	Top of layer	Relative density	Unit weight	Strength parameters		Stifness	Settlement parameters		
	m + NAP		γ kN/m^3	c kPa	ϕ degr	E100 MPa	$C_c/(1+e_0)$	$C_{sw}/(1+e_0)$	C_a
Landfill 1 – Sand	5.0	Loose	16 - 20 (moist) 18 - 20 (wet)	0	25 – 30	15-20	0.0075 – 0.05	0.003-0.01	0
Landfill 1 – Silty sands	-3.0 – -4.5		16 - 18	0-1	20 – 25	1 – 3	0.05 – 0.25	0.01-0.075	0.001 – 0.015
Naaldwijk (sand)	-15.2 – -16.3	Medium dense – dense	19.5 - 20.5	0	31 – 33	30 – 70	0.0025 – 0.0075	0.001-0.003	0
Organic (organic clays and peat)	-20.0 – 21.0		14 - 16	1	15	1 – 3	0.15 – 0.25	0.05-0.075	0.01 – 0.015
Kreftenheye (sand)	-21.4 – -23.5	Medium dense	19.5 - 20.5	0	31 – 33	30 – 70	0.0025 – 0.0075	0.001-0.003	0

Table 6-3 Summary of the material properties for Subarea 3.

layer	Top of layer	Relative density	Unit weight	Strength parameters		Stifness	Settlement parameters		
	m + NAP		γ kN/m^3	c kPa	ϕ degr	E100 MPa	$C_c/(1+e_0)$	$C_{sw}/(1+e_0)$	C_a
Landfill 1	5.0	Medium dense	16 - 20 (moist) 19 - 21 (wet)	0	33 – 36	30 – 70	0.0025 – 0.0075	0.001-0.003	0
Landfill 2 – Sand	-3.0 – -4.5	Loose – medium dense	19 - 21	0	29 – 31	15 – 30	0.0075 – 0.05	0.003-0.01	0
Landfill 2 – Silty sands	-3.0 – -4.5		16 - 18	0-1	20 – 25	1 – 3	0.05 – 0.25	0.01-0.075	0.001 – 0.015
Landfill 3 – Sand	-9.5 – -13.2	Loose – medium dense	19 - 21	0	29 – 31	15 – 30	0.0075 – 0.05	0.003-0.01	0
Landfill 3 – Silty sands	-9.5 – -13.2		16 - 18	0-1	15 – 25	1 – 3	0.05 – 0.25	0.01-0.075	0.001 – 0.015
Naaldwijk (sand)	-15.2 – -16.3	Medium dense – dense	19.5 - 20.5	0	31 – 33	30 – 70	0.0025 – 0.0075	0.001-0.003	0
Organic (organic clays and peat)	-20.0 – 21.0		14 - 16	1	15	1 – 3	0.15 – 0.25	0.05-0.075	0.01 – 0.015
Kreftenheye (sand)	-21.4 – -23.5	Medium dense	19.5 - 20.5	0	31 – 33	30 – 70	0.0025 – 0.0075	0.001-0.003	0

6.4.1 Attention points

With the exception of the landfill, subsurface conditions are similar for all subareas. The landfill consists of sands and silts, which are especially loose towards the bottom of the landfill. In the upper parts of the landfill thin clay and organic layers are present. Their thickness varies and the layers are non-continuous.

The parameters derived here are based on CPT data using correlations and Dutch standards and additional laboratory testing has not yet been performed. Since the CPTs do not reach deeper than -25 m NAP, to geotechnical information is present for deeper parts. Further investigation at larger depths is required before more detailed design phases are started. Also, laboratory testing on soil samples is required for future design phases.

Due to the presence of loose sand, densification of the landfill may be required before construction. Due to the heterogeneity of the landfill and varying thickness of the soft (clayey) layers uneven settlements may be expected.

7 Subsidence, settlements and bearing capacity

7.1 Subsidence of the shallow subsurface

This section gives an overview of the potential subsidence which may occur at the surface of the MV2 site. Subsidence in this area is mostly the result of ongoing compaction of the landfill to reclaim this area as well as compaction of the material underneath the MV2 due to the weight of the reclamation. Additional subsidence originates from long-term geological subsidence.

The long-term geological subsidence component has been modelled to 0.35 mm/yr for the study area (Hijma, 2022). Just north of the MV2 site there is increased subsidence as a consequence of the extraction of gas from both on- and offshore fields. The fields are relatively small, though, and the associated subsidence is estimated to be only 0.01 or 0.02 m in the coming decades (Hijma, 2022). It is possible that the southern edge of the gas-extraction related subsidence bowl will extend across the planned MV2 site.

Rates of subsidence related to compaction can be estimated from the *Bodemdalingskaart 2.0* and the *European Ground Motion Service*. Both show ground motion data on a local, national and continental scale with millimetre accuracy. They are derived from Sentinel-1 radar images at full resolution, on which a multi-temporal interferometric analysis (InSAR) is done. These data includes both geological and anthropogenic subsidence.

Figure 7-1 shows the results from the *Bodemdalingskaart 2.0 (NCG et al., 2025)* both at a regional and a local scale. The upper panel shows that the MV2 clearly stands out as a region of increased subsidence in comparison to the surrounding areas. Rates lie between 2-7 mm/yr, while east of the MV2 rates drop to 1 mm/yr. The lower panel shows that highest rates of subsidence are found at the location of the levees, which is not surprising since at those locations the anthropogenic deposit is thickest. The rates of subsidence are lower at the construction sides. It also shows that the Maasvlakte 1, that was built in the 1960's, does not show increased rates of subsidence. This means that it can be expected that increased rates of subsidence due to land reclamation diminish after several decades.

Figure 7-2 shows the results from the *European Ground Motion Service* (Copernicus Land Monitoring Service, 2024). Datapoints do not cover the study area, but nearby points show rates of 2 to 5 mm/yr, in general the average rates of subsidence are somewhat higher than follows from the *Bodemdalingskaart.*

Figure 3-11 shows that the plots in MV2 are not built in one go, but that new plots are added gradually. After construction of a plot, the Port of Rotterdam estimates that it takes about half a year to a couple years before a plot can be used (DCMR Milieudienst Rijnmond, 2024). This time is required for the sand to settle, prepare the terrain and build the required (energy) infrastructure. For example, the construction of a plot of 55 ha area south of the Alexiahaven was started in 2022 and finished in 2024 (DCMR Milieudienst Rijnmond, 2024).

In summary: based on satellite measurements subsidence rates of 2-7 mm/yr can be expected for the coming decades. These rates are substantial and since these rates will vary across the study area due to both differences in thickness and composition of the reclamation deposits as well in the underlying geology, differential subsidence should be accounted for. Note that the subsidence is less sever at the construction sides. On the long term, rates of subsidence will slowly move toward the expected rate of geological subsidence (0.35 mm/yr).

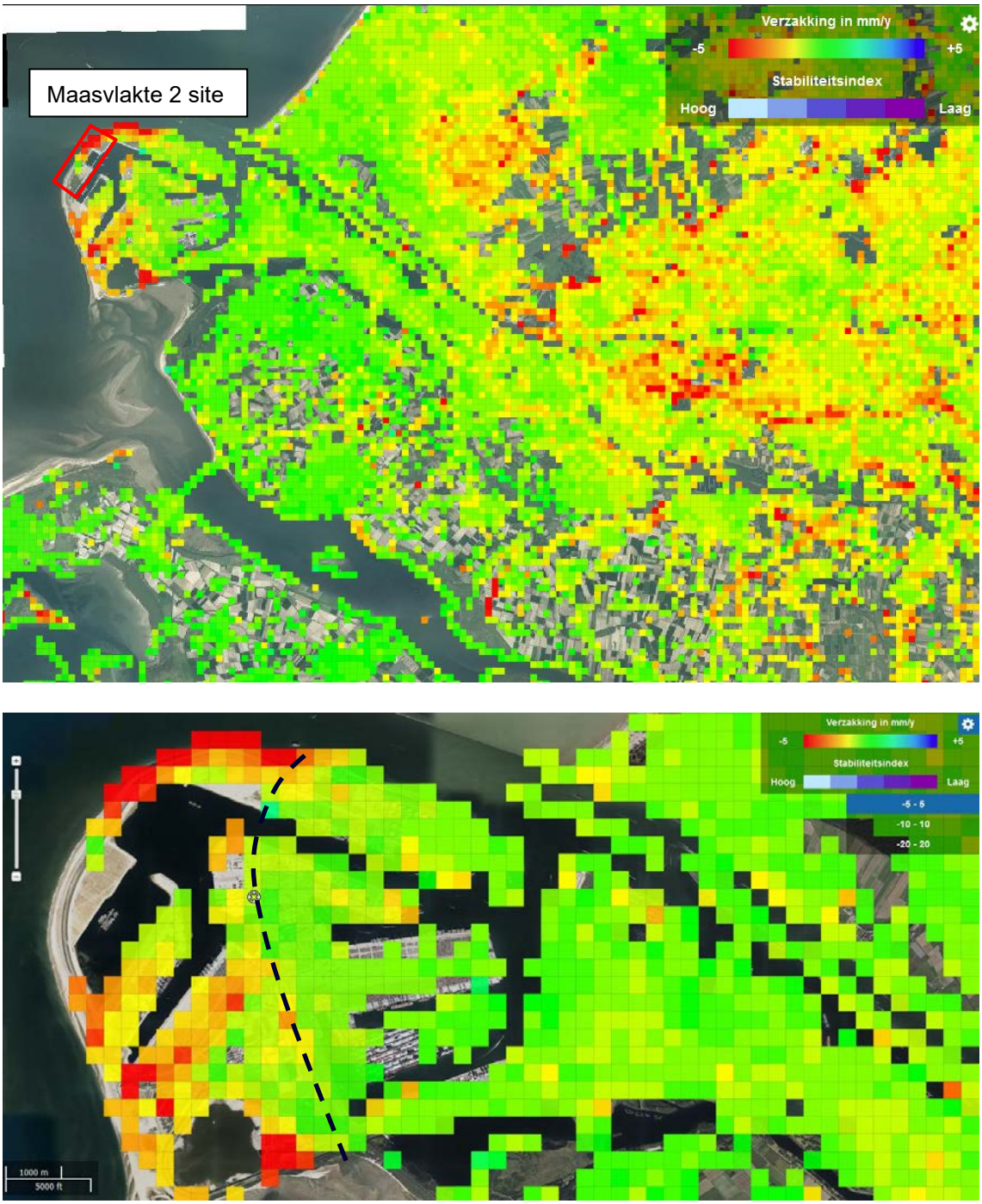

Figure 7-1 The ground motion in mm/year for the period October 2017 to October 2022 shown on the regional scale in the upper image (red box outlines the study area) and the local scale of the site area in the lower image (Bodemdalingskaart 2.0). The black dashed lines separates Maasvlakte 2 (left of it) from Maasvlakte 1.

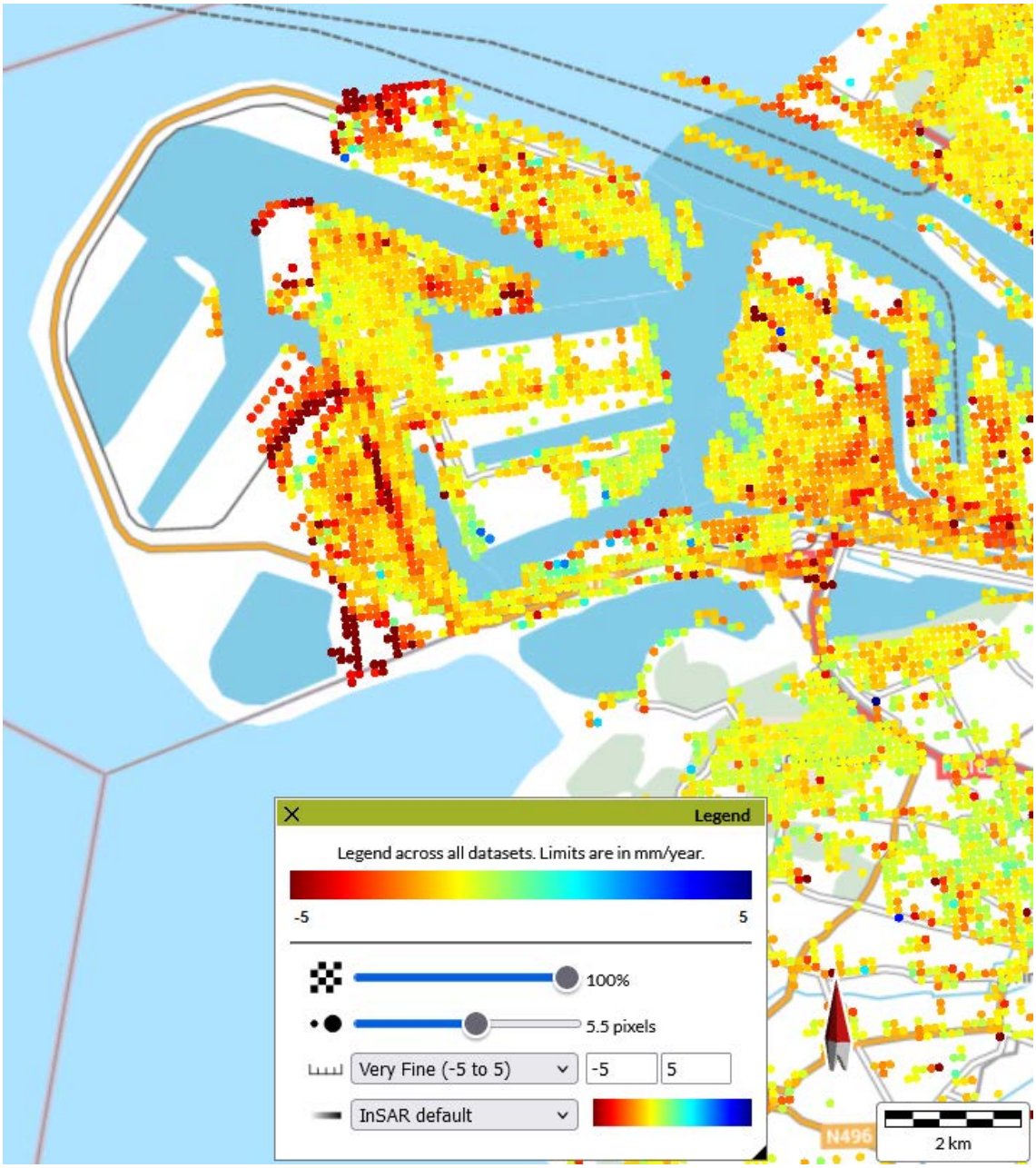

Figure 7-2 Subsidence rates from InSar (Copernicus: https://egms.land.copernicus.eu/) for the period January 2019 – December 2023.

7.2 Settlements

This section provides a first assessment of the potential settlement of the building at the MV2 site. The objective of the settlement calculations is to get a first estimate (order of magnitude) of the settlements to be expected when building a power plant at the envisaged locations.

7.2.1 Building dimensions

The final building dimensions will be determined by the vendors. For the first estimate of the settlement and bearing capacity the following building dimensions are used:

- Length: 100 m
- Width: 60 m
- Basement depth: 15 m below ground level

The load at foundation level was provided by the client as 690 kPa. This is equivalent to roughly 27.5 m of solid reinforced concrete.

Additionally, it is assumed that the local ground level will be raised from NAP +5 m to a platform height of NAP + 8 m before building construction starts. Raising will be done with well compacted sand.

According to the information provided, the building will be founded on a shallow foundation, i.e no piled foundation is used. Installation of piles is considered by one or more vendors. However, these piles will not be used as a direct foundation, but with the objective to enhance strength and stiffness of the subsurface. The top of these piles will be below the foundation level of the reactor building. The building will not rest directly on these piles. For the present analyses the presence of these piles will be ignored.

7.2.2 Building timeline

For the analyses the following timeline will be used:

- Year 0: start preparation site, increase surface level to desired platform height of NAP +8 m by applying a well compacted sand layer
- Year 1-3: consolidation time, to limit the residual settlements due to backfilling area to required platform height
- Year 3: start construction of the civil works. (among others: building the concrete structures)
- Year 8: start installation turbine etc.

7.2.3 Calculation methodology

The settlement calculations are performed with the program D-Settlement of Deltares. The new reactor building is modelled as a vertical load at foundation level (15 m below ground level). This is below ground water level, so the structure experiences an upward force due to the groundwater pressure at foundation level. The applied net load at foundation level is therefore reduced in order to take into account this upward force. The load is applied such that the total vertical stress at foundation level (GL – 15 m) equals the surcharge load.

Figure 7-3 provides the cross-sectional setup of the model, while Figure 7-4 provides the top view of the load. The settlements are computed at the centre of the building, i.e point 2 in Figure 7-4.

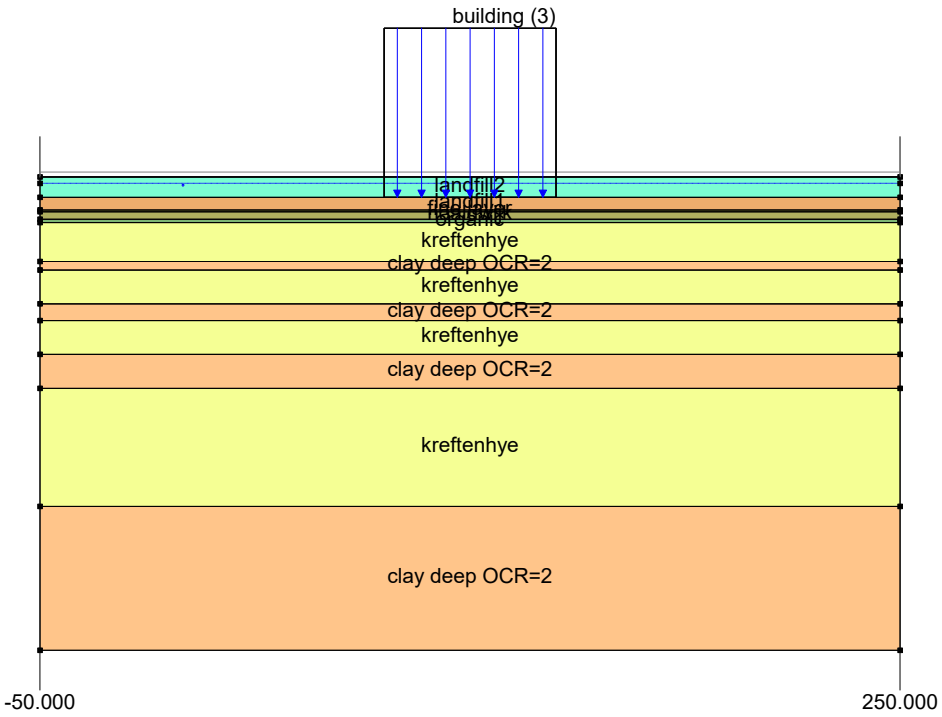

Figure 7-3 Cross section of applied load, modelled depth is 275 m

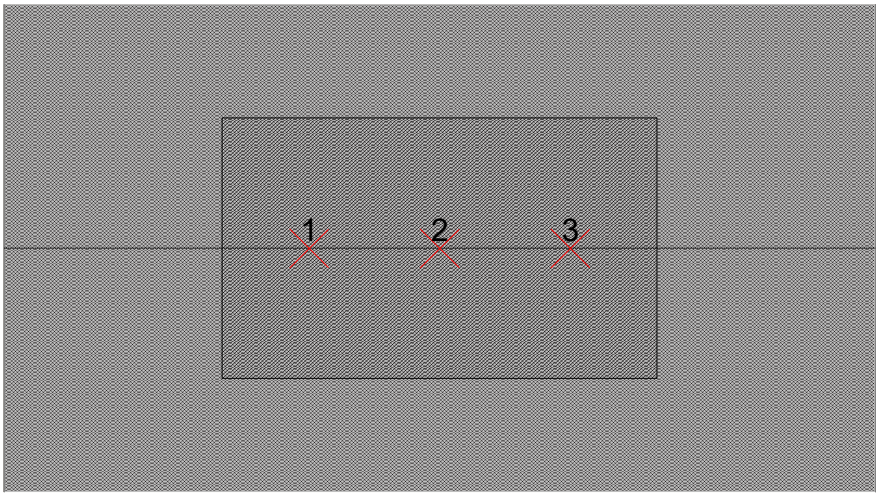

Figure 7-4 Top view of applied load

7.2.4 Settlement parameters

The settlement parameters are taken from the geotechnical parameter selection (see section 6.3). However, the contribution of the deeper clay layers (below NAP – 30 m) cannot be ignored for the calculation of the total settlement. No sufficient information on the properties of these layers is available. Therefore, some assumptions are made.

The depth and thickness of these layers are selected using the geological soil description. The settlement parameters are selected based on the given soil description and, in absence of a qualitative description, values from NEN-9997-1 for clay are used. The Dutch code NEN-9997-1 combines the Eurocode NEN-EN 1997-1 and the Dutch national annex.

Settlement behaviour of these layers greatly depends on the overconsolidation ratio (OCR). As these layers are of older age, overconsolidation due to aging will be present. For the calculations OCR = 2 is used.

7.2.5 Calculated settlement

For the settlement calculations, the deep subsurface, to a depth of NAP – 275 m, is modelled, as shown in Figure 7-3.

In the absence of data on the settlement parameters of the deep clay layers two situations are considered:

- Settlement parameters for medium stiff clay
- Settlement parameters for stiff clay

The construction time of the reactor building is taken into account by applying the load in 4 steps with a 1 year interval. The settlement as function of time at foundation level is shown in Figure 7-5.

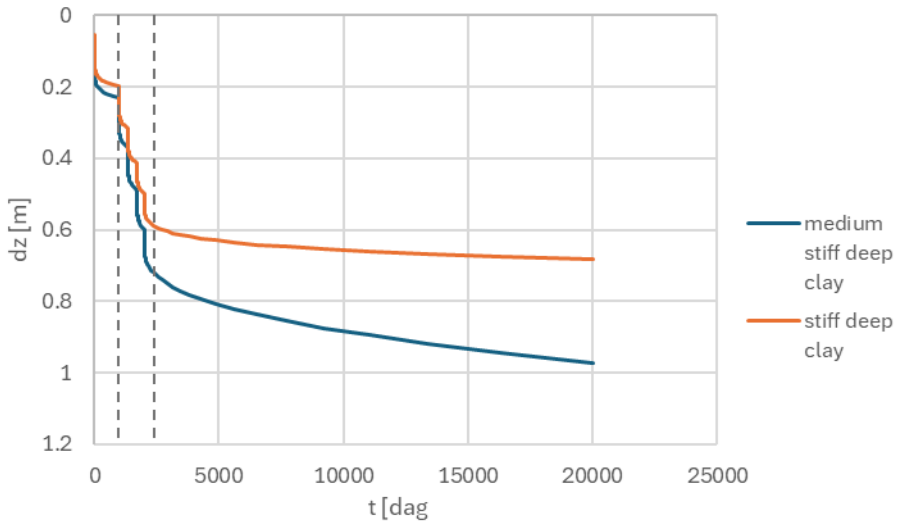

Figure 7-5 Settlement-as function of time at foundation level (z = NAP – 7 m). t = 0 days represents the start of the preparation of the site. The dashed lines indicate the start and end of the reactor construction.

The following values for the settlement are obtained:

- With deep clay modelled as medium stiff clay
  - Since start building : dz = 0.74 m
  - Since end of construction works: dz = 0.37 m
- With deep clay modelled as stiff clay
  - Since start building: dz = 0.49 m
  - Since end of construction works: dz = 0.19 m

This shows the effect of the settlement behaviour of the deep clay layers on the total settlement, and implies that these layers cannot be ignored when considering the building settlement.

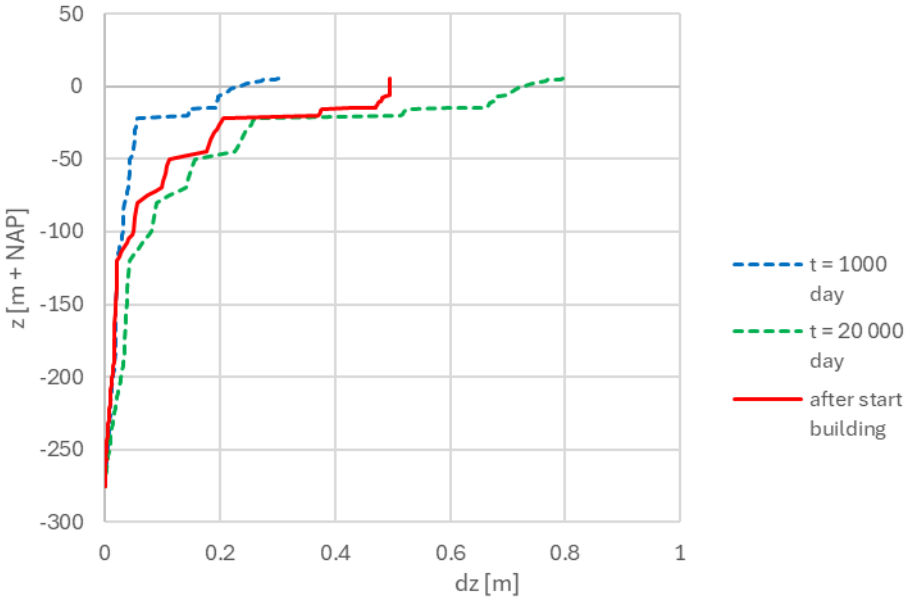

Figure 7-6 Settlement as function of depth, deep clay layers modelled as stiff clay. The red line indicates the additional settlement since the construction of the building, i.e. the difference between the green and blue lines.

A significant part of the total settlement is caused by the organic layer at NAP – 21 m. Additional soil investigation for determination of the settlement parameters of this layer can reduce the uncertainty in the expected settlement. For the situation presented in Figure 7-6 with an overconsolidated stiff deep clay, about 25% of the settlement after start building originates from the layers below NAP – 50 m. The contribution of these deeper layers to the total settlement will increase when these layers are less stiff and/or less overconsolidated. As mentioned no settlement parameters for these layers are known, and further investigation of the deeper layers is vital.

7.3 Bearing capacity

The objective of these bearing capacity calculations is to estimate the bearing capacity of the subsurface, and the result may be used to decide whether a non-piled foundation may be used or if a piled foundation is needed.

The assumed building dimensions and building timeline are provided in sections 7.2.1 and 7.2.2.

7.3.1 Calculation methodology

For the bearing capacity calculations the foundation of the structure will be considered as a shallow foundation. Bearing capacity will be assessed using the Brinch-Hansen approach, as described in the governing Dutch geotechnical code (NEN-9997-1). In the present calculations any horizontal load, e.g. due to wind, is not taken into account.

According to the Dutch code NEN-9997-1 the settlement of the building should be within certain limits. For this report the check on settlement is omitted when checking the bearing capacity, as these settlements are already calculated in section 7.2.

The calculations are performed with the program D-Foundation of Deltares.

7.3.2 Soil parameters

The used soil parameters are taken from the geotechnical parameter selection, see section 6.2. For the deeper soil layers an estimate is made, using the given soil description.

In the calculations the applicable partial factors, as prescribed in NEN-9997-1, are used. These are:

- Angle of internal friction: 1.15
- Effective cohesion: 1.6
- Undrained shear strength: 1.35

No partial factor on the load is applied as these calculations are for comparative purposes.

7.3.3 Bearing capacity calculation

For the bearing capacity calculations two soil profiles are considered. The difference between the considered soil profiles is the soft layer at NAP – 15m, which is not present over the total area. Figure 7-7 and Figure 7-8 show the used soil profiles.

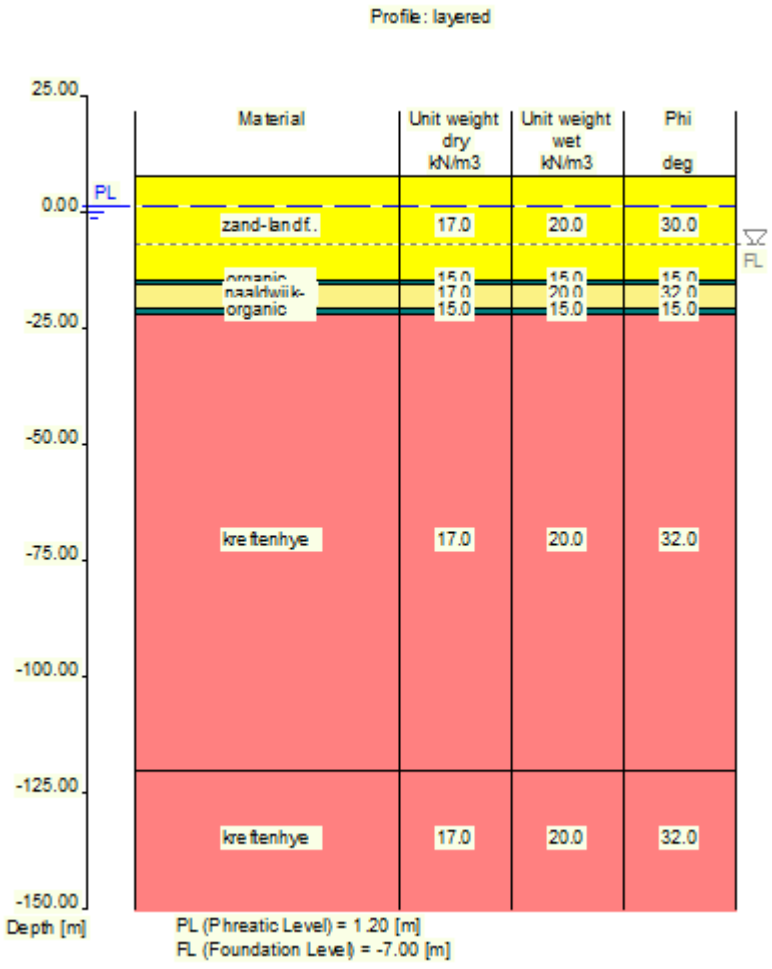

Figure 7-7 Soil layering used in bearing capacity calculation. All older sediments are labelled Kreftenheye in this figure, because they were all given the same parameter value. In reality (see Figure 4-1), the older sediments consists of several geological formations.

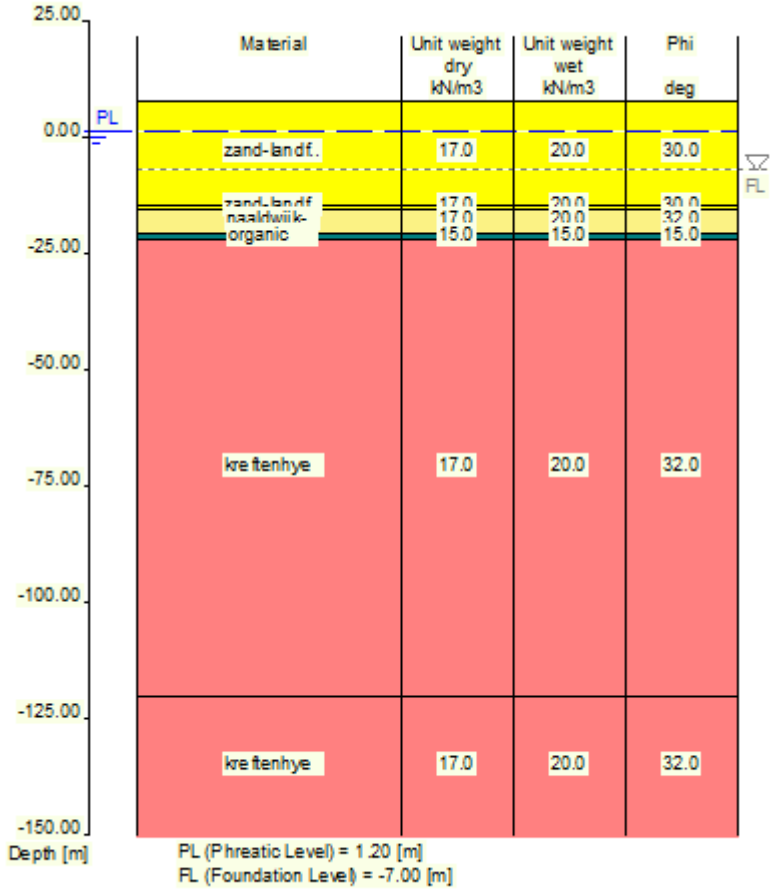

Figure 7-8 Soil layering used in bearing capacity calculation. All older sediments are labelled Kreftenheye in this figure, because they were all given the same parameter value. In reality (see Figure 4-1), the older sediments consists of several geological formations.

The following values for the total bearing capacity are calculated:

- Situation with two soft layers (Figure 7-7): q = 632 kPa
- Situation with one soft layer (Figure 7-8): q = 661 kPa.

The bearing capacity is close to the load provided by the client. The bearing capacity with two soft layers is governed by the punch-trough mechanism of the first soft layer at NAP – 15 m. From the second calculation it follows that the bearing capacity is governed by the punch-trough mechanism of the soft layers at NAP – 21 m. In other words, the bearing capacity is governed by the two soft layers.

The punch-trough mechanism is a standard check required by the Dutch code NEN-9997-1. Given the limited thickness of the layer, the long expected construction time, and the dimensions of the building, it is doubtful whether punch-trough is realistic for this situation. Therefore, a third scenario has been calculated ignoring these layers, which results in a total bearing capacity exceeding 6400 kPa. Further investigation, with for example finite element calculations of the construction, are required on the impact of these soft layers.

8 Seismic hazards

8.1 Faults in the vicinity of MV2

The MV2 site lies on the southern edge of the West Netherlands Basin (WNB), a subregion of the wider North Sea Basin (Figure 3-1). It is not known as a tectonically active region. This is evidenced by the instrumental (since 1911) and historical (since 1142) records that indicate no recent earthquake activity in the region (see Kruiver & Spetzler, 2024).

Figure 8-1 shows that within a distance of 100 km only a few earthquakes are present in the KNMI-database (KNMI, 2025). Most earthquakes occur around the active bounding faults of the Roer-Valley Graben (RVG) in the southeast of the Netherlands (Figure 3-1). The nearest point of the geologically active Gilze-Rijen Fault on the western side of the RVG is located approximately 55 km to the east of Maasvlakte 2. The Peel Boundary Fault on the eastern side of this actively subsiding region is located 90 km away. Among the larger recorded earthquakes are the Uden earthquake from 1932 (Richter-Magnitude (ML) of 5; 100 km distance from MV2) and the Roermond earthquake from 1992 (ML of 5.8; 160 km distance). Farther towards the southwest, the Sangatte Fault in northern France is the next nearest active fault at 180 km distance.

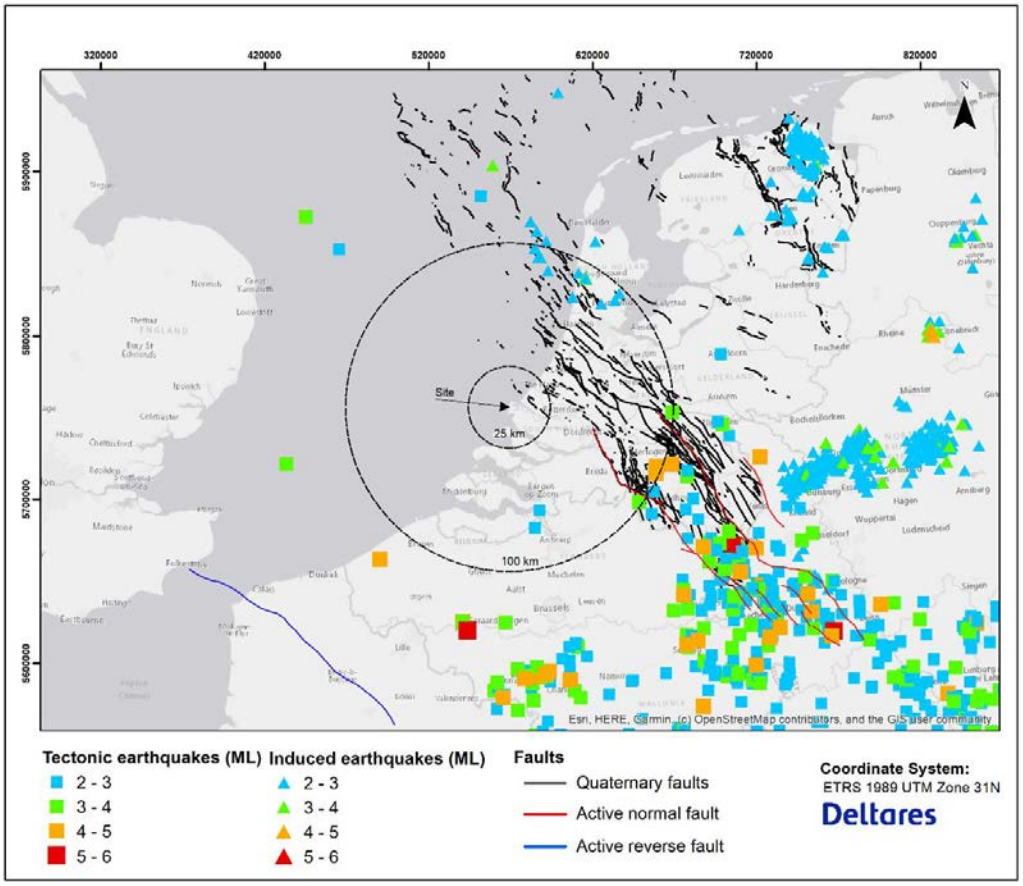

Figure 8-1 Regional map with the location of the MV2 site and the tectonic and induced earthquakes from the KNMI-database, including their local Richter-Scale magnitude (ML). Also indicated are the Dutch Quaternary faults in the upper 500 m from the HIKE-database and the active faults according to the EFSM.

At a local scale, the subsurface site evaluation based on all currently available CPTs and borehole descriptions did not suggest any faults in the geological record at the MV2 site. This is supported by the regional geological mapping at the surface and in the subsurface as compiled in Dutch regional subsurface models GeoTOP and REGIS/DGM. These models do not require the presence of faults to explain any of the geological data for the last millions of years. In deeper lying layers, however, a fault of the Jurassic Altena Group can be identified that crosses the MV2 site (Figure 8-2).

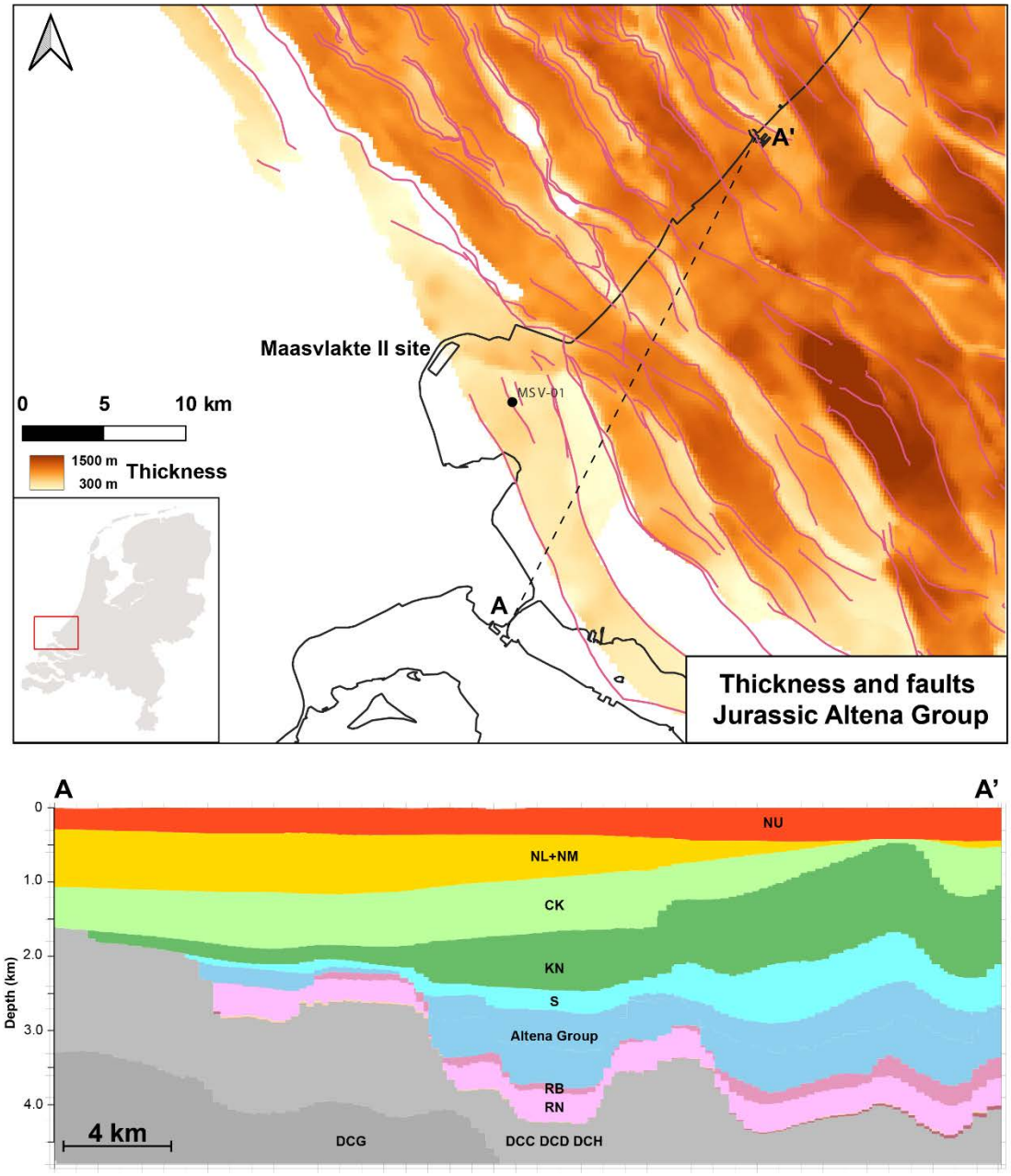

Figure 8-2 Top: thickness of the Jurassic Altena Group in the region around the MV2 site. Thickness of the deposited sedimentary rocks varies between 300 and 1500 m thick with numerous NW-SE oriented faults (in pink) separating individual sub-basins. Map based on DGMDeep5 (https://www.nlog.nl/en/dgm-deep-v5-and-offshore). Bottom: Cross-section A-A' oriented SSW-NNE in the vicinity of the MV2 site highlighting the subsurface build-up at group level. Note the depth of the Altena Group of which the faults are indicated in the top panel. Location of line A-A' is indicated on the top panel.

Nearby faults active during the Quaternary (most recent 2.6 million years) are largely constrained to the Roer-Valley Graben and its northwestern propagation underneath the North Sea (Figure 3-1). Tectonic earthquakes were rarely recorded in this region, with only one ML 2 to 3 earthquake recorded underneath the North Sea. A small number of induced earthquakes (ML 2 to 3) have been recorded in this region, likely related to hydrocarbon extraction. Farther to the north, a larger number of induced earthquakes (mainly ML 2 to 3) have been recorded in the north of the Netherlands related to hydrocarbon extraction in the major Groningen gas field.

At a site vicinity scale of the MV2 site the subsurface site evaluation based on all currently available CPTs and borehole descriptions did not suggest the presence of any faults in the geological record of the past 5 million years. This is supported by the regional geological mapping at the surface and in the subsurface as compiled in Dutch regional subsurface models GeoTOP and REGIS/DGM. These models do not require the presence of faults to explain any of the geological data for the last millions of years.

Deeper in the subsurface faults are present near the MV2 locality. For construction purposes, these faults do not need to be considered. They are geologically inactive and are located at depths greater than 2000 m (Figure 8-2). They date back to the Jurassic period (Altena Group) and are about 200 million years old. At the time, regionally extensive rifting occurred, forming the Central Netherlands Basin. Notably the MV2 site is located directly on top of the southwestern flank of this extensional basin.

Induced seismicity due to recent geothermal activities or the extraction of gas in the nearby gas fields in the North Sea has not been accounted for within this overview. Further investigation is required to estimate their impact. Note that, the gas extraction within this vicinity is small when compared to the extraction in Groningen.

8.2 Initial assessment of liquefaction potential

As no results of a recent site-specific seismic hazard analysis are available, indicative values for the seismic loading are used. Note that a full Probabilistic Seismic Hazard Analysis according to the latest scientific standards and SSHAC recommendations is recommended. The properties used are derived from the hazard curve shown in Figure 8-3. The vertical lines indicate a PGA of 0.065, 0.21 and 0.55 g, which correspond to yearly probability of exceedance of 10^{-4},10^{-5} and 10^{-6} respectively.

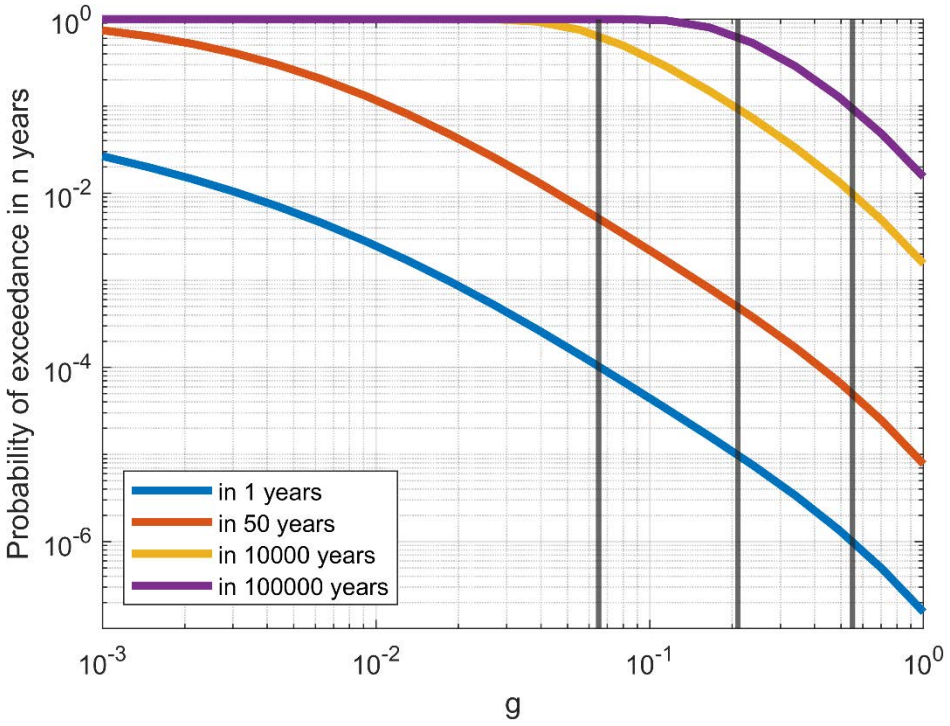

Figure 8-3 PGA Hazard Curves for MV2. Derived from the publicly available European Seismic hazard model ESHM20 (Danciu et al., 2021). The curves have been derived with the following settings: Longitude 3.982, Latitude 52.000, ESHM20, PGA, rock_vs_30_800ms-1 and the arithmetic mean.

The PGA determined in Figure 8-3 represents the acceleration at MV2 at bedrock level. According to Eurocode 8-1 (2004), in combination with n the local soil conditions, an amplification factor of 1.15 is used, such that the PGA at ground level becomes PGA = 0.075g. The moment magnitude (Mw) is used as an indication of the duration of the vibrations. Theoretically, the moment magnitude that correlates with the most impactful PGA's at the site should be used. However, further investigation is required to derive these earthquake statistics. Here, a conservative estimate of Mw = 6 is used based on the earthquake in Roermond in 1992, the largest measured earthquake in NW Europe, with measured Mw = 5.3 (Braunmiller et al., 1994).

To summarize, the following seismic parameters are used for the preliminary assessment:

- PGA = 0.075 g (higher than the value used for the stress test for Borssele NPP)
- Mw = 6 (which is conservative when compared to the earthquake in Roermond in 1992, but again, a full PSHA will be needed to detail this).

The approach outlined by Boulanger & Idriss (2014) is used as liquefaction model. In the analyses no thin layer correction or any other correction for the measured cone resistance at layer boundaries is applied. This may underestimate the cone resistance, and thus overestimate the risk of liquefaction, in strongly layered soils. Results are shown in the next figures for the three subareas. A groundwater level of 1.2 m NAP is used. No liquefaction will

occur in the soil layers above the groundwater level. Additionally, the current ground level is used in the approach. Raising the ground level will increase the effective soil stress, thereby reducing the liquefaction potential. Subarea 2 is not modelled, since the soil conditions for liquefaction will not be representative of the final configuration once the landfill has been completed. Therefore, the liquefaction potential of subareas 1 and 3 is more representative for subarea 2. The figures below provide the Factor of Safety (FS) against liquefaction. If FS is higher than one, liquefaction will most likely not occur given the seismic conditions.

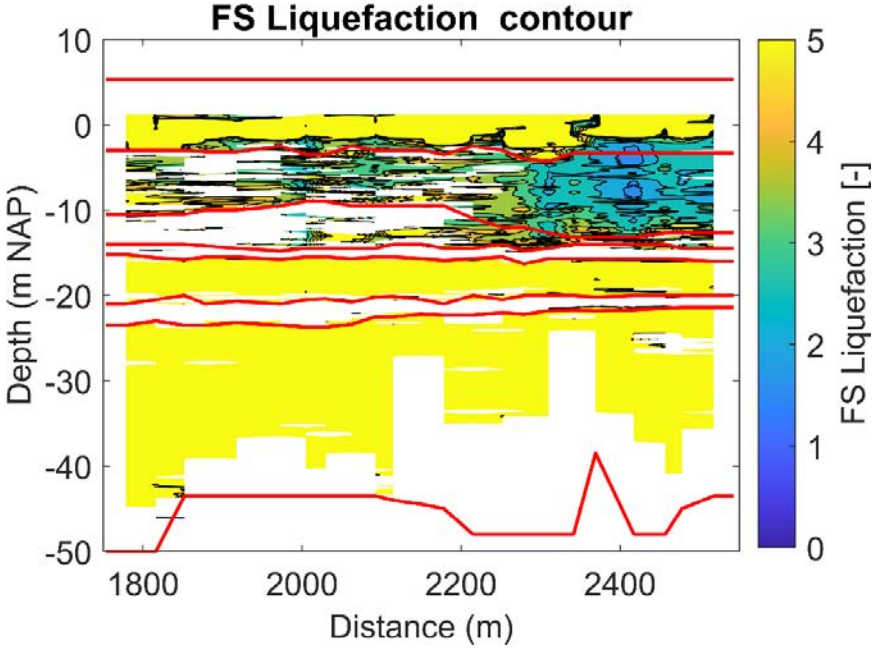

Figure 8-4 Liquefaction assessment of Subarea 1 based on the closest CPTs. The liquefaction potential is only assessed for sand and silt layers, clayey parts thus remain white.

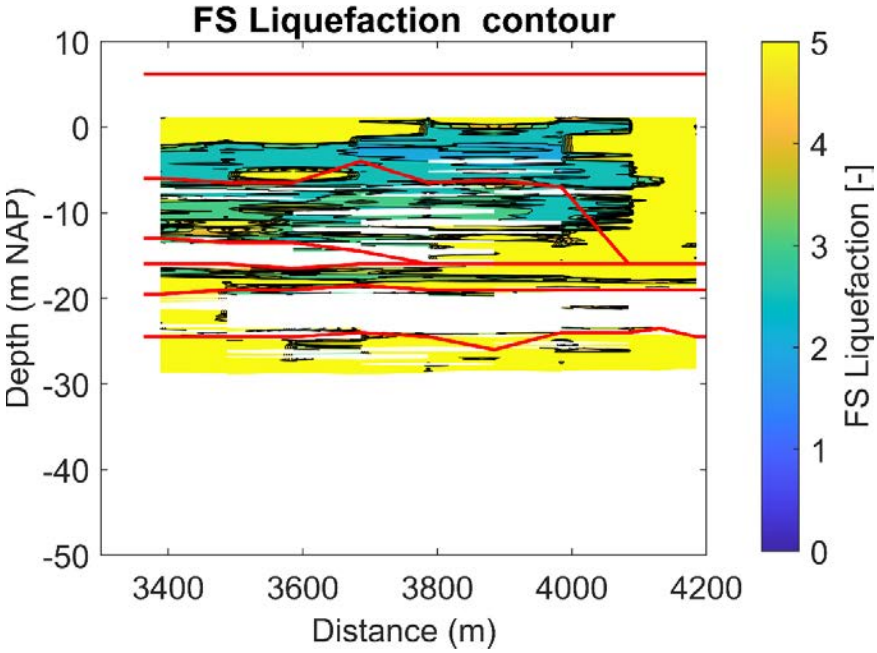

Figure 8-5 Liquefaction assessment of Subarea 3 based on the closest CPTs. The liquefaction potential is only assessed for sand and silt layers, clayey parts thus remain white.

The landfill has the lowest factors of safety, but since FS is mostly higher than 2, the risk for liquefaction is generally very low. Especially near the bottom of the landfill, however, the sand

is in a looser state. However, due to the low expected earthquake loads, liquefaction is still not expected. The denser Naaldwijk and Kreftenheye Formations below the landfill are unlikely to trigger liquefaction.

Additionally the liquefaction assessment is performed for Subarea 1 with the higher PGA values of 0.24 g (Figure 8-6) and 0.63 g (Figure 8-7). These studies indicate the liquefaction potential for rare earthquakes. Especially, the landfill may be prone to liquefaction at these higher earthquake loads. However, given the low likelihood of these events, further investigation is required to better estimate the earthquake loads and effects. According to Figure 8-7, also the lower layers must be investigated, as liquefaction may be triggered during the extreme load of 0.63 g.

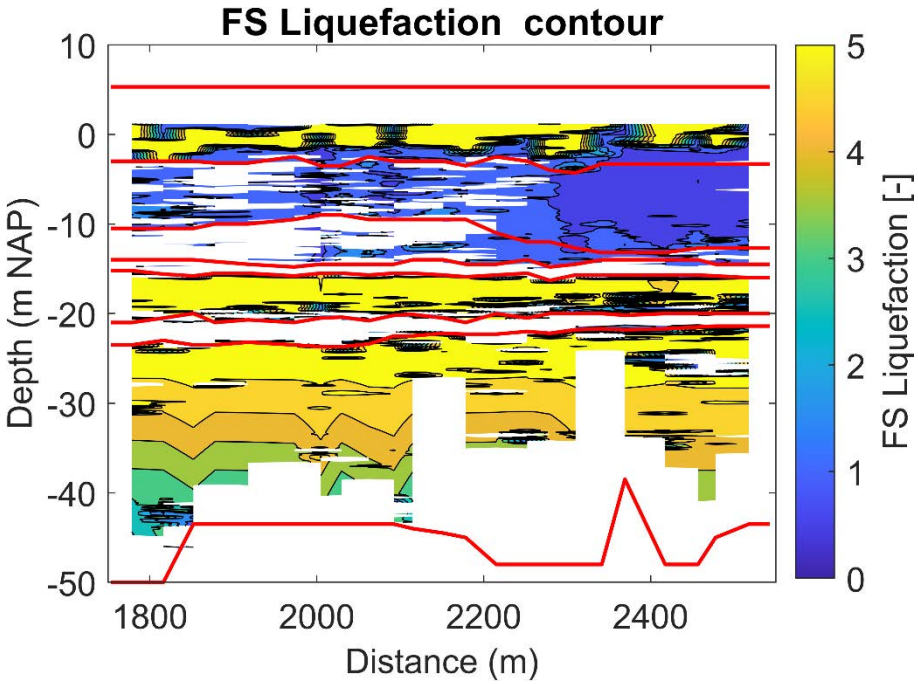

Figure 8-6 Liquefaction assessment with PGA = 0.24 g at ground level, a yearly probability of exceedance of 10^{-5}, of Subarea 1 based on the closest CPTs. The liquefaction potential is only assessed for sand and silt layers, clayey parts thus remain white.

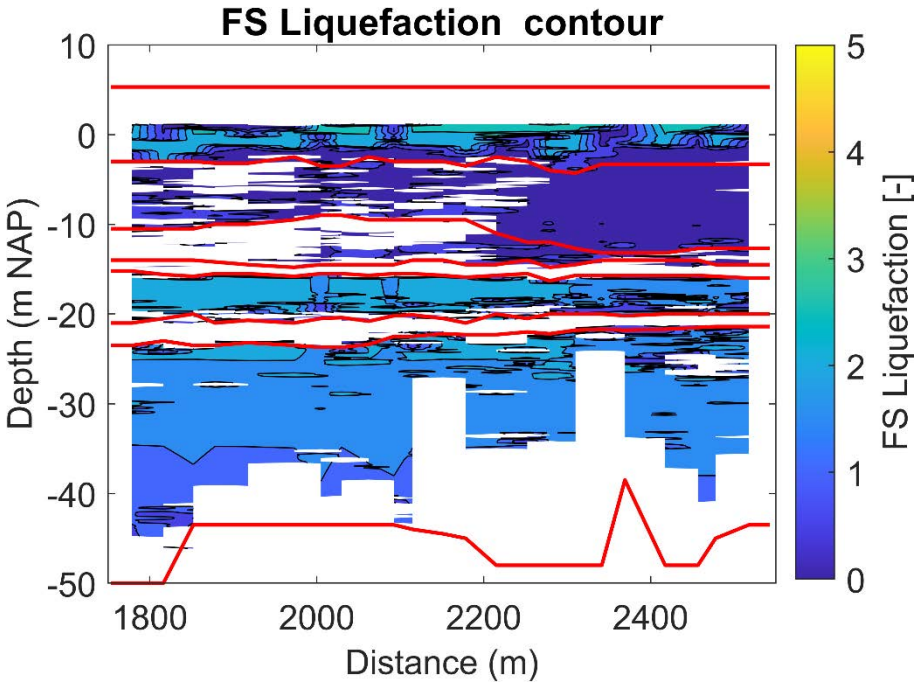

Figure 8-7 Liquefaction assessment with PGA = 0.63 g at ground level, a yearly probability of exceendance of 10^{-6}, of Subarea 1 based on the closest CPTs. The liquefaction potential is only assessed for sand and silt layers, clayey parts thus remain white.

9 Volcanic risks

No volcanic activity is known to have taken place in the Netherlands during the last 10 Ma. In this section we will discuss the nearest regions that were volcanically active during the Holocene and Pleistocene. This is far from a complete study on all volcanic activity in northwestern Europe, but within the scope of the current report it provides first insights towards a potential volcanic hazard risk assessment for the MV2 site.

9.1 Western and Eastern Eifel Volcanic Fields

The nearest volcanoes are the West and East Eifel Volcanic Fields in Germany. The West Eifel Volcanic Field is located southwest of Bonn and the East Eifel Volcanic Field is situated approximately 40 km to the northeast (Bogaard & Schmincke, 1985). These regions are located approximately 275 km to the southeast of the MV2 site.

Volcanic activity in the West and East Eifel Volcanic Fields first took place during the early parts of the Neogene, approximately until the late Miocene. After a quiet period, volcanic activity restarted in the Quaternary at 850 ka. The last eruption of the East Eifel Volcanic Field was at the Laacher See at approximately 12.9 ka. The last eruption of the West Eifel Volcanic Field was approximately 11 ka due to the Ulmener Maar (Förster & Sirocko, 2016; Hensch et al., 2019). Given this relatively recent age, these volcanic fields are considered active on geological time scales according to the IAEA guidelines (Committee & Connor, 2012) and should therefore be considered for the MV2 site.

The West Eifel Volcanic Field contains scoria cones, maars (tuff rings) and small stratovolcanoes. The East Volcanic Field contains scoria cones, maars, lava flows and the three larger caldera complexes of Wehr, Rieden and Laacher See volcano (Förster & Sirocko, 2016). Volcanic phenomena which occurred include tephra fall out, lava flows, slumps triggered by volcanic earthquakes or base surges. Tephra fall out is one of the volcanic phenomena which can have relatively large travel distances. During the large eruption of the Laacher See volcano about 20 km^3 of tephra was produced (Global Volcanism Program, 2024). Figure 9-1 shows the different lobes of the tephra deposits of the Laacher See volcano, which can be found close to the border of the province of Limburg in the southeasternmost part of the Netherlands. Maps of the areal distribution of ash layers in Bogaard & Schmincke (1985) show similar patterns as in Figure 9-1.

All other volcanically active regions in Europe are schematically indicated in Figure 9-2. These are all located farther from the MV2 site and include the volcanoes at the Massif Central in France (~600 km) and the Icelandic volcanoes (~1800 km). Since the historical effects of these volcanoes did not reach the Netherlands to a significant degree, we will only briefly mention them.

9.2 Chaîne des Puys

Holocene volcanic activity has taken place in the Chaîne des Puys, situated in the Massif Central, France. This chain consists of 80 cinder cones, maars and lava domes.
Latest volcanic activity occurred at approximately 8.6 ka during the eruption of the La Vache and Lassolas cone complex. This was also one of the most powerful eruptions of the Chaîne des Puys. Tephra and lava flow deposits of this eruption were found in the surrounding dozens of kilometres within the Chaîne des Puys (Jordan et al., 2016).

9.3 Icelandic volcanoes

Effects of eruptions of Icelandic volcanoes such as the eruption of the Eyjafjallajökull volcano in Iceland in 2010 were relatively limited in the Netherlands. This eruption led to disruption of the air traffic in Europe due to the large volcanic ash cloud (>8 km height; Petersen et al., 2012). The size of the ash particles that reached northwestern Europe were only submillimeter to tens of nanometers in size (Gislason et al., 2011).

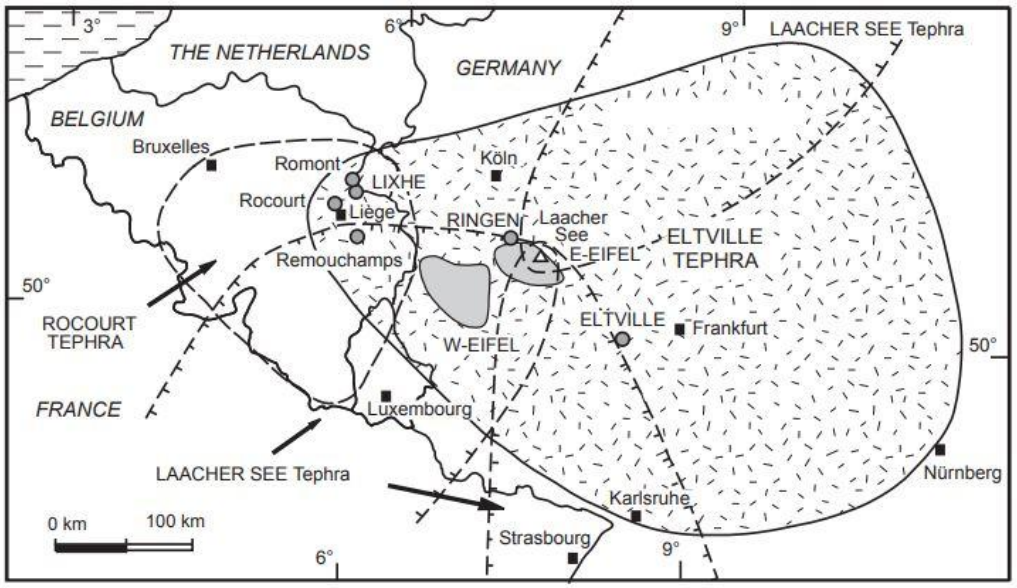

Figure 9-1 Lobes of the Lacher See tephra deposits (Pouclet & Juvigné, 2009).

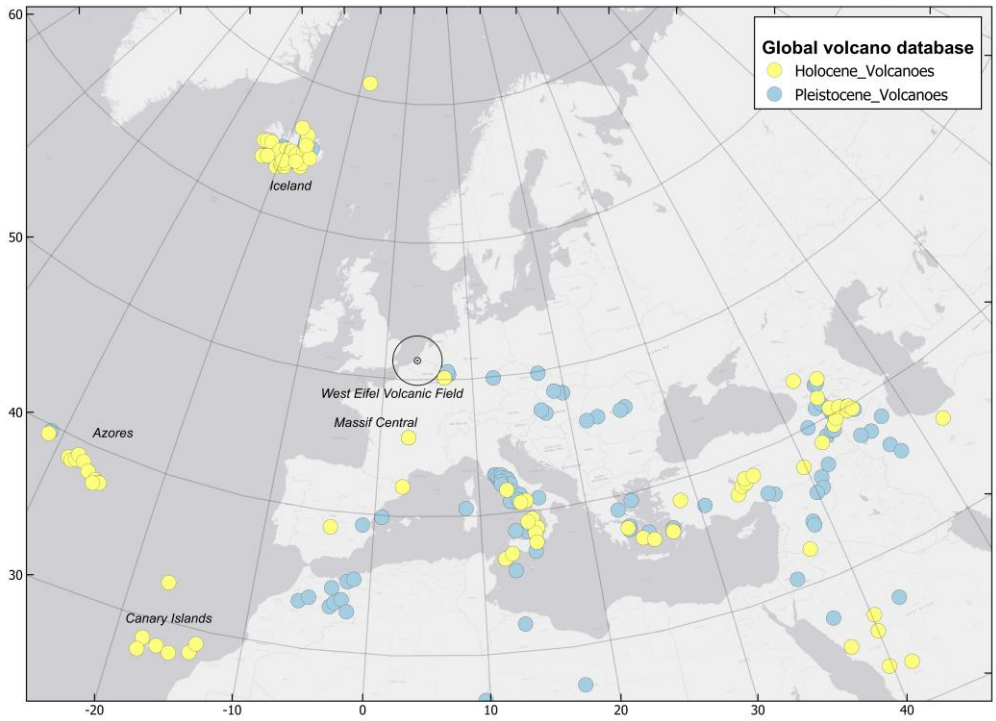

Figure 9-2 Holocene and Pleistocene volcanoes in and around Europe, based on the Smithsonian Institution's Global Volcanism Program database (Global Volcanism Program, 2024).

10 Conclusions and recommendations

10.1 Site evaluation

The site evaluation focused on the build-up and properties of the subsurface, but has also addressed potential risks associated with subsidence, settlements, bearing capacity, seismicity and volcanic activity. With respect to subsidence, seismicity and volcanic activity, no major upfront constraints for the development of MV2 were identified. Relative high rates of subsidence and low relative densities of the landfill do indicate, however, that the landfill is not yet consolidated and additional subsidence can be expected in the coming years. Since parts of the site are still water, these parts will be filled in as well when a NPP is built and will need time to consolidate as well. An additional point to consider is that plans for a third Maasvlakte are presently constructed which may impact MV2 as well.

The bearing capacity of the subsurface is below the given surcharge load of the reactor building, based on the preliminary investigation. Due to the given load of the reactor building large settlements, in the order of 0.5 m, during and after construction are expected. The expected settlements and the bearing capacity are uncertain due to a lack of site specific lab testing, a lack of information on deeper clay layers, and unclear building dimensions. Additionally, soil improvement has not been accounted for in this preliminary study.

In terms of the shallow subsurface the site can be geotechnically divided into three areas (Figure 6-1). In subareas 1 and 3 the landfill starts at about 5 m NAP, while in subarea 2 water is present and the landfill starts at -5 to -8 m NAP. The landfill in subarea 1 consists of three layers: a sandy top layer with high cone resistances, a middle layer with small clay and sand layers and lower cone resistances and a bottom layer with increasingly more fine layer. In subarea 2 the landfill has relatively low cone resistances and contains loose silty sand and clay layers. In subarea 3 the landfill has lower cone resistances than in subarea 1, perhaps because it was constructed more recently. In the landfill cone resistance increase towards the northeast.

Below the landfill a mostly sandy unit is present, in general consisting of shoreface deposits from the Southern Bight Formation on top of tidal deposits from the Naaldwijk Formation. The shoreface deposit is 0.5-1.0 m thick. The Naaldwijk Formation is more heterogenous, relatively fine and shows frequent alternations between clay/silt and sand. At locations of former tidal channels the Naaldwijk Formation is thickest and lies incised into the Kreftenheye Formation, locally to depths of nearly -30 m NAP.

The Naaldwijk Formation is underlain by a complex sequence of clayey freshwater-tidal fluvial deposits (Echteld Formation), a peat layer (Basal Peat Bed of Nieuwkoop Formation) and a loamy and stiff overbank deposit from the Kreftenheye Formation (Wijchen Member) and aeolian river dunes (Delwijnen Member). The dunes are known for their archaeological importance and it needs to be taken into account that additional geoarchaeological research may need to be executed when disturbed during the construction of the NPP. The Kreftenheye Formation below is 20-25 m thick and consists of stacked sandy deposits from both meandering and braided rivers. Cone resistance values indicate the Kreftenheye Formation consists of well compacted sands.

From public resources, there is no piezometric measurement available at the project site. With the Dutch Hydrological Model a simulation of groundwater is computed, indicating average groundwater levels between 0.5 and 1.0 m NAP, with fluctuations of 0.1 m between

seasons and of 0.5 m between years. Daily fluctuations due to the influence of the tidal cycle can be expected. It is expected that tidal effects influence the groundwater level on a hourly base. The salt concentration in the uppermost part of the subsurface is simulated to be currently ~2.0 g/l. It is expected that in 2045 a six metre thick freshwater lens will be present.

10.2 Recommendations

Based on the current assessment of the subsurface at the MV2 site and the regional geological setting no additional subsurface data is needed. When an actual NPP will be built at MV2, detailed subsurface information will be needed (also depending on how the NPP will be constructed), but this can be planned in a later stage. Attention should be given to the (deeper) soft layers, and additional studies regarding the settlement and bearing capacity must be performed.

To characterize the geohydrological situation, more data is needed urgently. At this point it is advisable to already install monitoring wells with filters at different depths to measure the piezometric head. Monitoring should continue for at least one year to capture seasonal effects.

For the potential risks associated with seismic hazards, a full Probabilistic Seismic Hazard Analysis is recommended. Based on preliminary assumptions it is concluded that the risk of full liquefaction is very low for earthquake events with a recurrence interval 10.000 years, but that during larger earthquakes liquefaction may occur.

In our view, a full PSHA and more insight into the plans for a third Maasvlakte would be essential information when ranking the four proposed locations in terms of suitability. The other attention points can be addressed in a later phase.

References

Bogaard, P.V., Schmincke, H.-U., 1985. Laacher See Tephra: A widespread isochronous late Quaternary tephra layer in central and northern Europe. Geological Society of America Bulletin, 96 (12), 1554-1571.

Bosch, J., 2000. Standaard Boorbeschrijvingsmethode: versie 5.1. Nederlands Instituut voor Toegepaste Geowetenschappen TNO.

Boulanger, R.W., Idriss, I.M., 2014. CPT and SPT based liquefaction triggering procedures. Report No. UCD/CGM.-14, 1, 134.

Braunmiller, J., Dahm, T., Bonjer, K.-P., 1994. Source mechanism of the 1992 Roermond, the Netherlands, earthquake from inversion of regional surface waves. Netherlands Journal of Geosciences, 73, 225-227.

CEN, 2004. Eurocode 8: Design of structures for earthquake resistance-part 1: general rules, seismic actions and rules for buildings. Brussels: European Committee for Standardization.

Cohen, K.M., Stouthamer, E., Pierik, H.J., Geurts, A., 2012. Digitaal Basisbestand Paleogeografie van de Rijn-Maas Delta / Rhine-Meuse Delta Studies' Digital Basemap for Delta Evolution and Palaeogeography. Dept. Physical Geography. Utrecht University. Digital Dataset.

Committee, Connor, C.B., 2012. Volcanic Hazards in Site Evaluation for Nuclear Installations. School of Geosciences Faculty and Staff Publications 789. https://digitalcommons.usf.edu/geo_facpub/789.

Copernicus Land Monitoring Service, 2024. European Ground Motion Service: Basic 2019-2023 (vector), Europe. https://egms.land.copernicus.eu/. https://doi.org/10.2909/7eb207d6-0a62-4280-b1ca-f4ad1d9f91c3.

Danciu, L., Nandan, S., Reyes, C.G., Basili, R., Weatherill, G., Beauval, C., Rovida, A., Vilanova, S., Sesetyan, K., Bard, P.-Y., 2021. The 2020 update of the European Seismic Hazard Model-ESHM20: model overview, EFEHR Technical Report.

DCMR Milieudienst Rijnmond, 2024. Integrale rapportage visie en vertrouwen 2024. Afsprakenkader Borging Project Mainportontwikkeling Rotterdam

de Jager, J., 2003. Inverted basins in the Netherlands, similarities and differences. Netherlands Journal of Geosciences - Geologie en Mijnbouw, 82 (4), 339-349. 10.1017/S0016774600020175.

De Mulder, E.F.J., Geluk, M.C., Ritsema, I.L., Westerhoff, W.E., Wong, T.E., 2003. De ondergrond van Nederland. NITG-TNO, Utrecht.

Doornenbal, P.J., 2023. Uitwerkingen boorgatmetingen Rotterdam World Gateway, Deltares report 11207991-006-BGS-0004.

Förster, M.W., Sirocko, F., 2016. The ELSA tephra stack: Volcanic activity in the Eifel during the last 500,000years. Global and Planetary Change, 142, 100-107. https://doi.org/10.1016/j.gloplacha.2015.07.012.

Fugro, Deltares, Waterschap Hollandse Delta, 2020. Onderzoeksproject Anisotropie - Eindrapportage, Fugro rapportnummer 1217-0051-000.R17 | 6-11-2020.

Gislason, S.R., Hassenkam, T., Nedel, S., Bovet, N., Eiriksdottir, E.S., Alfredsson, H.A., Hem, C.P., Balogh, Z.I., Dideriksen, K., Oskarsson, N., Sigfusson, B., Larsen, G., Stipp, S.L.S., 2011. Characterization of Eyjafjallajökull volcanic ash particles and a protocol for rapid risk assessment. Proceedings of the National Academy of Sciences, 108 (18), 7307-7312. doi:10.1073/pnas.1015053108.

Global Volcanism Program, 2024. [Database] Volcanoes of the World (v. 5.2.7; 21 Feb 2025). Distributed by Smithsonian Institution, compiled by Venzke, E. https://doi.org/10.5479/si.GVP.VOTW5-2024.5.2.

Hensch, M., Dahm, T., Ritter, J., Heimann, S., Schmidt, B., Stange, S., Lehmann, K., 2019. Deep low-frequency earthquakes reveal ongoing magmatic recharge beneath Laacher See Volcano (Eifel, Germany). Geophysical Journal International, 216 (3), 2025-2036. 10.1093/gji/ggy532.

Hijma, M.P., Cohen, K.M., Hoffmann, G., Van der Spek, A.J.F., Stouthamer, E., 2009. From river valley to estuary: the evolution of the Rhine mouth in the early to middle Holocene (western Netherlands, Rhine-Meuse delta). Netherlands Journal of Geosciences - Geologie en Mijnbouw, 88 (1), 13-53.
Hijma, M.P., Cohen, K.M., 2010. Timing and magnitude of the sea-level jump preluding the 8200 yr event. Geology, 38 (3), 275-278.
Hijma, M.P., Cohen, K.M., Roebroeks, W., Westerhoff, W.E., Busschers, F.S., 2012. Pleistocene Rhine-Thames landscapes: geological background for hominin occupation of the southern North Sea region. Journal of Quaternary Science, 27 (1), 17-39. 10.1002/jqs.1549.
Hijma, M.P., Cohen, K.M., 2019. Holocene sea-level database for the Rhine-Meuse Delta, The Netherlands: Implications for the pre-8.2 ka sea-level jump. Quaternary Science Reviews, 214, 68-86. doi.org/10.1016/j.quascirev.2019.05.001.
Hijma, M.P., 2022. Bodemdalingsmonitor 2022 Kustfundament en de getijdenbekkens - Overzicht onderzoek 2018-2021, Deltares report 11208035-003-ZKS-0003.
Hijma, M.P., Bradley, S.L., Cohen, K.M., van der Wal, W., Barlow, N.L.M., Blank, B., Frechen, M., Hennekam, R., van Heteren, S., Kiden, P., Mavritsakis, A., Meijninger, B.M.L., Reichart, G.-J., Reinhardt, L., Rijsdijk, K.F., Vink, A., Busschers, F.S., 2025. Global sea-level rise in the early Holocene revealed from North Sea peats. Nature, 639 (8055), 652-657. 10.1038/s41586-025-08769-7.
Hoek, W.Z., 2001. Vegetation response to the ~14.7 and ~11.5 ka cal. BP climate transitions: is vegetation lagging climate? Global and Planetary Change, 30 (1-2), 103-115.
Hoek, W.Z., 2008. The Last Glacial-Interglacial transition. Episodes, 31 (2), 226-229.
Janssen, G., Vermeulen, P., Van Walsum, P., Prinsen, G., Nogueira, G.E.H., Verkaik, J., Delsman, J., Kok, H., Leander, R., Klapwijk, E., Kroon, T., 2025. Veranderingsrapportage LHM 4.3.3 - De nieuwe release van het Landelijk Hydrologisch Model in het voorjaar van 2025, Deltares report 11211537-001-BGS-0001.
Jordan, S.C., Le Pennec, J.L., Gurioli, L., Roche, O., Boivin, P., 2016. Highly explosive eruption of the monogenetic 8.6ka BP La Vache et Lassolas scoria cone complex (Chaîne des Puys, France). Journal of Volcanology and Geothermal Research, 313, 15-28. https://doi.org/10.1016/j.jvolgeores.2015.12.006.
KNMI, 2025. Aardbevingcatalogus. https://www.knmi.nl/kennis-en-datacentrum/dataset/aardbevingscatalogus.
Kruiver, P.P., Spetzler, J., 2024. Seismological quickscan for Borssele - Available data and recommendations for approach, Royal Netherlands Meteorological Institute.
Lengkeek, H.J., De Greef, J., Joosten, S., 2018. CPT based unit weight estimation extended to soft organic soils and peat, Cone Penetration Testing 2018. CRC Press, pp. 389-394.
Lunne, T., Christoffersen, H.P., 1983. Interpretation of Cone Penetrometer Data for Offshore Sands, Offshore Technology Conference.
Michon, L., Van Balen, R.T., Merle, O., Pagnier, H., 2003. The Cenozoic evolution of the Roer Valley Rift System integrated at a European scale. Tectonophysics, 367 (1-2), 101-126.
Moree, J.M., Sier, M.M. (Eds.), 2015. Interdisciplinary Archaeological Research Programme Maasvlakte 2, Rotterdam BOORrapporten 566.
Moree, J.M., van Trierum, M.C., Carmiggelt, A., Bureau Oudheidkundig Onderzoek Rotterdam, Gemeente Rotterdam. Archeologie Rotterdam, 2018. Onderzoeksagenda Archeologie van de gemeente Rotterdam (ROA): prehistorie en Romeinse tijd. Archeologie Rotterdam (BOOR).
NCG, SkyGeo, TU Delft, 2025. Bodemdalingskaart 2.0. Geraadpleegd in februari 2025. https://bodemdalingskaart.nl/nl/.
Petersen, G.N., Bjornsson, H., Arason, P., 2012. The impact of the atmosphere on the Eyjafjallajökull 2010 eruption plume. Journal of Geophysical Research: Atmospheres, 117 (D20). https://doi.org/10.1029/2011JD016762.

Pouclet, A., Juvigné, E., 2009. The Eltville Tephra, a late pleistocene widespread tephra layer in Germany, Belgium and Netherlands; Symptomatic compositions of the minerals. Geogica Belgica, 12 (1-2), 93-103.
Rasmussen, S.O., Andersen, K.K., Svensson, A.M., Steffensen, J.P., Vinther, B.M., Clausen, H.B., Siggaard-Andersen, M.L., Johnsen, S.J., Larsen, L.B., Dahl-Jensen, D., Bigler, M., RÃ¶thlisberger, R., Fischer, H., Goto-Azuma, K., Hansson, M.E., Ruth, U., 2006. A new Greenland ice core chronology for the last glacial termination. Journal of Geophysical Research, 111 (Journal Article), D06102-D06102.
Robertson, P.K., 1990. Soil classification using the cone penetration test. Canadian Geotechnical Journal, 27 (1), 151-158. 10.1139/t90-014.
Stafleu, J., Maljers, D., Busschers, F.S., Gunnink, J.L., Schokker, J., Dambrink, R.M., Hummelman, H.J., Schijf, M.L., 2013. GeoTOP modelleringTNO 2012 R10991, TNO - Geological survey of The Netherlands, Utrecht.
Ten Veen, J.H., Vis, G.-J., De Jager, J., Wong, T.E. (Eds.), 2025. Geology of the Netherlands. Amsterdam University Press B.V.
TNO-GDN, 2019. DGM-diep v5.0. TNO - Geological Survey of the Netherlands (TNO-GDN), Utrecht, The Netherlands.
TNO-GDN, 2023. Geologische Kaart van het Koninkrijk der Nederlanden 1:600 000. TNO-Geological Survey of the Netherlands.
TNO-GDN, 2025. Digital Geological Model of the shallow subsurface of the Netherlands (DGM), version v2.2.1. TNO - Geological Survey of the Netherlands (TNO-GDN), Utrecht, The Netherlands.
Törnqvist, T.E., Weerts, H.J.T., Berendsen, H.J.A., 1994. Definition of two new members in the upper Kreftenheye and Twente Formations (Quaternary, the Netherlands): a final solution to persistent confusion? Geologie en Mijnbouw, 72 (Journal Article), 251-264.
Van Adrichem-Boogaert, H.A., Kouwe, W.F.P., 1993. Stratigraphic nomenclature of the Netherlands, revision and update by RGD and NOGEPA. Mededelingen Rijks Geologische Dienst, 50.
Van Balen, R.T., Van Bergen, F., De Leeuw, C., Pagnier, H., Simmelink, H., Van Wees, J.D., Verweij, J.M., 2000. Modelling the hydrocarbon generation and migration in the West Netherlands Basin, the Netherlands. Netherlands Journal of Geosciences - Geologie en Mijnbouw, 79 (1), 29-44.
Van Geel, B., Bohncke, S.J.P., Dee, H., 1980. A palaeoecological study of an upper late glacial and holocene sequence from "de borchert", The Netherlands. Review of palaeobotany and palynology, 31 (Journal Article), 367-392.
Van Ginkel, M., 2019. Design of the subsurface of land reclamations for freshwater storage and recovery - A new view on land reclamations. Ph.D.-thesis, Delft University of Technology.
Van Huissteden, J., Kasse, C., 2001. Detection of rapid climate change in Last Glacial fluvial successions in The Netherlands. Global and Planetary Change, 28 (1-4), 319-339.
Vandenberghe, J., 1985. Paleoenvironment and stratigraphy during the last glacial in the Belgian-Dutch border region. Quaternary Research, 24 (1), 23-38.
Vermeer, N., Hijma, M.P., Maarse, M., Quataert, E., 2025. Beheerbibliotheek Kust Voorne en Goeree -Beschrijvingen van de kustvakken ter ondersteuning van het beheer en onderhoud van de kust, Deltares, The Netherlands.
Vos, P.C., Bazelmans, J., Weerts, H.J.T., Van der Meulen, M.J., 2011. Atlas van Nederland in het Holoceen, RCE, TNO en Deltares.
Vos, P.C., 2015. Origin of the Dutch coastal landscape. Ph.D.-thesis, Utrecht University, Utrecht, The Netherlands, 359 pp.
Vos, P.C., Bunnik, F.P.M., Cohen, K.M., Cremer, H., 2015. A staged geogenetic approach to underwater archaeological prospection in the Port of Rotterdam (Yangtzehaven, Maasvlakte, The Netherlands): A geological and palaeoenvironmental case study for local mapping of Mesolithic lowland landscapes. Quaternary International, 367, 4-31. http://dx.doi.org/10.1016/j.quaint.2014.11.056.

Appendices

A Lithological description of the geological units

In this section, characteristics of each of the geological units will be described in detail. This includes the depositional age, lithology and related depositional environments, defining characteristics of the lower and upper boundaries of each unit, the thickness and typical depths at MV2. In addition, defining characteristics of these units in cone penetration test (CPT) results are discussed in combination with specific points of attention related to geotechnical investigations. The geological formations will be discussed from young to old. Interfingering Holocene members of the Naaldwijk and Nieuwkoop formations are described as part of the formation and are therefore not strictly discussed in chronological order.

For the current report we limit ourselves to the formations that make up the top 180 m of subsurface at MV2.

A.1 Anthropogenic deposits

- Link to Dutch stratigraphic nomenclature

https://www.dinoloket.nl/en/stratigraphic-nomenclature/antropogenic-deposits

- Age

Last 20 years.

- Lithological description

Mostly sand, increasingly clayey below -10 m NAP.

- Depositional environments

Landfill

- Lower boundary

Stratigraphically above the Southern Bight Formation or the Naaldwijk Formation, as a conformable landfill drape.

- Thickness indication and typical depth interval

At MV2 the landfill is generally 18-22 m thick. Below water bodies the thickness is less and estimated at 8-10 m. Typical depth interval ranges from 5 to -15 m NAP.

- Points of attention

Heterogenous, with a complex 3D-structure of different relative densities and lithologies.

A.2 Southern Bight Formation

A.2.1 Bligh Bank member

- Link to Dutch stratigraphic nomenclature

https://www.dinoloket.nl/en/stratigraphic-nomenclature/bligh-bank-member

- Age

Holocene (Atlantic-Subatlantic). Top part active until 20 years ago, below up to a few thousands year old.

- Lithological description

Very fine to moderately coarse sand, contains shell fragments. Homogenous.

- Depositional environments

Shallow marine, upper to lower shoreface .

- Lower boundary

Stratigraphically above the Naaldwijk Formation. Boundary clearly defined by an erosional contact with the underlying sediments. In most the cases it rests on top of the Naaldwijk Formation, but it could be in direct contact with the higher parts of the aeolian river dune deposits (Delwijnen Member) or the clay/peat complex (Echteld/Nieuwkoop Formations)

- Upper boundary

Formed the seafloor until the creation of the landfill. Mostly conformably overlain by the landfill.

- Thickness indication and typical depth interval

Mostly 0.5-2 m thick, starting around -15 m NAP.

- Points of attention

None

A.3 Naaldwijk Formation

A.3.1 Wormer Member

- Link to Dutch stratigraphic nomenclature

https://www.dinoloket.nl/en/stratigraphic-nomenclature/wormer-member

- Age

Holocene (Boreal-Subatlantic). Younger than 8250 years.

- Lithological description

Clay, grey, poor in humus, strongly silty and layered with few to many sand layers. But thicker sand layers do occur.

- Depositional environments

Estuarine or back-barrier, tidal channel.

- Lower boundary

In most cases an erosive unconformity with the Echteld Formation, but at places also with the Delwijnen Member. Tidal channels cut into the Kreftenheye Formation.

- Upper boundary

Erosively overlain by the Bligh Bank Member.

- Thickness indication and typical depth interval

Mostly varying between 2 and 4 m. In tidal channels thickness can reach 10 m. The top lies around -16/-18 m NAP, its base generally around -20/-21 m. The deepest parts of tidal channels reach close to -30 m NAP.

- Points of attention

Heterogeneous, with complex shifts between clayey and sandy parts. At tidal-channel locations, weaker layers can reach to considerable depths. Locally not present due to erosion by tidal channels (Naaldwijk Formation).

A.4 Echteld Formation

- Link to Dutch stratigraphic nomenclature

https://www.dinoloket.nl/en/stratigraphic-nomenclature/echteld-formation. In Hijma et al. (2009) it is part of the Terbregge Member.

- Age

Holocene (Preboreal-Boreal). 8700-8250 years old.

- Lithological description

Silty clay, grey brown and often organic. Can consist of gyttja. Lies on top of the basal peat. Wood remains and reed roots are present. In the top, also thin layers of silt occur.

- Depositional environments

Fluvial-tidal flood basins, fresh to slightly brackish.

- Lower boundary

Conformably overlying the Basal Peat Bed.

- Upper boundary

Erosively overlain by the Wormer Member, sometimes by the Bligh Bank Member.

- Thickness indication and typical depth interval

Thin, mostly 0.1-0.5 m. Occurs around -21/-22 m NAP.

- Points of attention

Weak layer. Locally not present due to erosion by tidal channels (Naaldwijk Formation).

A.5 Nieuwkoop Formation

A.5.1 Basal Peat Bed (NIBA)

- Link to Dutch stratigraphic nomenclature

https://www.dinoloket.nl/en/stratigraphic-nomenclature/basisveen-bed

- Age

Early Holocene (Preboreal-Boreal). 9250-8450 years old.

- Lithological description

Amorphous, compact, brown to dark brown peat. Macroscopic plant remains fragments of reed, roots and small pieces of wood. The layer is generally clayey, and may contain distinct clay layers.

- Depositional environments

Peat bog, frequently flooded.

- Lower boundary

Conformably overlying the Wijchen Member, sometimes also the Delwijnen Member.

- Upper boundary

The Basal Peat Bed is commonly conformably overlain by the Echteld Formation.

- Thickness indication and typical depth interval

Generally 0.05-0.3 m thick. Occurs around -21/-22 m NAP.

- Points of attention

Locally not present due to erosion by tidal channels (Naaldwijk Formation).

A.6 Boxtel Formation, Delwijnen member

- Link to Dutch stratigraphic nomenclature

https://www.dinoloket.nl/en/stratigraphic-nomenclature/boxtel-formation

- Age

Early Holocene (Preboreal). Mostly between 11.000-9.000 years old.

- Lithological description

Well sorted fine sands, median grain size 150-210 µm. Where not eroded, a dark humus soil is present in the top.

- Depositional environments

Aeolian, river dune.

- Lower boundary

Mostly overlying a thin Wijchen Member, but sometimes directly on top of the Kreftenheye Formation.

- Upper boundary

Conformably overlain by the Basal Peat Bed. Sometimes erosively overlain by the Naaldwijk Formation.

- Thickness indication and typical depth interval

The dunes are generally present as a sheet-like deposit of 1-2 m thick, locally 3 m thick.

- CPT characteristics

- Points of attention

The top of the dunes are often archaeologically rich (Moree & Sier, 2015; Vos et al., 2015). When being disturbed, additional archaeological research could be required. Locally not present due to erosion by tidal channels (Naaldwijk Formation).

A.7 Kreftenheye Formation, Wijchen member

- Link to Dutch stratigraphic nomenclature

https://www.dinoloket.nl/en/stratigraphic-nomenclature/wijchen-bed-0

In the nomenclator this unit is labelled as the Wijchen Bed, but this will change soon to the Wijchen Member.

- Age

Early Holocene (Preboreal). Mostly between 11.700-9.000 years old.

- Lithological description

Below the Delwijnen Member, the Wijchen Member consists of laminated grey loam, sandy clay and clayey sand (Vos et al., 2015). Above the Delwijnen Member it is a stiff grey clay, with medium to high silt content. At the base it is often very loamy and laminated with fine sand layers. Dark zones are present consisting of charred plant material and fine charcoal particles. Towards the top increasingly organic.

- Depositional environment

Fluvial floodplain.

- Lower boundary

Either conformably overlying the Kreftenheye Formation or the Delwijnen Member.

- Upper boundary

Either conformably overlain by the Delwijnen Member or the Basal Peat Bed.

- Thickness indication and typical depth interval

Below the dunes a few centimetres to decimetres thick. Above the dunes the thickness can be 1 m. Occurs between anywhere between -21 and -23 m NAP.

- Points of attention

Locally not present due to erosion by tidal channels (Naaldwijk Formation).

A.8 Kreftenheye Formation

- Link to Dutch stratigraphic nomenclature

https://www.dinoloket.nl/en/stratigraphic-nomenclature/kreftenheye-formation

- Age

Top part Late Glacial to Early Holocene (Preboreal). Deepest sections can be significantly older, up to 130.000 years old (Hijma et al., 2012).

- Lithological description

Medium to coarse sand, could be gravelly at places.

- Depositional environment

A mix of braided and meandering river floodplains.

- Lower boundary

Erosively overlying the Waalre Formation.

- Upper boundary

Mostly conformably overlain by the Wijchen Member. Locally incised by tidal channels of the Naaldwijk Formation.

- Thickness indication and typical depth interval

Starting between -22 and -25 m NAP, with its base around -41/-42 m NAP. Average thickness is thus 20-22 m.

- Points of attention

A long time hiatus of 1 to 2 million years exist between the Kreftenheye and Waalre Formation.

A.9 Waalre Formation

- Link to Dutch stratigraphic nomenclature

https://www.dinoloket.nl/en/stratigraphic-nomenclature/waalre-formation

- Age

Early Pleistocene (Praetiglian-Menapian). Between 2.6 and 1.1 million years old.

- Lithological description

Very variable. In the study area consisting of alternations of metre-thick clay and sand units. The sandy units seem to contain mostly fine sand.

- Depositional environment

Fluvial to estuarine, including high energy channel deposits as well as low energy flood basin and perhaps lagoonal.

- Lower boundary

Commonly sharp transition towards the Maassluis Formation. If the lowest part of the Waalre Formation consists of channel deposits, the boundary is strongly erosive.

- Upper boundary

Erosively overlain by the Kreftenheye Formation.

- Thickness indication and typical depth interval

Starting around -41/-42 m NAP, with the base around -70/-80 m NAP. Thickness thus 30-40 m.

- Points of attention

None.

A.10 Maassluis Formation

- Link to Dutch stratigraphic nomenclature

https://www.dinoloket.nl/en/stratigraphic-nomenclature/maassluis-formation

- Age

Early Pleistocene (Praetiglian-Tiglian). Between 2.6 and 1.8 million years old.

- Lithological description

Very variable. In the study area mostly consisting of fine to medium sand, but thin to thick clay layers do occur. In general the Maassluis Formation shows a coarsening upward trend. Slightly glauconitic.

- Depositional environment

Shallow marine, near coastal.

- Lower boundary

Mostly gradual transition into the slightly finer and more glauconitic Oosterhout Formation.

- Upper boundary

Commonly sharp contact with the Waalre Formation, but transition can also be diffuse with reworked Maassluis shells in the Waalre Formation.

- Thickness indication and typical depth interval

Starting around -70/-80 m NAP, with the base around -180 m NAP. Thickness thus 100-110 m.

- Points of attention

None.

B Cross sections including point data

B.1 Cross-section for the wider MV2 site (detailed version Figure 4-1)

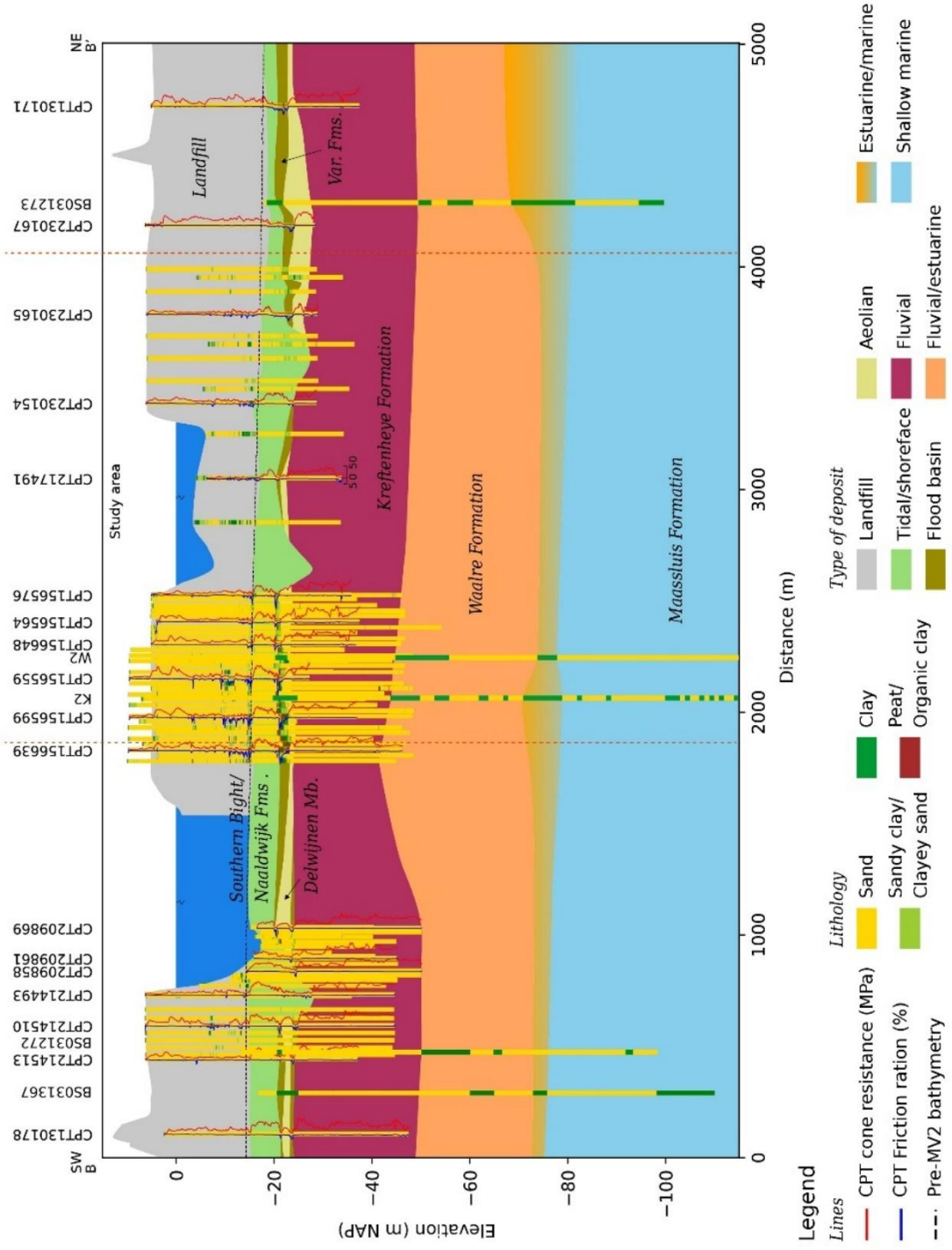

B.2 Close-up cross-section across the actual MV2 site (detailed version Figure 4-2)

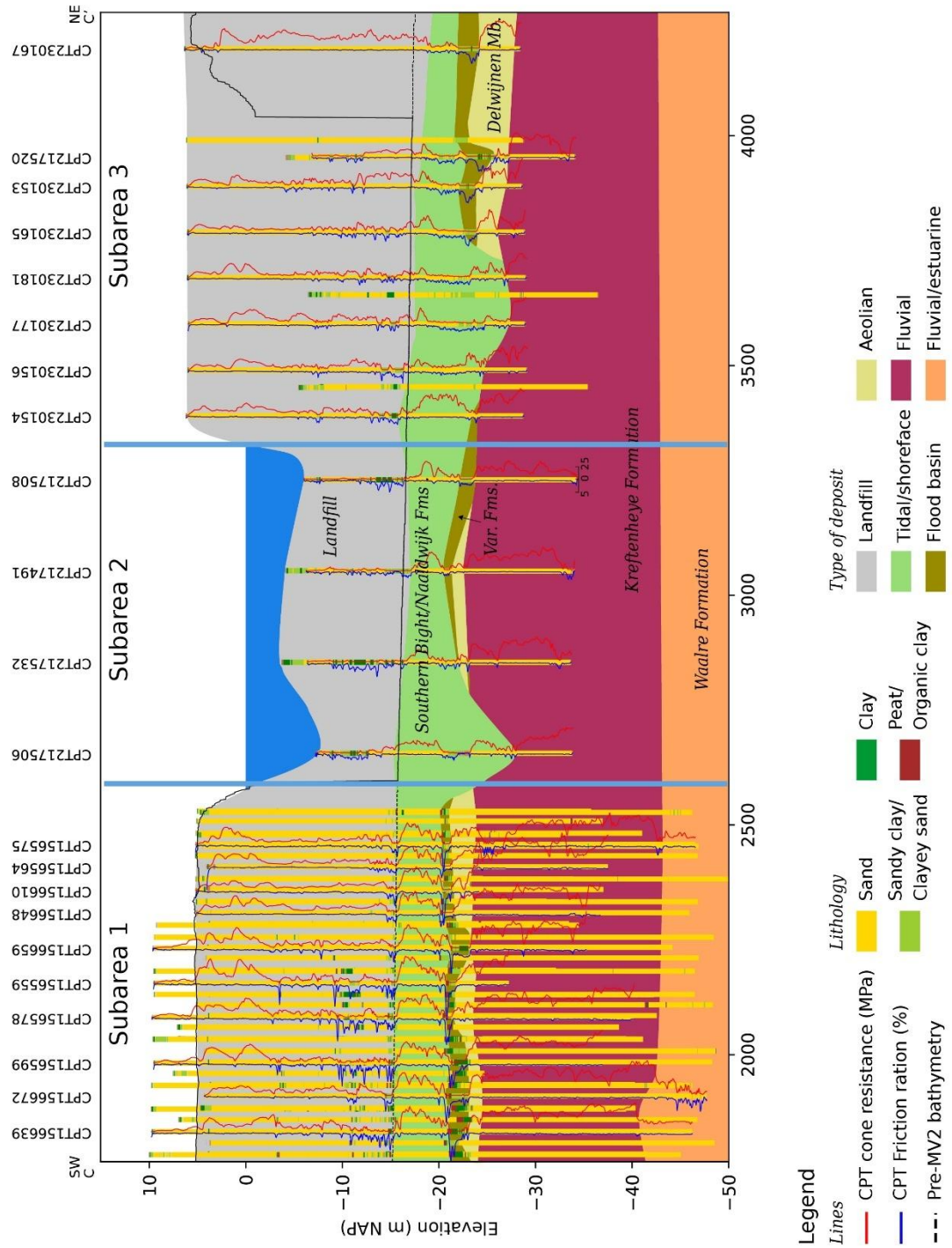

C Additional information geotechnical parameters

C.1 Layer boundaries

Table C.1 Layer boundaries for Subarea 1.

Length along cross section (m)	Layer boundaries (m)							
	1	2	3	4	5	6	7	8
1779	5.3	-3.0	-10.5	-14.0	-15.2	-21.0	-23.5	-50.0
1816	5.3	-3.0	-10.5	-14.0	-15.6	-20.5	-23.0	-50.0
1852	5.3	-3.0	-10.5	-14.0	-15.8	-20.0	-23.5	-43.5
1878	5.3	-3.2	-10.0	-14.2	-15.5	-21.0	-23.5	-43.5
1918	5.3	-3.2	-10.0	-14.5	-15.5	-20.7	-23.2	-43.5
1973	5.3	-2.5	-9.5	-14.8	-15.8	-21.0	-23.5	-43.5
2005	5.3	-3.5	-9.0	-14.5	-15.5	-20.5	-23.7	-43.5
2030	5.3	-3.5	-9.0	-14.5	-15.5	-20.4	-23.7	-43.5
2062	5.3	-2.5	-9.5	-14.5	-15.7	-20.8	-23.4	-43.5
2092	5.3	-3.0	-9.5	-14.5	-15.5	-20.2	-22.5	-43.5
2115	5.3	-3.0	-9.5	-14.0	-15.5	-20.1	-22.5	-44.0
2156	5.3	-3.0	-9.5	-14.0	-15.7	-20.5	-22.2	-44.5
2178	5.3	-3.5	-9.5	-14.5	-15.9	-21.0	-22.3	-45.0
2215	5.3	-2.5	-11.0	-14.5	-15.7	-20.0	-22.3	-48.0
2252	5.3	-3.0	-12.0	-14.0	-15.5	-20.5	-22.0	-48.0
2279	5.3	-4.0	-12.0	-14.8	-16.3	-20.0	-22.2	-48.0
2310	5.3	-4.3	-12.7	-14.5	-15.7	-20.0	-21.8	-48.0
2341	5.3	-3.3	-13.2	-14.0	-15.7	-20.0	-21.7	-48.0
2369	5.3	-3.3	-13.2	-14.0	-15.7	-20.2	-21.8	-38.5
2417	5.3	-3.3	-13.2	-14.0	-15.7	-20.0	-21.7	-48.0
2457	5.3	-3.3	-12.7	-14.0	-15.7	-20.0	-21.5	-48.0
2478	5.3	-3.3	-12.7	-14.5	-15.8	-20.0	-21.4	-45.0
2518	5.3	-3.3	-12.7	-14.5	-16	-20.0	-21.4	-43.5

Table C.2 Layer boundaries for subarea 2.

Length along cross section (m)	Layer boundaries (m)			
	1	2	3	4
2664	-4.2	-12.5	-20.0	-23.5
2850	-4.2	-16.5	-20.0	-23.5
2875	-4.2	-16.5	-20.5	-23.2
3048	-4.2	-17.0	-20.5	-23.2
3074	-4.4	-17.0	-20.5	-24.0
3259	-4.4	-16.8	-20.5	-24.0

Table C.3 Layer boundaries for Subarea 3.

Length along cross section (m)	Layer boundaries (m)					
	1	2	3	4	5	6
3388	6.2	-6.0	-13.0	-16.0	-19.5	-24.5
3487	6.2	-6.5	-13.5	-16.0	-19.0	-24.5
3586	6.2	-6.5	-13.5	-16.5	-19.0	-24.5
3686	6.2	-4.0	-14.5	-16.0	-18.5	-24.0
3786	6.2	-6.5	-16.0	-16.0	-19.0	-24.5
3884	6.2	-6.2	-16.0	-16.0	-19.0	-26.0
3984	6.2	-7.0	-16.0	-16.0	-19.0	-24.0
4084	6.2	-16	-16.0	-16.0	-19.0	-24.0
4131	6.2	-16	-16.0	-16.0	-19.0	-23.5
4185	6.2	-16	-16.0	-16.0	-19.0	-24.5

C.2 NEN9997 Interpolation table

Table C.4 Interpolation table for all layers with mostly non-organic materials

$q_{c,norm}$	phi (degrees)	E100 (MPa)	$C_c/(1+e_0)$	C_α	$C_{sw}/(1+e_0)$
0.1	15	0.2	0.46	0.023	0.1533
0.5	15	1	0.23	0.0115	0.0767
0.7	22.5	1.5	0.23	0.0092	0.0767
1.0	27.5	2	0.092	0.0037	0.0307
2	27.5	3	0.0511	0.0020	0.017
5	30	15	0.0115	0	0.0038
15	32.5	45	0.0038	0	0.0013
25	35	75	0.0023	0	0.0008
45	40	110	0.0015	0	0.0005

Table C.5 Interpolation table for the layers with mainly organic materials

$q_{c,norm}$	phi (degrees)	E100 (MPa)	$C_c/(1+e_0)$	C_α	$C_{sw}/(1+e_0)$
0.1	15	0.2	0.46	0.023	0.1533
0.2	15	0.5	0.3067	0.0153	0.1022
0.5	15	1	0.23	0.0115	0.0767
1.0	15	2	0.1533	0.0077	0.0511
2	27.5	3	0.0511	0.0020	0.017
5	30	15	0.0115	0	0.0038
15	32.5	45	0.0038	0	0.0013
25	35	75	0.0023	0	0.0008
45	40	110	0.0015	0	0.0005

Deltares is een onafhankelijk kennisinstituut voor toegepast onderzoek op het gebied van water en ondergrond. Wereldwijd werken we aan slimme oplossingen voor mens, milieu en maatschappij.

Deltares

www.deltares.nl